The GEOLOGICAL BULLETIN of the PANJAB UNIVERSITY

Number Six
DECEMBER 1967

The
GEOLOGICAL BULLETIN
of the
PANJAB UNIVERSITY

Number Six December 1967

CONTENTS

THE PETROLOGY OF SOME CHLORITOID AND STAUROLITE-BEARING SCHISTS FROM THE MANSEHRA-AMB STATE-AREA, NORTHERN WEST PAKISTAN

BY

F. A. SHAMS*

Abstract : *Petrographic description is given of some chloritoid and staurolite-bearing pelitic schists from the Mansehra-Amb State Area, Northern West Pakistan. Textural evidence suggests possibility of the following reactions :—*

$$\underset{\text{Amesitic Chlorite}}{H_2(Mg, Fe)_2 Al_2 Si0_9} + 2\underset{\text{Muscovite}}{H_2 KAI_3 Si_3 0_{12}} + \underset{\text{Hematite}}{Fe_2 0_3} = 4\underset{\text{Chloritoid}}{H_2(Mg, Fe) Al_2 Si0_7} + 3\underset{\text{Quartz}}{Si0_2} + 2 KOH$$

$$\underset{\text{Muscovite}}{H_2 KAI_3 Si_3 0_{12}} + 2\underset{\text{Biotite}}{H_2 K (Mg, Fe)_3 AlSi_3 0_{12}} = 2\underset{\text{Staurolite}}{H_2 Fe Al_2 Si0_7} + \underset{\text{Phlogopite}}{H_2 K Mg_3 Al Si_3 0_{12}} + 4\underset{\text{Quartz}}{Si0_2} + K_2 0 + \underset{\text{Ore.}}{Fe0}.$$

Petrochemistry of the rocks is discussed. The ratio $FeO+MnO/FeO+MnO+MgO$ for the co-existing chloritoid and staurolite is 0.89 and 0.87 respectively, which suggests that there can be only a very narrow P—T range of co-existence of these minerals.

INTRODUCTION

Occurrence of chloritoid and staurolite have been described from various parts of the world. The minerals generally occur as constituents of regional crystalline schists of the orogenic belts and are commonly known to have grown in media which were rich in iron, alumina, and silica while being poor in lime; otherwise a mineral of the epidote group may appear instead. Many reactions to explain their genesis have been proposed, *e.g.* by Tilley (1925) for the minerals in the Frenchman schists of Australia by Williamson (1953) for the Kincardineshire schists and by Shelling (1957) in the case of the schists of Glen Esk, Scotland. Investigation of some chloritoid and staurolite-bearing rocks from the Mansehra-Amb State area† has been undertaken in order to ascertain the validity of the mechanisms proposed.

A preliminary account of the geology of the Mansehra area was published some years ago (Shams 1961) while a major paper is under preparation. The area is part of a major syntaxial bend of the Himalayas (Wadia, 1931) and consists of (Fig. 1) Palaeozoic (?) pelitic and psammitic schists and quartzites, intruded by granites of different ages ; all are cut by basic minor intrusives.

THE OCCURRENCES OF CHLORITOID

The chloritoid-bearing rocks have been seen at two stratigraphical levels, one falling in the chlorite and the other in the garnet zone of regional metamorphism ; they are now considered separately :

(*i*) The chlorite-grade, chloritoid-bearing rocks make the south-eastern marginal zone of the Potha schist formation and are in contact

* Department of Geology, Panjab University, Lahore.

† This is the first record and description of chloritoid and staurolite bearing rocks from the Hazara District.

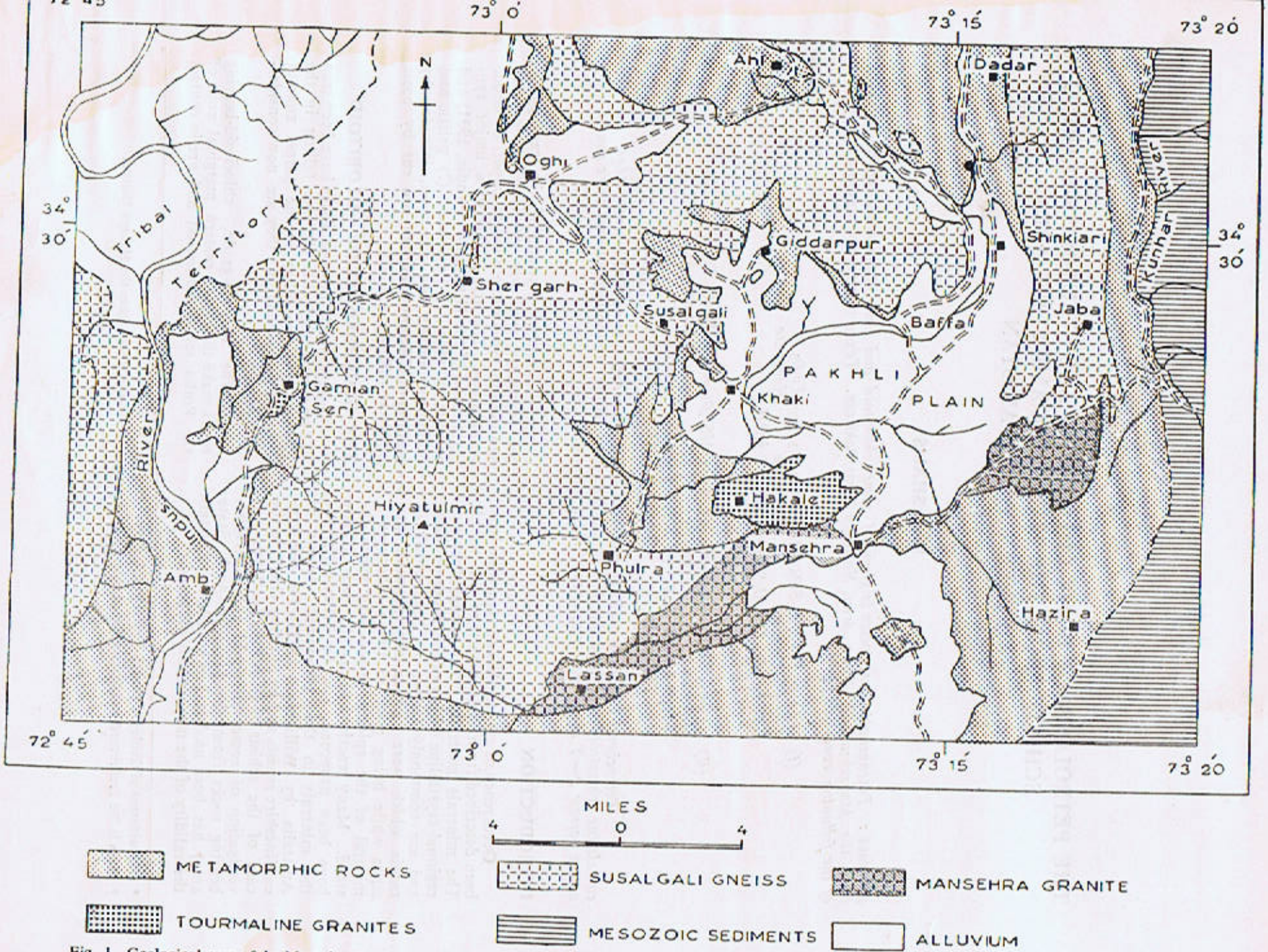

Fig. 1. Geological map of the Mansehra-Amb State Area, (Geology by F. A. Shams). Dots mark location of the specimens described in the text of the paper.

with the younger sedimentary rocks. The older schists have actually been thrust over the sedimentary strata and the marginal rocks are strongly sheared, in the direction of the regional strike. The contact marks a major thrust shear zone which can be traced over very long distances.

The chloritoid-bearing rocks are silvery grey, strongly sheared grits and conglomerates, with a micaceous matrix. The quartz grains and pebbles (upto 1 inch in the longer dimension) are granulated and stretched and the rocks show a gneissic foliation. The chloritoid occurs as tiny bluish-black specks within the micaceous folia.

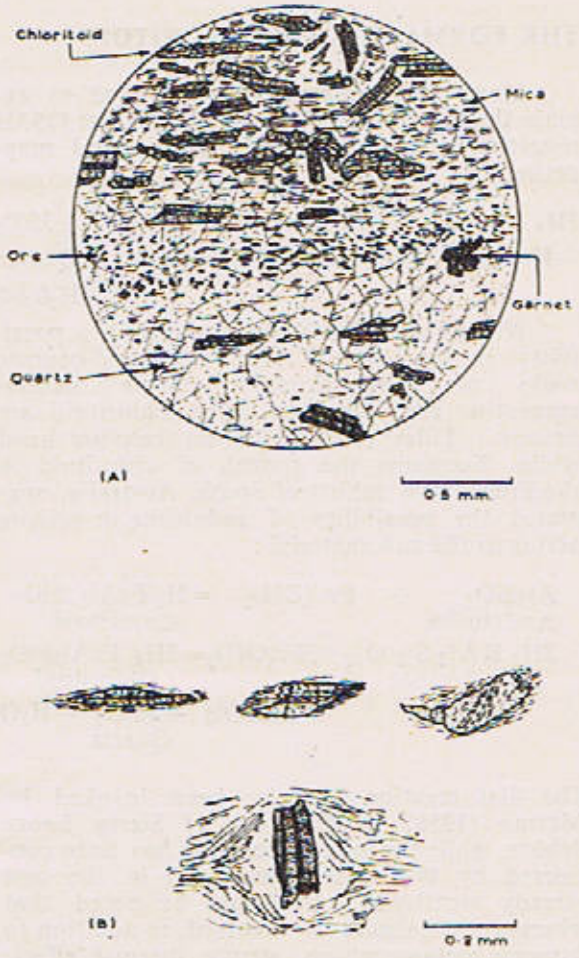

Fig 2. Thin section drawings from a specimen of chloritoid bearing schist (MNS 6658) from near Hazira. Fig. 2A shows the general rock texture and mineralogy and Fig. 2B shows habit and nature of individual chloritoid crystals.

In thin section (Fig. 2A), a typical specimen (MAS 6658,* grid 334309, 1" 43 F/7, about 1 mile south-west of Hazira) exhibits a very prominent, sheared texture. Quartz makes up 50% of the rock and occurs as strongly sheared large grains and comparatively strain-free, smaller grains. In general, unequidimensional quartz grains have their longer dimension conformable to the schistosity, which is otherwise marked by the orientation of predominant muscovite (25%) and subordinate chlorite (12%) flakes. Sometime, large quartz grains show an incipient fracture pattern which may be highly discordant to the rock foliation. Next, in the order of abundance, are hematite, magnetite and rutile, generally dispersed in the rock and also occasionally present in distinct bands. Rare, detrital grains of greenish-blue, pleochroic tourmaline and a colourless garnet are present These accessories, together, make up obout 5% of the rock. The chloritoid (8%) occurs as skeletal to well-formed, tiny to long, prismatic metacrysts, with ragged and drawn-out ends, and occasionally acquire augen-like or spindle-shaped forms (Fig. 2B). It shows distinct pleochroism from straw-yellow to greenish; has good (001) cleavage and a poor (100) parting. Lamellar twinning is very prominent and, rarely, an hour-glass structure is seen. It is biaxial with $2V_z$ nearly 42° and $C\hat{Z} = 16°$. Inclusions of quartz, mica and ore minerals are invariably present, sometimes in trails and suggesting a syntectonic growth of the mineral. Chloritoid crystals are sometime bent and curved in accordance with the attitude of the schistosity, while occasional crystals have been rotated into positions perpendicular to the foliation. The mineral is generally surrounded by micaceous veneers, not necessarily originating by the alteration of chloritoid.

(*ii*) The second occurrence of the chloritoid-bearing rocks is in the Khaki area, near margin of a tongue-like extension of the Susalgali granite gneiss. It is a dark, greyish black, somewhat massive-looking rock, with shining mica flakes and small, 1-2 mm. long, chloritoid porphyroblasts. The rock has a weak knotted appearance.

In the thin section (Fig. 3) of a typical rock (MAS 6851, grid 111412, 1" 43 F/3, about 1 mile west of Jabian), a weak schistose texture is seen, marked mainly by the micaceous minerals like muscovite, biotite and chlorite. The muscovite (10%) occurs as long individual flakes and as aggregates of small flakes. The biotite (25%)

* This and subsequent numbers refer to the catalogued collection of the Department of Geology, Panjab University, Lahore.

is a light brown, strongly pleochroic variety, sometime transitional to chlorite. The latter mineral (10%) is deep green; pleochroic and shows anomalous blue interference colour. It is generally present as porphyroblastic aggregates, as is also the case in the chloritoid-free schists of the immediately lower grade. Quartz (40%) is the most important mineral of the matrix and shows a weak directional orientation. Among the accessories (3%) are the generally dispersed ore minerals, rare garnet and detrital tourmaline grains, which are pleochroic and colour-zoned. The chloritoid (8%) generally occurs, within or close to the chlorite porphyroblasts, as well-formed prismatic crystals and plates. Polysynthetic twinning is very important and curved crystals are occasionally seen. The mineral is pleochroic from pale-yellow to light slaty-blue, and has inclusions of quartz and ore grains.

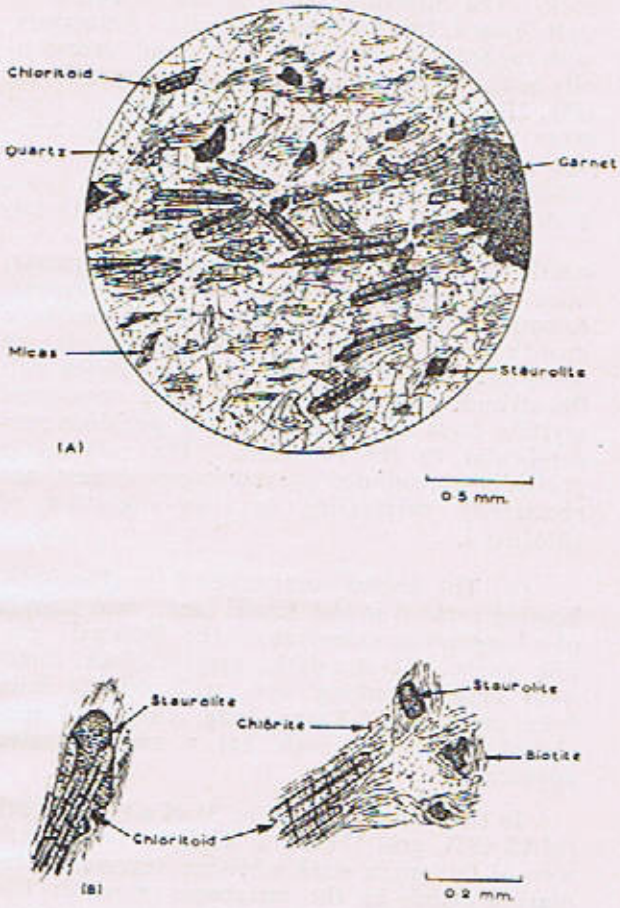

Fig. 3 Thin section drawings from a specimen of chloritoid-staurolite - garnet - mica schist (MNS 6851) from near Jabian. Fig. 3A shows general rock texture and mineralogy and Fig. 3B shows the independent genetic habits of chloritoid and staurolite crystals.

In addition to chloritoid, this rock has also staurolite (4%) which is in its initial stages of growth and, therefore, marks the pro-grade transition from the chloritoid grade. The staurolite is present as small anhedral grains and shows its typical pleochroism. Distinct from chloritoid, the staurolite is intimately associated with biotite and shows no direct relationship towards chloritoid (Fig. 3B). Quartz and ore minerals are the most common inclusions. Spongy and pink almandine garnet, with inclusions of ore, biotite and quartz, is another mineral of metamorphic origin. Its relationship towards the ferrous aluminium silicates could not be established with certainty, except that it appears to be younger than chloritoid and occasionally encloses the latter.

THE FORMATION OF CHLORITOID

Many reactions have been proposed to explain the formation of chloritoid. Harker (1932) suggested a reaction between kaolin and magnetite:

$$3H_4\ Al_2\ Si_2\ 0_9 + Fe_3\ 0_4 = 3H_2\ FeAl_2Si0_7 + 3Si0_2 + 3\ H_20 + 0$$

Kaolin — Magnetite — Chloritoid — Quartz

Williamson (1953) considered such a possibility in the case of the chloritoid-bearing rocks of Kincardineshire, where kaolin-magnetite pseudomorphs after chloritoid are present. Tilley (1925, 1926) on the other hand while discussing the growth of chloritoid in the Frenchman schists of South Australia, suggested the possibility of andalusite or sericite acting as the raw material:

$$Al_2SiO_5 + Fe\ (OH)_2 = H_2\ FeAl_2\ SiO_7$$

Andalusite — Chloritoid

$$2H_2\ KAl_3\ Si_3\ O_{12} + 3Fe(OH)_2 = 3H_2\ FeAl_2SiO_7 + 2KOH + 3SiO_2 + H_2O$$

Sericite — Chloritoid — Quartz

The first reaction has also been invoked by Marmo (1958) in the case of Sierra Leone Schists, while the second reaction has been considered by Williamson (loc. cit.) in the case already mentioned. It should be noted that wherever andalusite is involved, in addition to dynamic metamorphism, strong thermal effects have also taken place. This type of phenomenon has been called "piezocontact metamorphism" by Tilley (1925). The Hazira schists, however, do not fall into this category. In view of mineralogy of these schists, Tilley's second equation is applicable. The ferrous iron may have been

supplied by hematite and magnetite minerals through the agency of pore fluid. The iron ore minerals are present in the chloritoid.

The case of the Khaki schists is different. From the mineral paragenesis and their textural relationship, chloritoid seems to have developed from chlorite and muscovite. The following reaction is considered as a possibility :

$$H_2(Mg, Fe)_2\ Al_2\ Si0_9 + 2H_2\ KAl3\ Si_3\ 0_{12} + Fe_20_3$$
Amesitic Chlorite Muscovite Hematite
$$= 4H_2(Mg, Fe)\ Al_2\ Si0_7 + 3\ Si0_2 + 2\ KOH$$
Chloritoid Quartz

It is interesting to note that, in some instances, chloritoid is enclosed in chlorite flakes in a manner which suggests that it is developing solely from the latter. Although, from chemical consideration, such a possibility is not ruled out, yet the incorporation of muscovite is considered necessary because chloritoid aggregates are frequently surrounded by relatively muscovite-poor haloes Andalusite, being younger, could not be a reactant as was suggested by Tilley (loc. cit) in the case of Frenchman Schists.

Williamson (loc. cit.) noted in the Kincardineshire Schists that chloritoid and biotite do not form a stable assemblage. In case of the Khaki schists, although garnet is present and the chloritoid is at its best development, yet biotite does not show sign of mass transformation to garnet. The biotite was rather involved in reactions which gave birth to staurolite (discussed below). In the present case, chloritoid and chlorite show a clear antipathetic relationship. The expenditure of biotite seems hardly to have anything to do with the development of chloritoid and is simply due to rise in the grade of metamorphism. Even the Kincardineshire case may perhaps be explained on these lines.

THE OCCURRENCES OF STAUROLITE

In addition to the transitional rocks, as described above, staurolite-bearing rocks have been seen at other horizons too. Only two examples are considered here :

(*i*) The first example comes from within the thermal aureole of the Susalgali granite-gneiss, being only 300 yards from the contact. This aureole is very interesting because the country rocks, in addition to thermal metamorphism, are also veined by granitic material in lit-par-lit fashion. This seems to have happened during

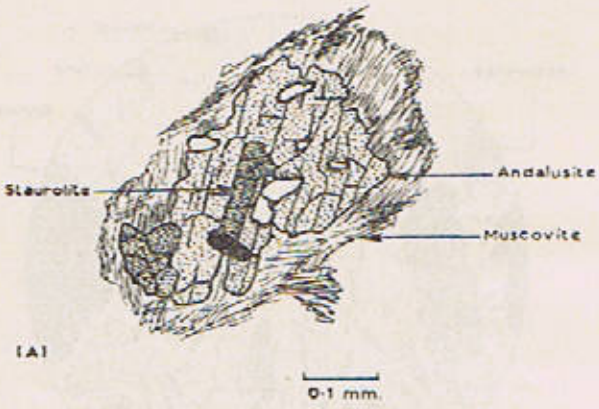

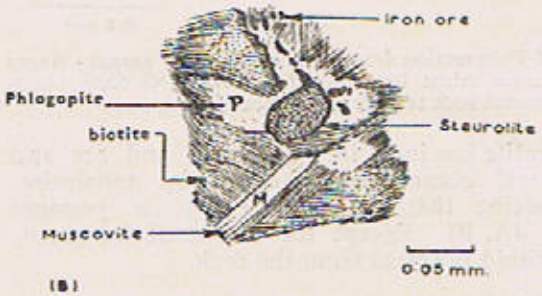

Fig. 4 Thin section drawings from a specimen of staurolite-andalusite - garnet mica hornfels (MNS 6881) from near Chorgali. Fig. 4A shows the textural relations of andalusite and staurolite and Fig. 4B shows evidence for the growth of staurolite grains.

the orogenic movements so that the hornfelsed country rocks underwent plastic deformation and contact migmatites*, of the type described from South Africa (Walker and Mathias, 1947), were developed. The specimen (MA S 6881, grid 128461, 1" 43 F/3), now to be described, was taken from eastern side of the Khaki-Oghi road, near the Chorgali crossing. It is composed of pink pleochroic andalusite (10%), which is developed within a matrix that is essentially composed of quartz (36%), muscovite (16%), biotite (28%) and ore minerals (2%). Porphyroblasts of almandine are present at places and are charged with ore grains and rods due to their thermal breakdown ; garnet and detrital tourmaline, make about 1% of the rock The staurolite (7%) is present as small grains within felts of mica minerals It is intimately attended by ore minerals and the biotite around staurolite is changed to weakly pleochroic, brownish-yellow to colourless, phlogopitic mica. The

* The term "contact migmatite" is used to distinguish them from the "regional migmatites" which are developed on regional scale, such as in Finland, Scotland etc.

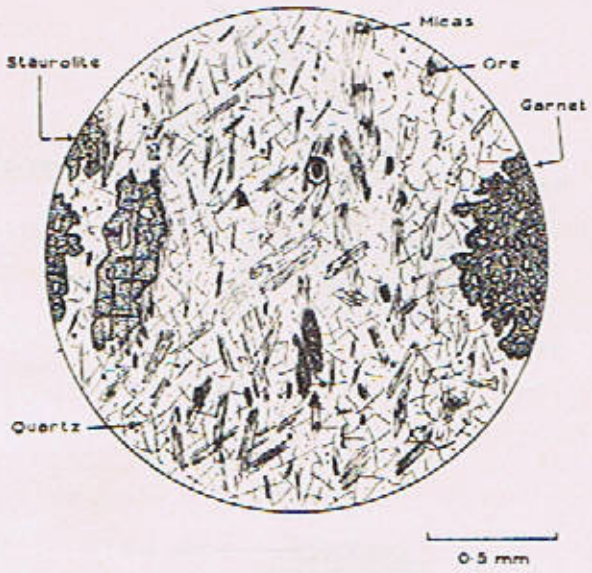

Fig. 5 Thin section drawing a specimen of garnet - staurolite - mica schist from near Tarkanal (MNS 6500), showing general rock texture and mineralogy.

staurolite has inclusions of quartz and ore and is itself occasionally enclosed by andalusite, suggesting that the latter may be younger (Fig. 4A, B) Except for one doubtful grain, chloritoid is absent from the rock.

(*ii*) The second example is taken from an area where the staurolite is at its best development. A typical specimen (MA S 6500, grid 272569, 1° 43 F/6 about ¼ mile south of Tarkanal) is a silvery white, mica-schist with large porphyroblasts of garnet (4%) and staurolite (10%). Thin, microfolded quartz-veins are present and a strain-slip cleavage sometime shows up. The matrix minerals (Fig. 5) are granular and include somewhat strain-free quartz (45%), muscovite (13%) and brown biotite (25%). Zoned tourmaline, apatite, hematite, magnetite and rutile make 2% of the rock. Staurolite makes big as well as small spongy crystals, poikilitically enclosing quartz, ore, muscovite and biotite and, rarely, garnet as well. It shows its typical pleochroism and is altered to hematite along cracks. Sometime curved crystals are seen and the mineral usually lies within mica and ore-rich zones.

These schists outcrop across the river Siran, north of the Dadar sanitorium, where excellent exposures are available along road cuts to Jabori. In these schists, due to inherent mineralogical banding related to the sedimentary origin, staurolite is mostly confined to definite bands which alternate with staurolite-free bands. Garnet does not show selective growth and is occasionally enclosed by staurolite.

THE FORMATION OF STAUROLITE

In all cases from the present area, it has been repeatedly seen that biotite was intimately involved in the growth of staurolite. In discussing the formation of this mineral in the Holnhead schists, Glen Esk, Snelling (1957) proposed following reaction :

$$x\mathrm{Fe_2Al_2(SiO_4)_3} + y\mathrm{K_2Al_4(Al_2Si_6O_{20})(OH)_4} + \left\{\begin{array}{l} n\mathrm{K_2Fe_6(Al_2Si_6O_{20})(OH)_4} \\ n\mathrm{K_2Mg_6(Al_2Si_6O_{20})(OH)_4} \end{array}\right. + 12\mathrm{H_2O}$$

almandine — muscovite — biotite — water

$$= 12\,\mathrm{FeAl_4Si_2O_{10}(OH)_2} + (x-14)\,\mathrm{Fe_3Al_2(SiO_4)_3} + (y-5)\,\mathrm{K_2Al_4(Al_2Si_6O_{20})(OH)_4} + \left\{\begin{array}{l} n+5\mathrm{K_2Fe_6(Al_2Si_6O_{20})(OH)_4} \\ n\mathrm{K_2Mg_6(Al_2Si_6O_{20})(OH)_4} \end{array}\right. + 18\,\mathrm{SiO_2}$$

staurolite — almandine — muscovite — biotite — quartz

Such a reaction could have been responsible for the growth of staurolite in the Shergarh, Tarkanai and Dadar Schists. However, it is noteworthy that, in these cases, garnet crystals do not show any sign of reactive dissipation and appear to have been accidently enclosed by the growing staurolite crystals. It is also noteworthy that chloritoid too is not directly involved in the manner, suggested by Tilley (1925) in case of the Piz Scopi schists

$$10\,\mathrm{H_2FeAl_2SiO_7} + \mathrm{H_2KAl_3Si_3O_{12}} + \mathrm{SiO_2} = 4\,\mathrm{HFeAl_5Si_2O_{13}} + 8\mathrm{H_2O}$$

chloritoid — muscovite — quartz — staurolite — water

$$+ \left\{\begin{array}{l} \mathrm{H_2KAl_3Si_3O_{12}} \\ 3\mathrm{Fe_2SiO_4} \end{array}\right.$$

biotite

This has also been accepted by Williamson (1953). In the case of Piz Scopi schists, the staurolite arose from the ruins of chloritoid. No such evidence was seen in the case under discussion. Such an evidence is missing in the Kincardineshire schists also. However, rarely (*e.g.* in MAS 6851) an association of chloritold and staurolite is seen (see Fig. 3 A) but it proves parallel growth rather than a mineralogical transformation.

In the case of Khaki schists, Snelling's equation does not apply at all because garnet is typically not involved. Textures, such as shown in the Fig No. 4 B, show that staurolite evolved by the reaction of biotite and muscovite, the former transforming to phlogopitic composition on the extraction of iron. The reaction can be written as follows :

$$\underset{\text{muscovite}}{H_2 KAl_3 Si_3 O_{12}} + 2\,\underset{\text{biotite}}{H_2 K (Mg, Fe)_3 Al Si_3 O_{12}} = 2\,\underset{\text{staurolite}}{H_2 Fe Al_2 Si O_7}$$

$$+ \underset{\text{phlogopite}}{H_2 KMg_3 Al Si_3 O_{12}} + 4\,\underset{\text{quartz}}{SiO_2} + K_2 O + \underset{\text{ore}}{FeO}$$

This reaction can be seen in its very initial stages in rocks from the Khaki area.

PETROCHEMICAL CONSIDERATIONS

Partial analyses of three schists from the Mansehra-Amb State area are given in Tables No. 1 and 2, in which are also included for comparison, analyses of rocks from some other occurrences of the world.

TABLE NO. 1

Chemical Analyses of the Chloritoid-Bearing Rocks.

		1	2	3	4	5
SiO_2	=	72 48	69.99	70.12	59.10	74.48
TiO_2	=	nd	nd	0.67	0.93	—
Al_2O_3	=	10.68	15.02	15.48	22 58	15 96
Fe_2O_3	=	9.06	9.86	0.68	0.97	0.87
FeO				5 98	4.40	2.02
MnO	=	nd	nd	0 23	0.09	nd
MgO	=	2.17	1.32	2.17	1.82	0.35
CaO	=	0.79	0.79	0.16	0.81	0.28
Na_2O	=	nd	nd	0.33	1.12	0.72
K_2O	=	nd	nd	0.99	3.74	3.88
P_2O_5	=	nd	nd	—	0.17	nd
H_2O^+	=	1.76	1.86	2.88	3.63	2.02
H_2O^-	=	0.06	0.22	0.32	0.16	0.13

(1) Quartz-chlorite-sericite-chloritoid schist from near Hazira, Mansehra-Amb State Area, Anal., Fazalur Rehman.

(2) Quartz-chlorite-muscovite-biotite-chloritoid-staurolite schist from near Jabian, Mansehra-Amb State Area, Anal., Fazalur Rehman.

(3) Muscovite-chlorite-chloritoid schist, Rawlinsville, Pennsylvania, Anal., Elsa Stahlberg.

(4) Chloritoid schist, Perthumie Bay, Stonehaven coastal section, Anal., Avery and Anderson, Melbourne.

(5) Chloritoid Schist, The Frenchman, Eyre Penninsula, S.Australia, Anal., Tilley.

TABLE NO. 2

Chemical Analyses of the Staurolite-Bearing Rocks.

		1	2	3
SiO_2	=	67.58	58.53	49.16
TiO_2	=	nd	2.53	1.01
Al_2O_3	=	17.16	18.55	28.21
Fe_2O_3	=	7.49	4.20	4.63
FeO	=		4.41	6.21
MnO	=	nd	0.05	0.19
MgO	=	1.35	2.24	1.84
CaO	=	0.75	0.97	0.88
Na_2O	=	nd	2.43	3.00
K_2O	=	nd	3.20	1.83
P_2O_5	=	nd	nd	0.47
H_2O^+	=	1.86	2.50	2.76
H_2O^-	=	0.04	0.17	0.28

(1) Quartz-Muscovite-biotite-andalusite-staurolite schist, from near Chorgali, Mansehra-Amb State Area, Anal., Fazal-ur-Rehman.

(2) Staurolite-garnet-mica schist, Holnhead, Glen Esk, Angus, Anal., Snelling.

(3) Staurolite schist, Limput Burn, Kincardineshire. Anal., Williamson.

The analyses show that rocks from the Mansehra-Amb State area, like similar rocks from other parts of the world, are rich in alumina and iron and poor in lime, which are the main chemical requirements for chloritoid and staurolite to crystallize provided that the suitable physical conditions are prevalent. However, their chemistry does not support Williamson's idea (loc. cit.) that a $Fe_2O_3 : Al_2O_3$ ratio of about 0·40 is critical for the formation of chloritoid and staurolite, which he found in case of the Kincardineshire schists. The theory is also not supported by data on rocks from other occurrences, as has been pointed out by Williamson himself.

The unique co-existence of chloritoid and staurolite in Jabian schist was further investigated because these two minerals are generally thought to be antipathetic and, therefore, are not expected to occur together. The minerals were concentrated out of schist, were purified and were subjected to partial chemical analysis.

The ratio $\frac{FeO + MnO}{FeO+MnO+MgO}$ is 0.89 and 0.87 in the case of chloritoid and staurolite respectively.

The close correspondence of $\frac{FeO+MnO}{FeO+MnO+MgO}$ ratio suggest a very narrow range of co-existence and thus upholds their antipathetic relationship as has been shown by Schreyer and Chinner (1956) also. This is further supported by the sudden disappearance of chloritoid as the staurolite grade sets in and the staurolite starts to grow in size and proportion.

STATUS OF CHLORITOID AND STAUROLITE IN REGIONAL METAMORPHISM

Study of rocks from the Mansehra-Amb State area, shows that chloritoid and staurolite have their own specific fields of stability and although sometime there may not be a mutual mineralogical transformation, yet staurolite prospers under those higher p—t conditions which are associated with dwindling chloritoid. There are transitional rocks which may be used to mark a metamorphic "isograd". However, in view of the chemical limits involved, these minerals cannot serve as index minerals or can be of restricted use only.

Alleged stress dependence of chloritoid, in the sense of Harker (1939), could not be checked. In the rocks of the Mansehra-Amb State area, chloritoid developed contemporaneously with regional movements but while the Hazira schists are strongly sheared, those of the Khaki area are not so violently involved. On the other hand, this mineral is much better developed in rocks of the Khaki area as compared with those from the Hazira area. This may mean that, in progressive regional metamorphism, rise in the geother-

mal heat may also favour growth of chloritoid. Under pure thermal metamorphism, however, chloritoid-bearing rocks give rise to cordierite and cordierite-spinel (corundum) hornfelses (Tilley, 1925).

The possibilities of new reactions show that, in nature, whenever critical physico-chemical conditions are prevalent, a certain mineral will grow by collecting constituent raw material out of a variety of mineral phases. The regional movemants may help in migration of chemical elements to produce favourable environments, as is suggested by Seki (1954).

REFERENCES

Schreyer, W. and Chinner, G.A. 1966 Staurolite-quartzite bands in kyanite quartzite at Big Rock, Rio Arriba County, New Mexico, *Min. and Pet. Contr.* **12**, 223-244.

Harker, A. 1939 Metamorphism, 2nd Ed. Methuen, London.

Marmo, V. 1958 Chloritoid schists of Central Sierra Leone. *Compt. Rend. Soc. Geol. Finlande*, No. **30**, 105.

Seki, Y. 1954 On chloritoid rocks in the Kitakami Median metamorphic zone, northeastern Japan. *Sci. Reports of Saitama Univ.* Ser. B, 1, 223.

Shams, F.A. 1961 A preliminary account of the geology of the Mansehra Area, District Hazara, West Pakistan. *Geol. Bull. Panjab Univ.* No. **1**, 57-62.

Snelling, N.J. 1957 Notes on the petrology and mineralogy of the Barrovian metamorphic zones. *Geol. Mag.* **94**, 297-304.

Tilley, C.E. 1925 Petrographical notes on some chloritoid rocks. *Geol. Mag.* **62**, 309-319.

..... 1926 Some mineralogical transformations in crystalline Schists. *Mineral. Mag.* **21**, 34-46.

Wadia, D.N. 1931 The syntaxis of the northwest Himalayas: Its rocks, tectonics and orogeny. *Rec. Geol. Surv. India* **45**, 89.

Walker, F. and Mathias, M. 1947 The petrology of two granite-slate contacts at Cape Town, South Africa, *Quart. Journ. Geol. Soc.* **102**, 499-521.

Williamson, D H. 1953 Petrology of chloritoid and staurolite rocks north of Stonehaven, Kincardine-shire. *Geol. Mag.* **90**, 353-361.

A GRAVITY AND MAGNETIC ($\triangle Z$) STUDY OF A DEEP-SEATED ANOMALY IN THE GUJRANWALA DISTRICT, WEST PAKISTAN

BY

AZIZ-UR-RAHMAN*

Abstract : *A gravity and magnetic ($\triangle Z$) survey was carried out covering an area of about 1600 sq. miles over an extensive predetermined aeromagnetic anomaly. Both the gravity and the magnetic anomalies thus found, were analysed for second vertical derivative on thebasis of the formulae due to Elkin and Rosenbach. Beside delineating the sub-surface features, the study provides a text-book example of a comparison between the two methods of second derivative determination for a deep-seated anomaly.*

INTRODUCTION

A total field magnetic anomaly was observed on the aeromagnetic map of the north-eastern areas of West Pakistan (Fig. 1). On the basis of this anomaly, a gravity and a vertical magnetic intensity survey was conducted, covering an area lying between Lat. 32° 0′ N to 32° 30′ N and Long. 73° 40′ E to 74° 15′ E (Fig. 2). About 600 observation stations were established at one mile interval along roads, canals and distributaries in this area, which has an extension of about 1600 sq. miles. Both the gravity and the magnetic observations were made at each station. The insruments used for the survey were the Worden Gravity Meter No. 372, with a scale constant of 0.0984 (4) mgal/s. d., and the ABEM Torsion Magnetometer No. 1081, having a scale constant of 10.5/s.d. The centre of the gravity and the magnetic anomalies were found to be situated about 20 miles NNW of the Gujranwala Town.

The area constitutes the flood plain of river Chenab having a surface gradient of about 1 ft/mile. The alluvium consists of sand, silt and clay; there are no outcrops in the area and the plain has an average height of about 600 feet above sea level. The nearest outcrops are at Sangla, which is a small town situated 30 miles south-west of the area. The Himalayan foothills flank the area and are situated on the eastern and north-eastern directions at a distance of about 30 miles.

Exploratory drilling in some areas of Indus plain of which this area makes a part, has shown that the Precambrian basement is overlain directly by the quaternary alluvium. Test drilling in this area has been carried to 1500 ft. depth, but the bed-rock has not been struck, hence the total thickness of the alluvium could not be determined (Kidwai, 1966). On the basis of test drilling it was found that the alluvium was more or less homogeneous and, therefore, it is believed that most probably the alluvium is not responsible for producing a gravity or a magnetic anomaly.

PART I : THE GRAVITY SURVEY

Accuracy of the Gravity Survey :

No geodetic survey was carried out to determine the elevations of the observation stations. However, the heights of the stations, on the natural ground surface were corrected by taking into consideration the surface, gradient of 1 ft./mile along NE-SW direction. The barometric altimeter was not used for height determination, firstly because of its overall low accuracy and secondly because the diurnal barometric variations were large and unsystematic. In case, where the observation was made on canal bank, higher than the natural ground surface, the corresponding height difference was taken into consideration for applying the Free-Air correction. The overall accuracy

* Geology Department, Panjab University, Lahore.

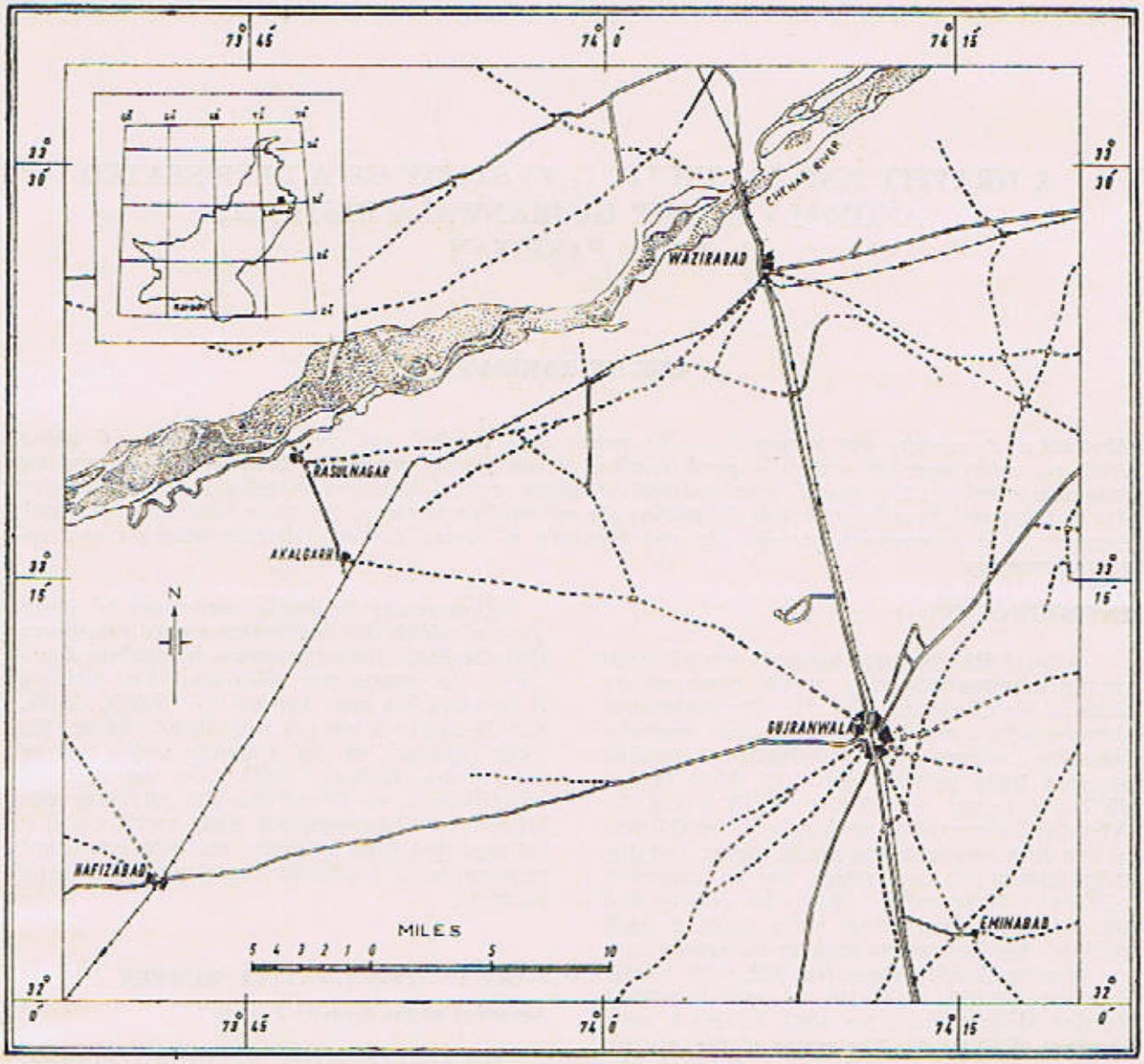

Fig. 1 The location map of the area.

of the vertical control achieved was of the order of ± 1 ft., which was better than the accuracy of the Worden Gravity Meter used in the present survey.

For horizontal control the milestones and the canal stones were taken into consideration. These horizontal distances were further checked by the milometer of the jeep, which was used during the survey. The accuracy of the horizontal control was better than ± 100 ft.

Considering the accuracy of the horizontal and the vertical controls, the drift of the instrument and the terrain correction, the accuracy of the gravity survey was better than ± 0.36 mgal.

Density Determination :

The geological evidences suggest that the underlying bed rock is an extension of the Aravallies. These are over-lain by the alluvial deposits of the Indus plain and outcrop as small

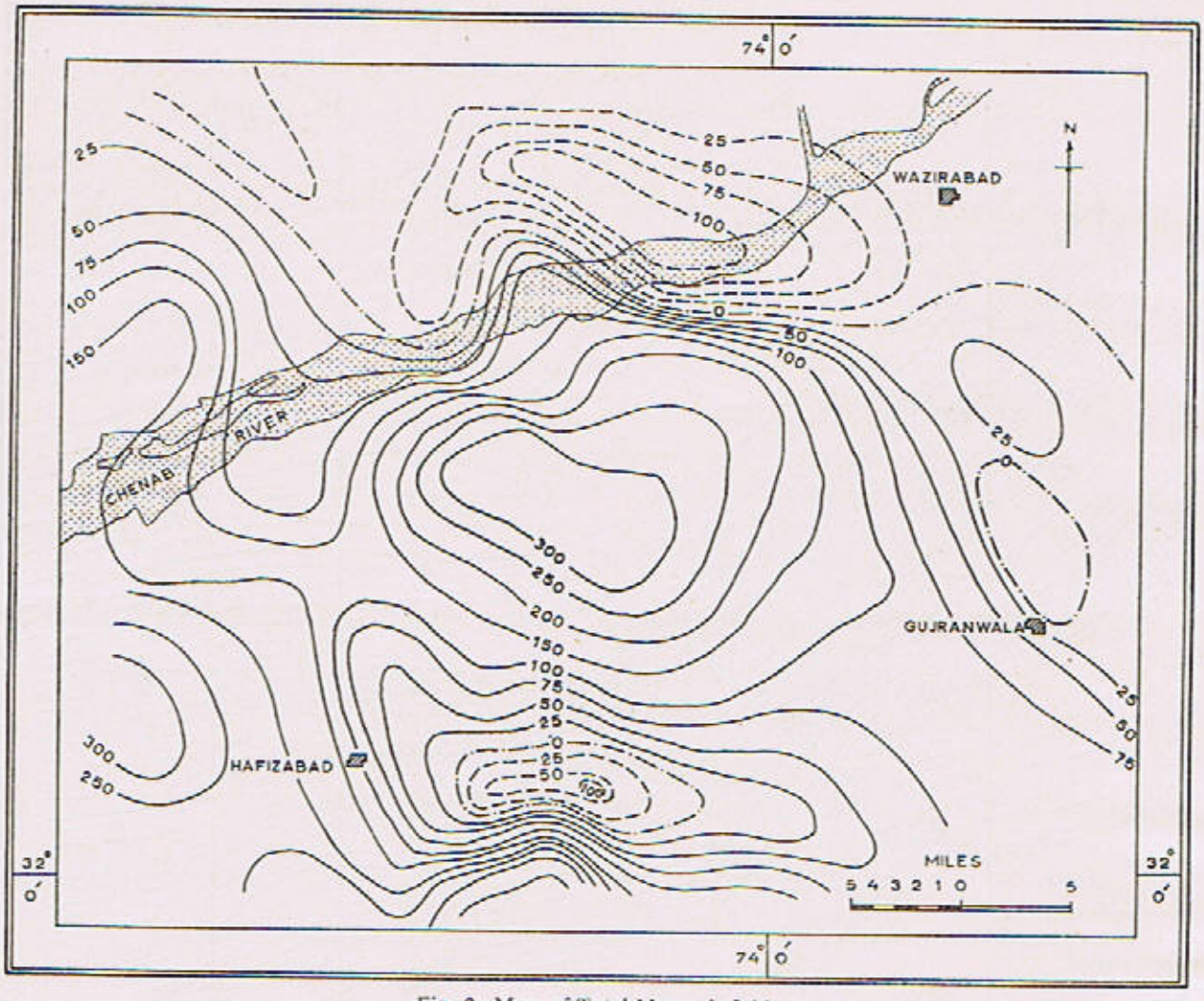

Fig. 2. Map of Total Magnetic field

hills near Sangla, Shahkot, Chiniot and Kirana (Wadia, 1961). For density determination, samples were collected from different localities, two in Sangla Hill and one in the Shahkot area. The specific gravities of the samples were determined by a Stanton-type balance. The specific gravity values of the samples are given below :

Table 1

No. of samples	Rock type	Average sp. gravity.
8	Baked quartzite	2.62
4	Unbaked quartzite	2.47
2	Quartzite	2.56
2	Garnet mica schist	2.61
3	Schistose quartzite	2.69
1	Quartz mica schist	2.55
2	Quartzose schist	2.70

The mean of the average sp. gravity data, thus calculated, was 2.60. Taking the average density of the alluvium to be 1.80 gm/cc, the density contrast came out to be 0.8 gm/cc. It was found, however, that the minimum density contrast considered most appropriate, by trial and error method, came out to be 1.00 gm/cc. This was perhaps due to increase in the density of the bed rock, under the alluvial overburden.

The Bouguer Anomaly Map of the Area :

The Gravity base at Wazirabad was connected to the base at Karachi International Airport by Dr. G. Norgaard in 1953 (Norgaard 1953). According to these values of observed gravity the Bouguer anomaly at Wazirabad was calculated to be −117.8 mgal with respect to the

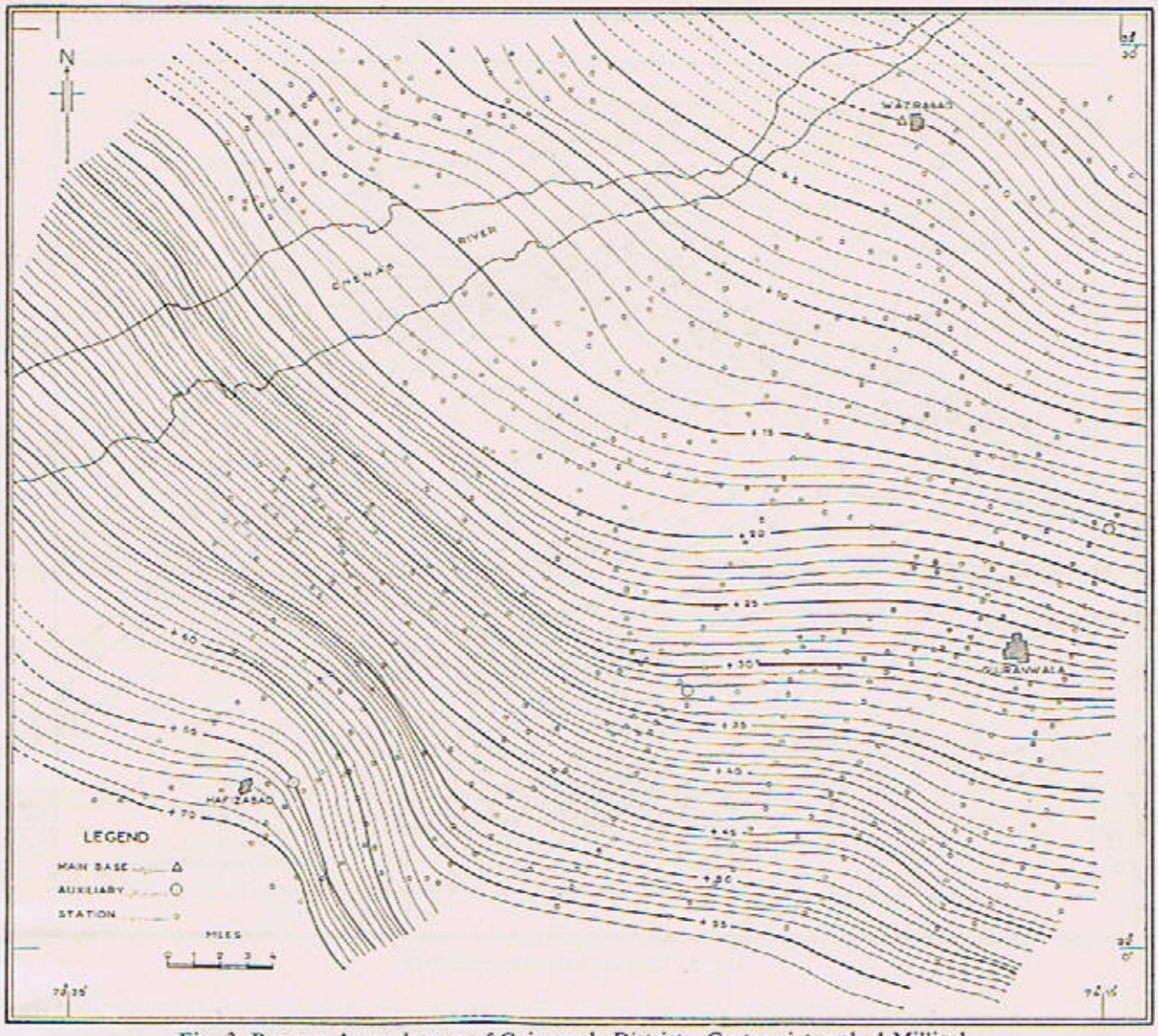

Fig. 3. Bouguer Anomaly map of Gujranwala District. Cantour interval : 1 Milligal.

Gravity Base at Karachi. The data of Karachi and Wazirabad bases are given below :

Gravity Base	Lat.	Elev. above sea level	Observed Gravity
Karachi Airport	24°54′	75 ft.	978963.0 mgal
Wazirabad	32°25′	740 ft. (approx.)	979376.4 mgal

Figure 3 shows map of the Bouguer anomaly, showing a gravity gradient in the NE-SW direction. The highest value of + 70 mgal was recorded near Hafizabad and the lowest value of −9 mgal appeared near Wazirabad; the highest and the lowest gravity values were separated by a distance of about 40 miles. From the SW to the NE regions of the map, *i. e.* in the direction of the Himalayan mass, a drop of 80 mgal in the gravity values has been recorded.

The value of the horizontal gradient of gravity was not constant throughout the area ; it was maximum in the north of Wazirabad, being 5 mgal/mile, and reduced in the north-eastern direction to a minimum value of 1.5 mgal/mile, recorded near Wazirabad. The contours in the region bounded by the isogals +20 and +10, in the central portion of the map, indicated a very low gradient *i.e.* 1 mgal/mile, which suggested the presence of a gravity low that was overshadowed by a strong regional effect.

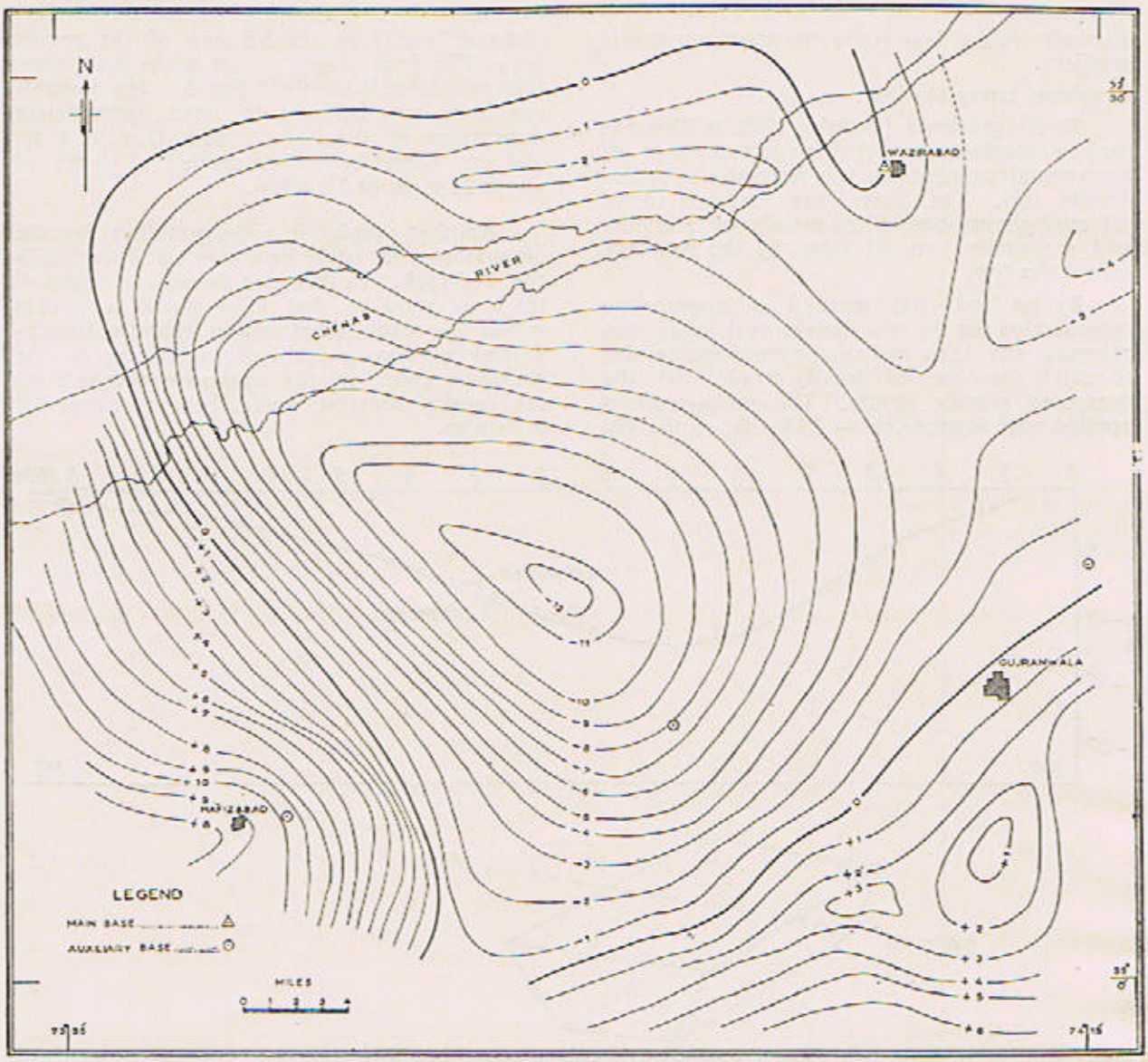

Fig. 4. Residual gravity Anomaly Map of Gujranwala District. Contour interval : 1 Milligal.

The residual gravity map of the area :

A residual gravity map (Fig. 4) was prepared after removing the regional effect from the Bouguer anomaly map. Since the contours in the Bouguer anomaly map were unidirectional, therefore, graphical method for removing the residual effect was employed (Dobrin, 1960) and the regional effect of 1.7 mgal/mile along the NE-SW direction, was removed. In the residual gravity map the contours resolved themselves into a well-defined negative anomaly, superposed on a smooth background. The magnitude of the anomaly was more than 40 times the maximum error of a single observation.

The close negative gravity anomaly was elongated in the NW-SE direction. The gravity gradient on the south-western side of the minimal trough was about 3 mgal/mile as compared to the average of 1 mgal/mile. The closed contouring of the map showed a localized geological feature at a depth corresponding to the depth of the bedrock. Applying formula of Bott and Smith (Parasnis, 1962, p. 52)

$$h \leqslant \frac{0.86 \triangle g\ max}{\triangle g'\ max},$$

the maximum depth of the anomalous body was calculated to be about 5.7 miles. In the formula $\triangle g_{max}$ is the maximum value of the

anomaly and $\triangle g'_{max}$ is the maximum horizontal gradient.

Graphical interpretation :

Skeel's graticule (Dobrin, 1960, p. 224) was used to calculate the probable size and shape of the anomalous mass that was responsible for this gravity low. The mass was assumed to be a trough-shaped body filled mainly by alluvium and surrounded on all sides by the bed-rock except the top.

By hit and trial method an appropriate cross-section for the two dimensional body was assumed and then end corrections were applied to match the observed gravity profile with the computed gravity profile. The end corrections applied were asymmetric — 35 k. ft. on the SW end and 70 k. ft. on the NE end of the profile XY. The final shape of the anomalous mass thus calculated is shown in Fig. 5. The anomalous body was believed to have approximate dimensions of 105 k. ft. × 80 k. ft. × 20 k. ft. and was considered to be buried at depth of about 22 k. ft. (4.23 miles).

Another probable interpretation for the anomalous mass could be a granitic intrusion in the bed-rock. In this case the size and mass of the body could be that of a pluton and thus would be many times bigger than the trough-shaped two-dimensional body considered in the previous case. In the case of a granite body the density contrast would be of the order of 0.2 gm/cc.

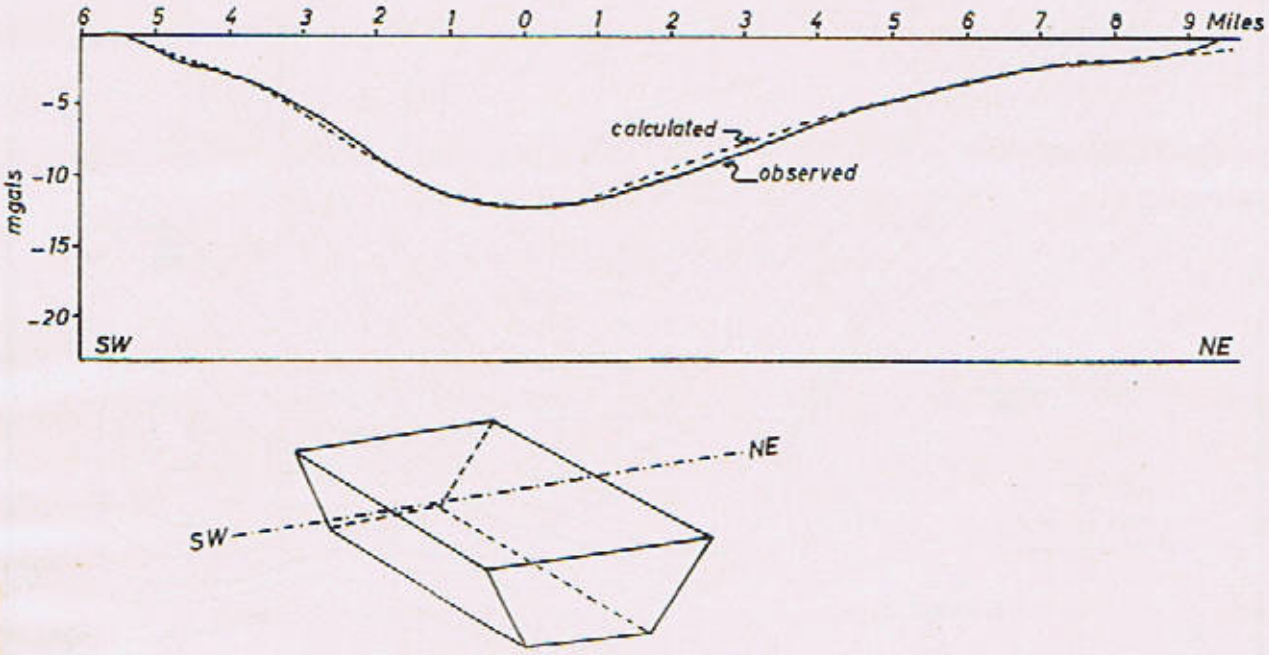

Fig. 5. Assumed 2-Dimensional Anomalous body.

Second derivative of gravity :

The residual gravity anomaly (Fig. 4) showed a classical example of an isolated geological feature buried under approximately 4 miles thick cover of alluvium. In order to confirm that the anomaly was due to some deep-seated mass-deficiency and to compare the results obtained from two different methods of second derivative, the second derivative analyses of the gravity field was carried out.

The double differentiation of the gravity field with respect to depth was accomplished by applying formulae of Elkin and Rosenbach which are based on a graphical analysis (Rosenbach, 1954). It was shown by Elkin (1951) that the second derivative methods used for three-dimensional bodies give correct results even when applied to two-dimensional features. Baranov's method (Baranov, 1953) of determining the vertical gradient of gravity was also applied to the data, and the results were compared with those of second derivative. The formulae used in the present analysis are given below :

1. $$gP \approx \frac{1}{s}\left\{ 23.0518\ g^{P} - 4.1587 \sum_{i=1}^{4} g_i^{A} + 0.6287 \sum_{i=1}^{4} g_i^{B} - 1.1165 \sum_{i=1}^{8} g_i^{C} \right\} \times 10^{-9}\ cgs$$ (Baranov)

2. $$g_{zz}^{P} \approx \frac{100}{62s^2}\left\{44\,g^{P}+4\sum_{i=1}^{4} g_i^{A}-3\sum_{i=1}^{4} g_i^{B}-6\sum_{i=1}^{8} g_i^{C}\right\}\times 10^{-15}\ cgs$$ (Elkins)

3. $$gP_{zz} \approx \frac{100}{24s^2}\left\{96\,g^{P}-18\sum_{i=1}^{4} g_i^{A}-8\sum_{i=1}^{4} g_i^{B}+\sum_{i=1}^{8} g_i^{C}\right\}\times 10^{-15}\ cgs$$ (Rosenbach)

In these equations s is the arbitrary distance in kms, this was taken to be 1.575 km, g^P is the Bouguer value of gravity at P in mgal and g^A , g^B and g^C are the values of gravity on the inner, the middle and the outer circles. These formulae are based on quadratic grid configuration.

Figure 6 shows the first derivative and figures 7 and 8 show the second derivatives of the gravity field. These three maps did not show any basic change w.r.t. the residual gravity map, however, few positive contours did appear in the Baranov's and Elkin's map. In these

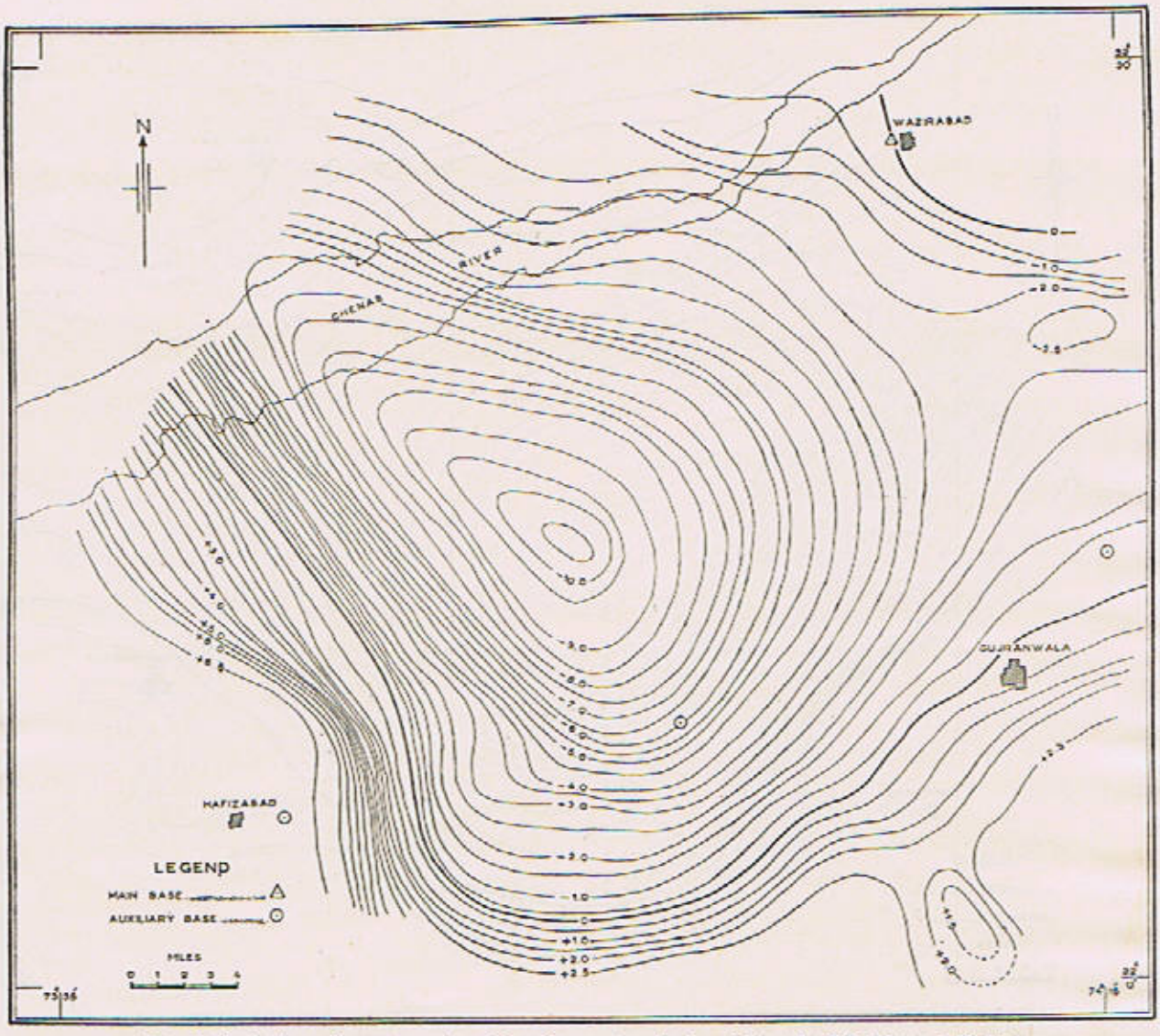

Fig. 6. Vertical gradient of gravity. (after Baranov). Contour interval : 0.5×10 c.g.s. Units.

maps the positive contours appeared in the NE and SE areas. The map due to Rosenbach's formula did not show any positive contours, however, there was an indication of positive values to be present in the SE part of the map. The positive closures mentioned above might have been caused due to an uplift in the basement rock. These closures could not be picked up in the map due to Rosenbach, because his formula is not so sensitive at greater depths as compared to the other two formulae. This might be due to a heavier weighting co-efficient for the inner circle as compared to the outer two, in the Rosenbach's formula. Elkin's formula is easy in its application and is lesser sensitive in shallower depths, its resolving power is also lesser than Rosenbach's formula. The weighting co-efficient of Elkin's formula is more important than the other factors, therefore it is more sensitive to the errors in the Bouguer gravity values. On the other hand it is less sensitive to errors in the mean gravity values around circles of the quadratic grid. Baranov's formula is rather difficult in its application and has very high weighting co-efficients. This is equally sensitive to the gravity values of the grid as well as to the mean gravity around a circle. (Baranov and Tassencourt, 1954).

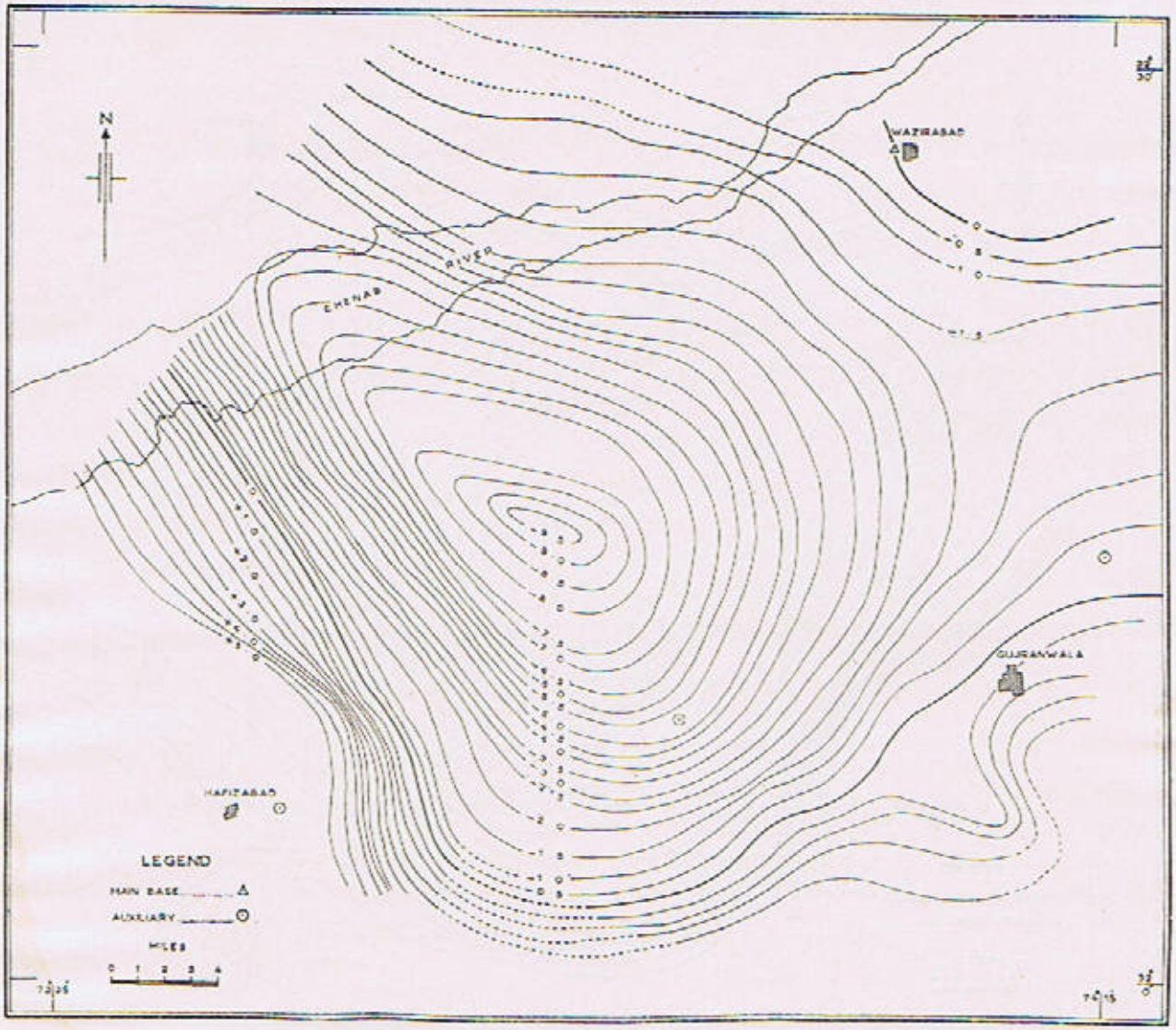

Fig. 7. Second derivative of gravity map. (after Rosenbach). Contour interval : 0.5×10^{-3} c.g.s. Units.

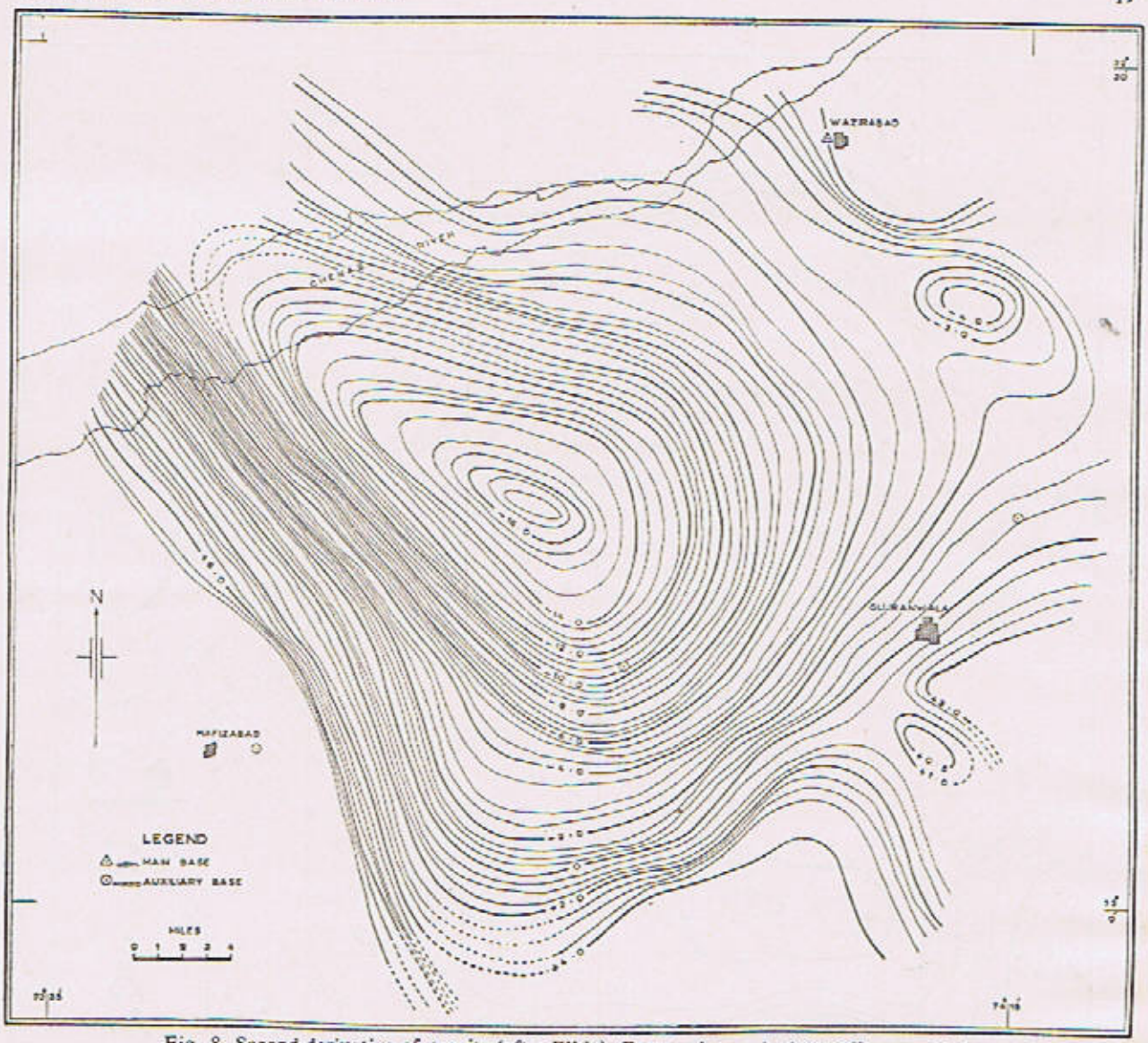

Fig. 8. Second derivative of gravity (after Elkin). Contour interval : 0.5×10^{-6} c.g.s. Units

PART II : THE MAGNETIC SURVEY

The aeromagnetic map (Fig. 1) shows a typical total magnetic anomaly over the area which was surveyed. In order to confirm this magnetic anomaly, a ground magnetic survey was conducted to measure the vertical magnetic intensity ($\triangle Z$). The observations were made at the same stations on which the gravity values were observed. Proper care was taken to carry out the survey on magnetically quiet days only. Normal correction of 21 γ/mile was applied to the observed data. No diurnal correction, which was expected to be very low, was applied. Contours showing equal value of $\triangle Z$ were drawn with 50 gamma interval (Fig. 9).

Interpretation of the magnetic anomaly

The axis of the negative and positive $\triangle Z$ anomaly was almost in the N—S direction, in the sense that the positive anomaly was lying to the north of the negative anomaly. The horizontal gradient of the vertical magnetic intensity was about 50 gamma/mile over whole of the area. To the south of both the positive and negative anomalies the values of the gradients were about 70 gamma/mile.

From the areal extension of the anomaly it appeared that, as in the case of the gravity anomaly, the probable source of the magnetic anomaly was also lying at a depth corresponding

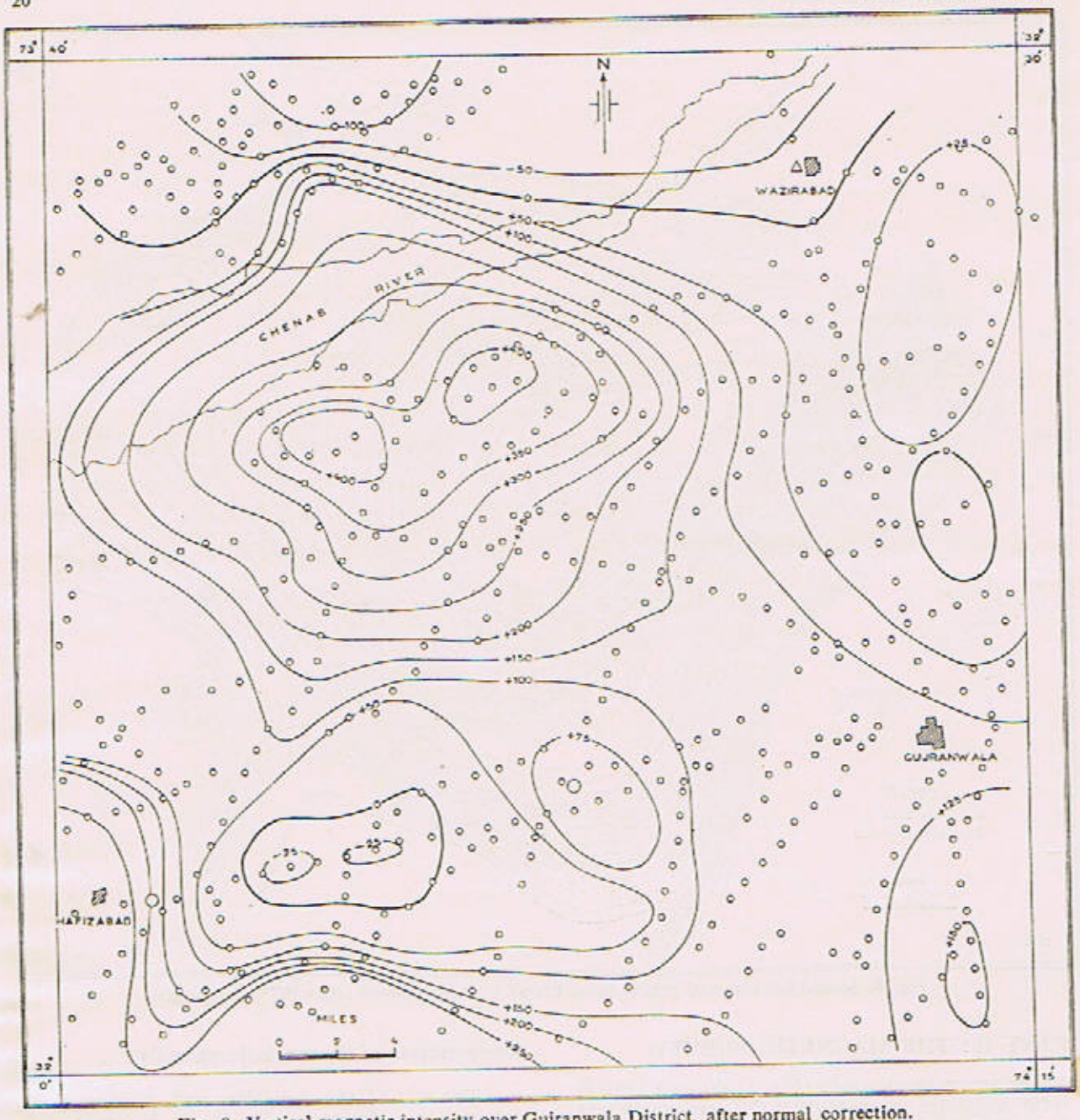

Fig. 9. Vertical magnetic intensity over Gujranwala District, after normal correction.

to the depth of the bed rock. It might also be just possible that the same body was causing both the gravity and magnetic anomalies.

The wide range of the magnetic susceptibilities of different rocks, and the direction as well as the magnitude of the remanent magnetization of rocks are the two major causes which make the interpretation of magnetic anomaly more ambiguous than even the interpretation of gravity anomaly. Thus, on the basis of a magnetic survey, it was practically impossible to find a unique solution of such a problem. Out of innumerable combinations of the variables, the following case was considered as an example :

Considering the anomalous body to be cylindrical (as a first approximation) with a radius of 5.5 k. ft., length of 50 k. ft. and

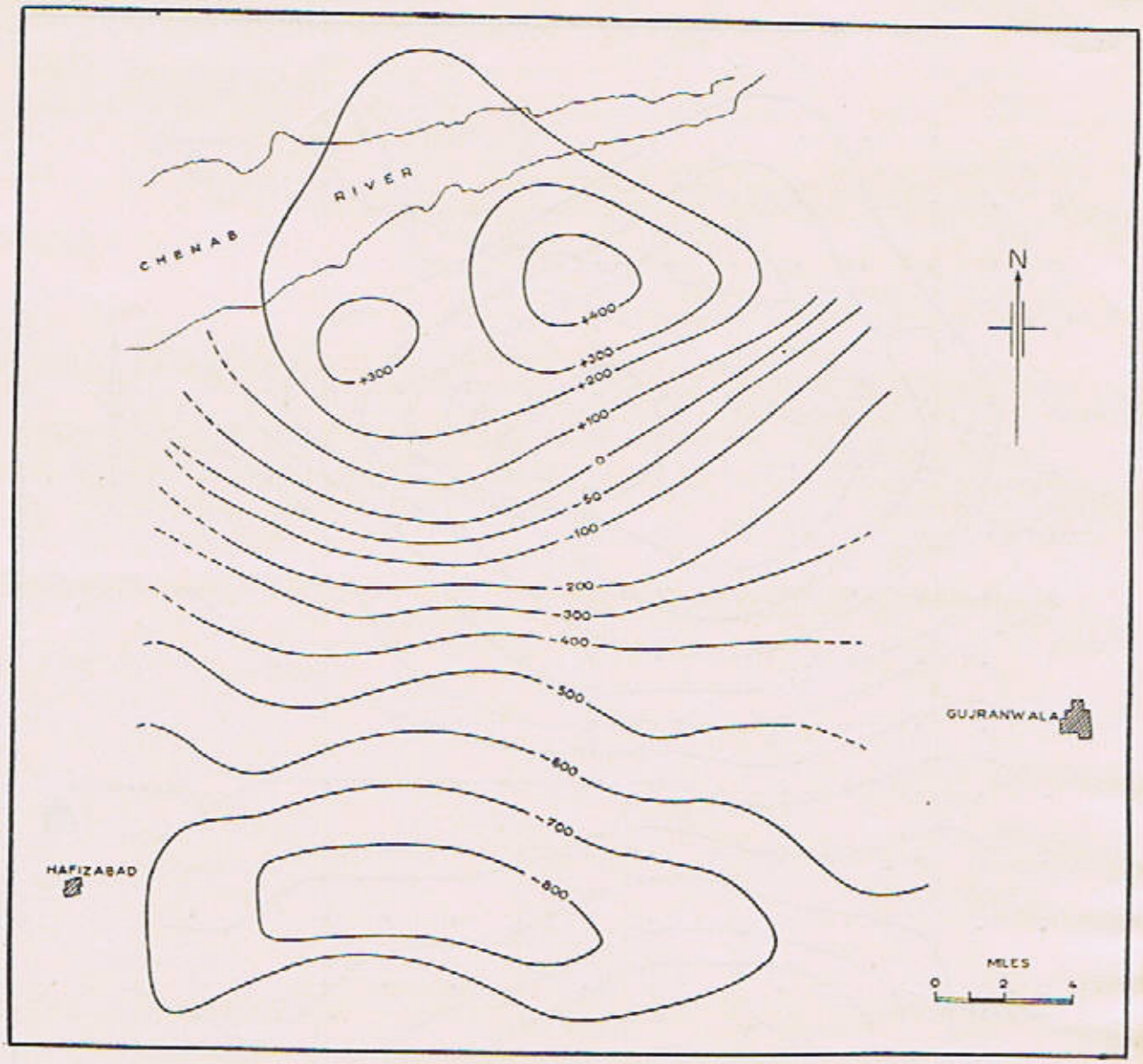

Fig. 10. Second vertical derivative of △T over Gujranwala District (Elkin's Formula). Contour interval 100×10^{-3} c.g.s. Units.

the intensity of magnetization to be 0.015 cgs units, the depth of burial came out to be 3.65 miles. This estimate of depth compared closely with the one which had been calculated for the body causing the gravity anomaly. These calculations were based on Peter's method (Dobrin, 1961). Accord to Smith's rule (Parasnis, op cit, p. 312) maximum depth of the anomaly came out to be 3.45 miles. These two results agree very closely and the mean of the two gave the probable depth of the anomalous body.

Second derivative of △Z

The formulae of Elkin and Rosenbach for the determination of second vertical derivatives for a vector field were applied to the data of △Z. The results are shown in Figs. 10 and 11. A comparison of these two maps with the map showing the vertical magnetic intensity (Fig. 9) revealed that there was not much difference between the contour pattern of these maps. Hence it was concluded that the cause of the

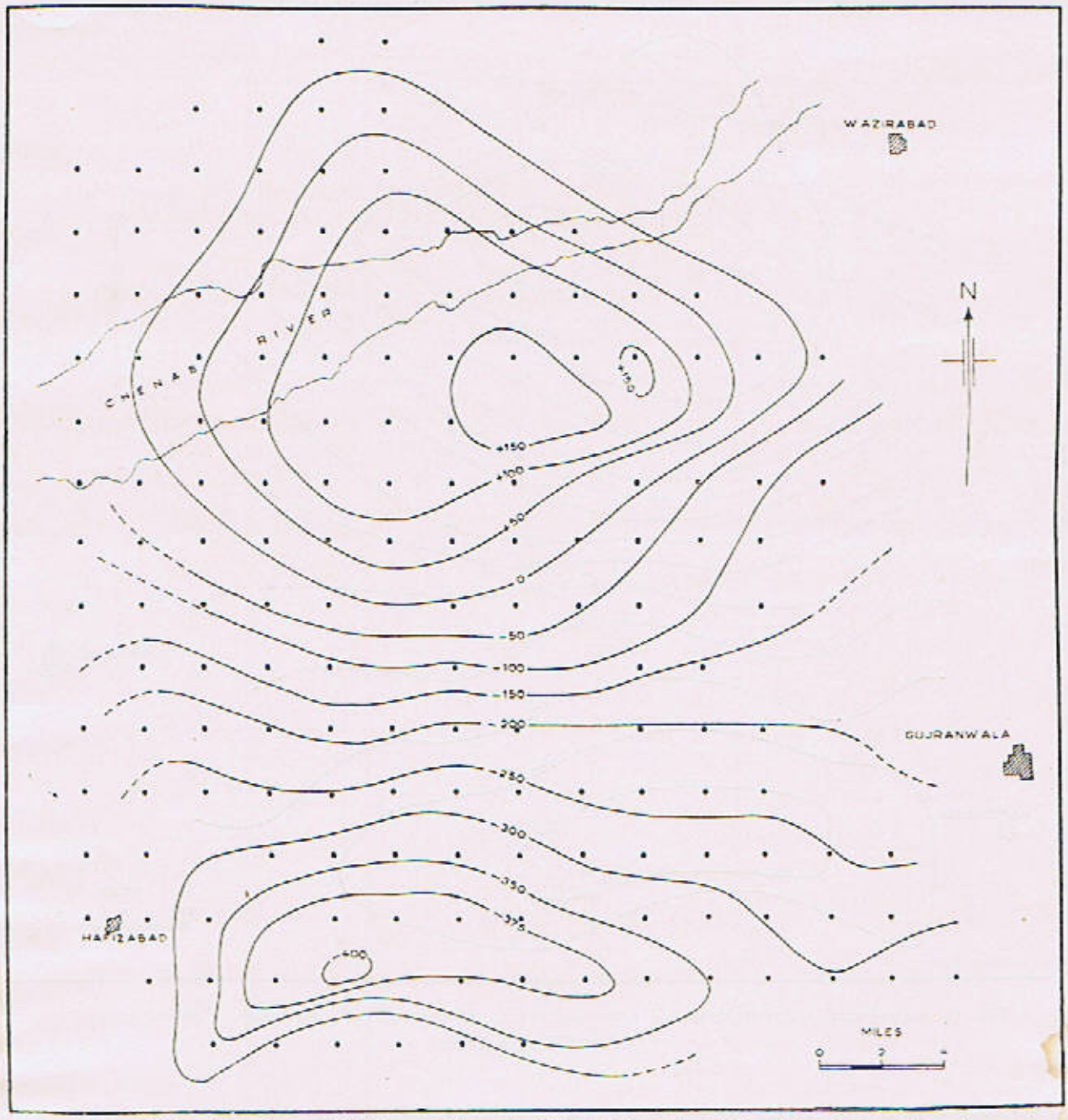

Fig. 11. Second derivative of △ T over Gujranwala District (Rosenbach's formula). Contour interval 50×10^{-3} c.g.s. Units

anomaly was lying at a greater depth and there was no anomalous feature lying at shallower depths.

Finally it must be emphasized that the knowledge of vertical derivatives does not reduce the fundamental ambiguity of interpretation of a gravity and a magnetic anomaly. The reason is that the derivatives are directly deduceable from the gravity or magnetic field and therefore do not contain any additional information not inherent in the original data.

CONCLUSION

It was found that the gravity and the magnetic anomalies were due to some deep-seated

cause, whose depth corresponded to the depth of the bedrock. The interpretation of the probable anomalous mass in terms of a trough-like depression in the bed-rock or a granitic intrusion in the Precambrian bedrock might not be considered as the unique solutions. In the absence of deep-drilling data in this area only refraction and reflection seismic methods could give some clue about the nature of the anomalous mass and its depth. A seismic survey in this area is strongly recommended.

ACKNOWLEDGEMENTS

The author is indebted to Prof. R. G. Davies, Department of Geology, University of the Panjab, for initiating the work. Grateful thanks are due to Mr. Ijaz Aziz for supervising the field work, and to the M.Sc. students, M/s Javid Durrani and Riaz Ahmad, who carried out the survey. Thanks are also due to Mr. Arshad, Geologic Illustrator, for redrawing various maps for publication.

REFERENCES

Abul Farah and Mohammad Ali 1964 *Rec. Geol. Surv. Pakistan* **11**, No. 2, 1-12.

Aeromagnetic map of Area 4A, Oil and Gas Development Corporation, Karachi. (Unpublished).

Baranov, V. 1953 Calcul du gradient vertical du champ de graviti ou du champ magnetique mesuri a la surface du sol. *Geophs. Prosp.* 1, 171-191.

.....and Tassencourt, J. 1954 Some remarks on the errors in the calculations. *Geophs. Prosp.*, **2**, No. 4, p. 285.

Dobrin, M.B. 1960 Introduction to Geophysical Prospecting. McGraw Hill Book Co. Inc.

Elkin, Thomas, A. 1951 The second derivative method of gravity interpretation. *Geophs.* **16**, 29-50.

Kidwai, Z. U. 1966 Personal Communication.

Norgaard, G., Abbas and Qudusi 1953 Gravity values in Pakistan. (Unpublished).

Parasnis, D.S. 1962 Principles of Applied Geophysics. London Methuen & Co., p. 52.

Rosenbach, O. 1954 Quantitative studies concerning the vertical gradient and second derivative method of gravity interpretation. *Geophs. Prosp.* **2**, 128-138.

Wadia, D. N. 1961 Geology of India. McMillan & Co. Ltd., London.

PALYNOLOGICAL BASIS FOR THE SUBDIVISION OF MIOCENE DEPOSITS IN BORE HOLES OF THE JALDI AREA, EAST PAKISTAN

BY

A. H. DZITIEV and SHAIKH M. AMIN*

Abstract : *The article gives results of palynological investigations of core material from bore holes of the Jaldi area. On the basis of defined spore-pollen assemblages it was possible to subdivide and correlate sections of the continental Miocene deposits, where the following formations were separated: Middle and Upper Bhuban, Boka Bil and Tipam.*

INTRODUCTION

The widespread continental Miocene deposits are significant in the stratigraphy and structure of the Chittagong Hill Tracts, East Pakistan. Their age is fixed conventionally by their comparison with similar deposits of the Upper Assam (India) and Burma. Their stratigraphic subdivision and correlation is, however, very difficult due to the following reasons :

(*i*) Miocene deposits are virtually devoid of marine fauna.

(*ii*) Within short distance, along their strike, these deposits undergo considerable lithological and facies changes with simultaneous variation in their thickness.

The subdivision and correlation of these Miocene deposits is considered very important because the present drilling for oil and gas is being conducted at Jaldi and Semutang structures in the Chittagong Hill Tracts. The solution to this problem has been provided by palynological investigations that have shown that, instead of marine organic remains, the Miocene deposits of East Pakistan contain rich spore-pollen assemblages.

The present investigation is based on the examination of 67 core samples from four bore holes of the Jaldi area, which have laid bare the geological section to a depth of 3360 m. The aims of palynological investigations were :—

(*i*) To trace vertical and horizontal variability of the plant kingdom in order to clarify the main transitional periods of development and extinction of flora and on this basis to subdivide and correlate well-section of the Jaldi area.

(*ii*) To make geological interpretation of the results obtained by palynological investigations.

TREATMENT OF SAMPLES

Two methods were used to extract spore and pollen from the rock samples :—

(*i*) The first method involved maceration of the rock sample with nitric acid and hydrofluoric acid and a later treatment with alkalies (NaOH, KOH).

(*ii*) The second method involved crushing of the rock to pea-size bits which were ground in acquous medium ; the solution was decanted and centrifuged in a heavy fluid.

Results obtained by the second method were very encouraging and spore and pollen were extracted invariably from more than 200 samples.

* Oil and Gas Development Corporation, Karachi.

SUBDIVISION OF THE JALDI SECTION

By tracing occurrence of individual genera and species of spore and pollen from bottom to top of the Jaldi section, a definite distribution pattern was recognized.

A particular palynological assemblage, confined to a definite horizon or a group, was found to have its own distinctive appearance and characteristic features.

On the basis of difference in their composition and quantity, 4 spore-pollen assemblages were defined and were made basis for subdivision of the Jaldi area cross-section.

THE ASSEMBLAGE I

It is defined in the interval 2600 to 3100 m. that marks the lowest level of drilled-in part of the Jaldi section.

The assemblage is confined to mudstones (sometimes called shales) that are dark-grey, hard and non-calcareous rocks with horizontal and oblique laminations and occasional lens-like streaks. Layers of light-grey and fine-grained sandstone are intercalated with mudstones ; the former are argillaceous in composition and are non-calcareous. The rocks of this horizon are highly compact, deformed and carry numerous friction planes ; the beds show variable dip upto vertical. The spore-pollen assemblage, extracted from these rocks, is poorly preserved and the grains show indications of effects that were suffered due to above mentioned geological processes.

The Filicales make predominant portion of this assemblage (up to 60%) with the most widespread being the small triradiate forms *Leiotriletes* Naum (25 %), *Matonia*, psilate *polypodium*.

The Gymnospermae comprise the next abundant component of this assemblage (upto 36%). These are represented mainly by *Pinus* and less commonly by grains of *Larix*, *Tsuga*, *Abies* and *Podocarpus*.

The Angiospermae make only upto 15% of the assemblage and show a rather restricted occurrence. The most frequently encountered forms are *Cyrilla barghoorniana* L., *Nipa*, *Magnolia*. The following forms may be defined as characteristic : *Leiotriletes* Naum., *Matonia* sp., *Matonia pectinata* R. Br., *Selaginellidites verrucosus* Cook et Pett., *Hymenophyllum asplenioides* Sw., *Pinus* subgen *Diploxylon*, *Tsuga pattoniana* Eng., *Pinus palustris* Mill., *Cyrilla barghoorniana* L., and others. The spore-pollen complex is illustrated in Plate 1. On the local geological scale the formation defined on the basis of assemblage I corresponds to the upper part of the Middle Bhuban with a drilled-in thickness of 627 m.

Immediately upwards (interval 1253 to 2600 m.), the lithological features of the Jaldi formation change. It is represented by an alternation of mudstones, siltstones and sandstones. The mudstones and siltstones are dark-grey in colour, hard, micaceous, non-calcareous and show horizontal and cross-lamination. The sandstones are grey-coloured, medium-grained, compact and non-calcareous rocks of homogeneous nature.

THE ASSEMBLAGE II

It is characterised by the predominance of Filicales (38-76%) over the Gymnospermae (15-40%) and Angiospermae (9-24%). This assemblage differs from the first one, due to a widespread occurrence of lycopods—*Selaginella granata* Bolch., *Lycopodium* sp.

The main back-bone in the composition of spores is provided by the representative forms of *Polypodium* genera (*Polypodium scouleri* Hook., *P. serratum* (Willd) Futo., *P. crassifolium* (L)., *P. punctatum* (L) Sw., and that of *Schizae* (*Schizaea fistulosa* Labill., *Schizaea dichotoma* (L) Sw.,). The most characteristic for this complex are the specimens of *Anemia* genera (*Anemia tricostata* Bolch., *A. mandioccana* Rud.

The occurrence of the Gymnospermae is indicated by the appearance of such species as *Araucaria schumaniana* Warb. A great variety of species is shown by Pinaceae—*Pinus* subgen *Diploxylon*, *P.* Subgen *Haploxylon*. Particularly flourishing is the genus *Tsuga*, which is an important index form for correlation. Angiospermae, the third important component in the complex, are characterised by the appearance of new genera and species such as *Betula*, *Corylus*, *Castanea*, *Myrica*, *Fagus*, *Juglans*, *Tilia*, *Alnus*, etc.

The following forms may be considered as leading :

Polypodium sp_1., *P. punctatum* (L) Sw., *P. serratum* (Willd) Futo., *P. scouleri* Hook., *Schizaea* sp_1., *Schizaea fistulosa* Labill., *Schizaea dichotoma* (L) Sw., *Anemia tricostata* Bolch., *A. mandioccana* Rud., *Matonia* sp_2., *Cyathea* sp_1., *Pinus* subgen *Haploxylon*, *P.* subgen *Diploxylon*, *Tsuga canadensis* (L) Carr., *Araucaria schumani-*

ana Warb., *Podocarpus nageiaformis* Zakl., *Betula* sp., *Corylus* sp., *Castania* sp., *Myrica* sp., *Fagus*, *Alnus*, *Tilia*, etc.

Side by side with spore and pollen, the fungal spores show a notable increase in the composition of their complex, (see Plate 2).

THE ASSEMBLAGE III

It is confined to deposits occurring in the interval 530 to 1250 m. Lithologically this interval shows an alternation of dark-grey, compact, non-calcareous mudstones and siltstones; the sandstones are subordinate in the section and are grey, fine-grained, homogeneous, loose and non-calcareous rocks.

The characteristic feature of this assemblage is the abundance in it of their species composition, particularly of certain species of Filicales. This gives a unique appearance to the whole complex, thus making it quite distinct from complexes of the underlying series and their assemblages. However, there is a considerable amount of species common with the Upper Bhuban which, probably, indicates their close relation in time. Nevertheless, this assemblage has its own peculiarities, such as :

(*i*) All the three classes—Filicales (48%), Gymnospermae (45%) and Angiospermae (40%)—play almost an equal part in its composition.

(*ii*) Fungal spores are extremely widespread in the complex and their content is upto 60%.

(*iii*) Simultaneously with quantitative increase of spore and pollen grains, there is an increase in their species contant as well. For instance, instead of the well-sculptured *Polypodium* spores, which were distinct in the underlying horizons, the leading part in this complex is taken by *Polypodium* spores with psilate surface (exine) and of small size. A similar conformity is shown by the representatives of Pinaceae also which exhibit changes in the nature of their air-sacs reticulum. Among these the appearance of such species is noted as *Keteleeria*, *Cedrus*, varieties of *Abies* and *Pinus*.

The Angiospermae in this assemblage are enriched by pollen grains, previously encountered either in single grains or not at all. These include *Juglans* sp., *Juglans polyporata* Vojc., *Ulmus*, *Engelhardtia vallichiana* Linde., etc. Following are the leading forms: *Selaginella granata* Bolch., *Lycopodium trigonium* K-M., *Polypodium aureum* L., *Matonia pectinata* R.Br., *Pinus peuce* Grisech., *Pinus* of section *Omarica* Willkm., new species of *Abies*, *Cedrus*, *Keteleeria*, *Picea*, *Juglans* sp$_1$., *Juglans polyporata* Vojc., *Ulmus*, *Engelhardtia wallichiana* Lind., *Liliacidites variegatus* Couper., *Acer* sp., *Betula americana*., Waet., *Corylus*, *Pterocarya*, *Palmae*, *Nipa*, *Magnolia*, etc.

The assemblage III corresponds to Boka Bill formation, with a thickess of 720 m.

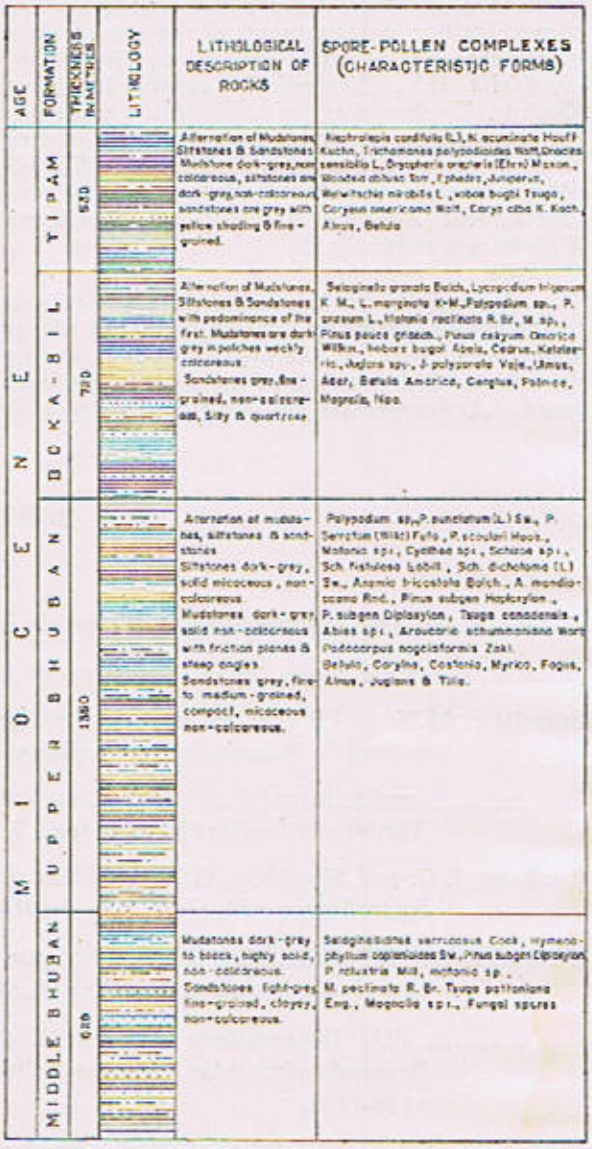

Fig. 1. COMPOSITE GEOLOGICAL AND PALYNOLOGICAL SECTION OF WELLS JALOI AREA

THE ASSEMBLAGE IV

It is characterised by an almost equal content of Filicales (17-45%) and Gymnospermae (18-40%). In the upper portion of the section, the lithological varieties remain unchanged and the section is composed of alternating mudstone and siltstone beds with subordinate sandstone.

The relationship between the Filicales and the Gymnospermae groups of plant remains is such that, down the section (interval 350 to 530 m.) while the significance of Filicales gradually increases that of the Gymnospermae on the contrary drops. Among spores the leading position is still that of *Polypodium* genus, which shows further development of species. There is appearance of such species as *Nephrolepis cordifolia* (L)., *Nephrolepis acuminata* Houff Kuchn., *Trichomanes polypodioides* Watt., *Onoclea sensibilis* L., *Dryopheris immersa* (Bb Kutze, *Dryopheris oreopteris* (Ehrh) Maxon., *Woodsia obtusa* Tanr., etc. In the pollen part of complex appear *Ephedra*, *Hyptostrobus*, *Juniperus*, *Welwitschia mirabilis* L.

Although the angiospermae were subordinate to the gymnosperms and spores, yet they played a significant part in the plant kingdom, during the period of deposition of the interval investigated. Angiospermae are characterised by high content of Betulacea, widespread occurrence of *Corylus*, *Carya alba* K. Koch., *Carypha australis* K. Br., *Alnus*, *Corylus americana* Watt, etc. The assemblages contain high quantity of pollen grains of uncertain systematic affiliation.

CONCLUSION :

The composite geological and palynological cross-section of the Jaldi area, based on results of the present investigations, is given in Fig. 1.

It should be mentioned, that the palynological assemblages defined in the present investigation cannot remain constant, these will be supplemented and confirmed with the treatment of new material from adjacent areas. However, even in their present stage these may be used as reliable guides for correlation.

The palynological investigations of core material from the Jaldi area as well as other areas of East Pakistan have shown, that it is quite possible to subdivide and correlate the continental Miocene deposits on the basis of spore-pollen assemblages which are confined to them The biostratigraphical basis for the subdivision and correlation of barren strata of East Pakistan will undoubtedly assist in the solution of many a practical problems of stratigraphical correlation.

BIBLIOGRAPHY

Bouché, P. M. 1962 Nannofossiles tertiaires du Bassin de Paris. *Somm. Soc. Fr.* **4** 106.

..... 1962 Nannofossiles calcaires du Lutétien du Bassin de Paris. *Rev. Micropal.* **5**, 75-103.

Bramlette, M.N. and Riedel, W. R. 1954 Stratigraphic value of Discoasters and some other microfossils related to Recent Coccolithophores. *Journ. Pal.* **28**, 385-403.

..... and Sullivan, F. R. 1961 Coccolithophorids and related Nannoplankton of the Early Tertiary in California, *Micropal.* **7**, 129-188.

Cookson, I. C. and Singleton, G. P. 1954 The preparation of transluscent fossils by treatment with hydroflouric acid, *Geol. Soc. Australia, News Bull* **2**.

Deflandre, G. 1947 Braarudosphaera nov, gen. type d'une famille nouvelle de coccolithophoridés actuels á éléments composites, *Acad. Sci., C. R.*, **225**, 439-441.

..... 1950 Observations sur les Coccolithophoridés, à propos d'un nouveau type de Braarudosphaeridae Micrantholithus, á éléments clastiques, *Acad. Sci. C. R.* **231**, 1156-1158.

Gorka, H. 1963 Coccolithophoridés, Dinoflagelles, Hystrichosphaerides et Microfossiles incertae sedis du Crétacé supérieur de Polonge. *Acta Pal. Polonica* **8**, 1-24.

Kamptner, E. 1949 Fossile Coccolithineen—Skelettreste aus dem Molukken—Archipel, *Osterr. Akad. Wiss., Math. Naturwiss, Kl., Anz.* **86**, 77-80.

Lohmann, H, 1902 Die Coccolithophoridae, eine Monographie der Coccolithen—bildenden Flagellaten, *Archiv. Protistenk* **1**, 89-165.

Martini, E. 1959 Pemma angulatum und Micrantholithus basquensis, zwei neue Coccolithophoriden—Arten aus dem Eozän, *Senckenbergiana Leth* **40**, 415-421.

Schiller, J. 1930 Coccolithinae. In : Rabenhorst, L., *Kryptogamen Flora*, Leipzig **10**, 89-267.

Tan Sin Hok 1927 Over de Samenstelling en het ontstaan van Krijt en mergelgesteenten van de Molukken, *Mijnw. Ned. Oost-Indie, Jarb.* (1926), 1-165.

Plate I

(All Figures ×280)

Figure 1	...	Selaginellidites Verrucosus Cook & Det.
Figure 2	...	Hymenophyllum asplenioides Sw.
Figures 3—6	...	Leiotriletes Naum.
Figures 7—8	...	Matonia pectinata R. Br.
Figures 9—10	...	Matonia sp_1.
Figure 11	...	Pinus subgen Diploxylon.
Figure 12	...	Tsuga pattoniana Eng.
Figure 13	...	Keteleeria sp.
Figure 14	...	Pinus palustris Mill.
Figures 15—16	...	Tsuga sp.
Figures 17 & 19	...	Pinus sp.
Figure 18	...	Podocarpus sp.
Figure 20	...	Gingko sp.
Figures 21 & 24	...	Indeterminate.
Figures 25—26	...	Magnolia sp.
Figures 27 & 30	...	Liquidambar sp.
Figure 31	...	Williamsonia peeten Carr.
Figure 32	...	Cycaditus sp.
Figure 33	...	Betula sp.
Figure 34	...	Pterocarya sp.
Figure 35	...	Carya sp.
Figure 36	...	Cycadeoidae.
Figure 37	...	Algae.
Figure 38	.	Diatomaceae.

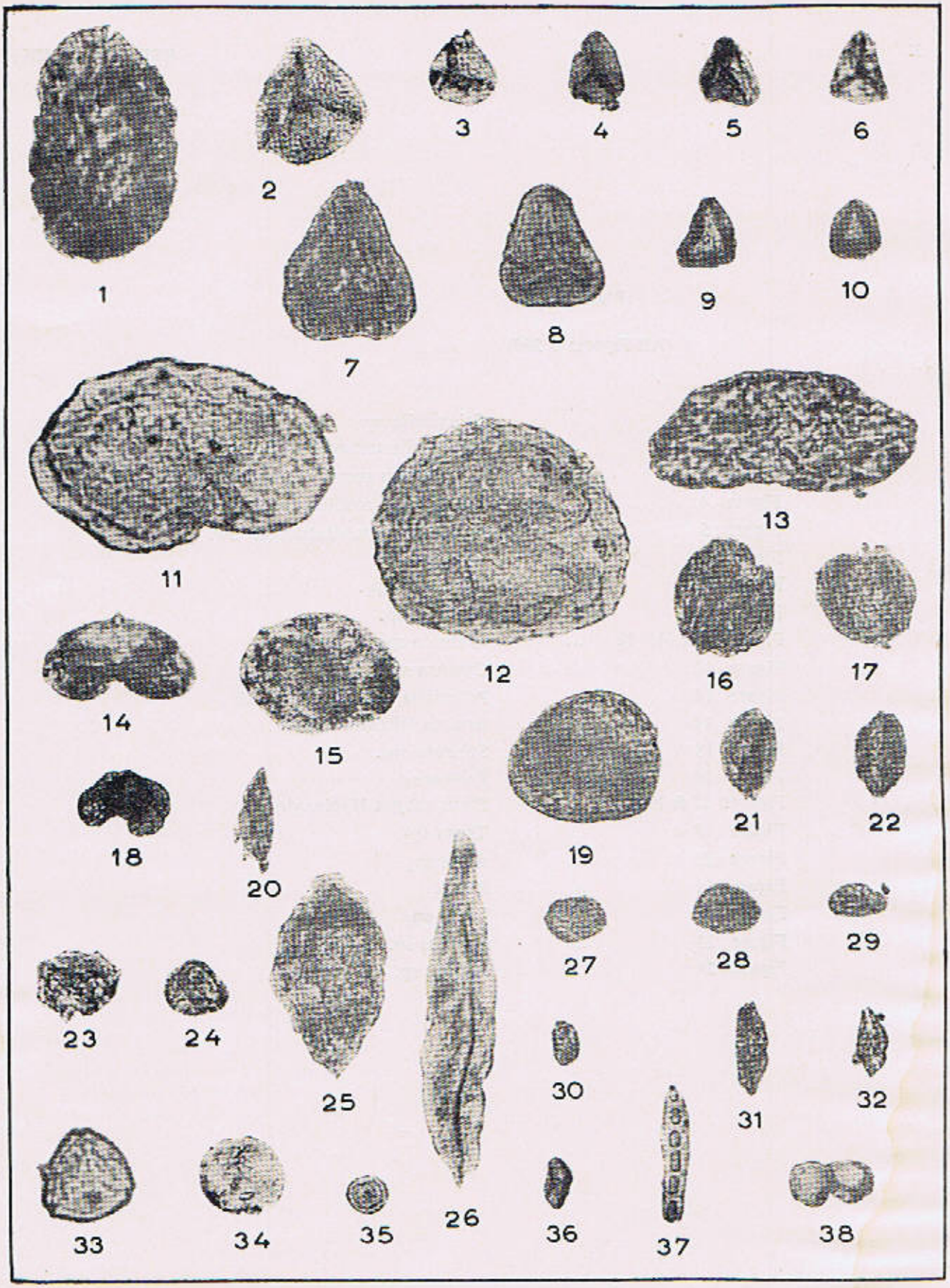

Geol. Bull. Panj. Univ. no. 6 Plate 1

Plate II

(All Figures ×280)

Figure 1	...	Selaginella sp.
Figure 2	...	Selaginella tuberculata Bolch.
Figure 3	...	Polypodium serratum (Willd) Futo.
Figure 4	...	Polypodium scouleri Hook.
Figure 5	...	Polypodium punctatum (L) Sw.
Figure 6	...	Cyathea sp_3.
Figure 7	...	Dicksonia sp_1.
Figure 8	...	Matonia sp.
Figures 9 & 11—12	...	Matonia sp_2.
Figure 10	...	Cyathea sp_1.
Figure 13	...	Pelletieria medostriata Bolch
Figure 14	...	Anemia tricostata Bolch.
Figure 15	...	Schizaea sp_1.
Figure 16	...	Palmae sp.
Figures 17 & 19	...	Pinus subgen Haploxylon.
Figure 18	...	Tsuga sp_2.
Figure 20	...	Abies sp_1.
Figure 21	...	Algae.
Figure 22	...	Tsuga sp_1.
Figure 23	...	Quercus sp.
Figure 24	...	Juglans sp.

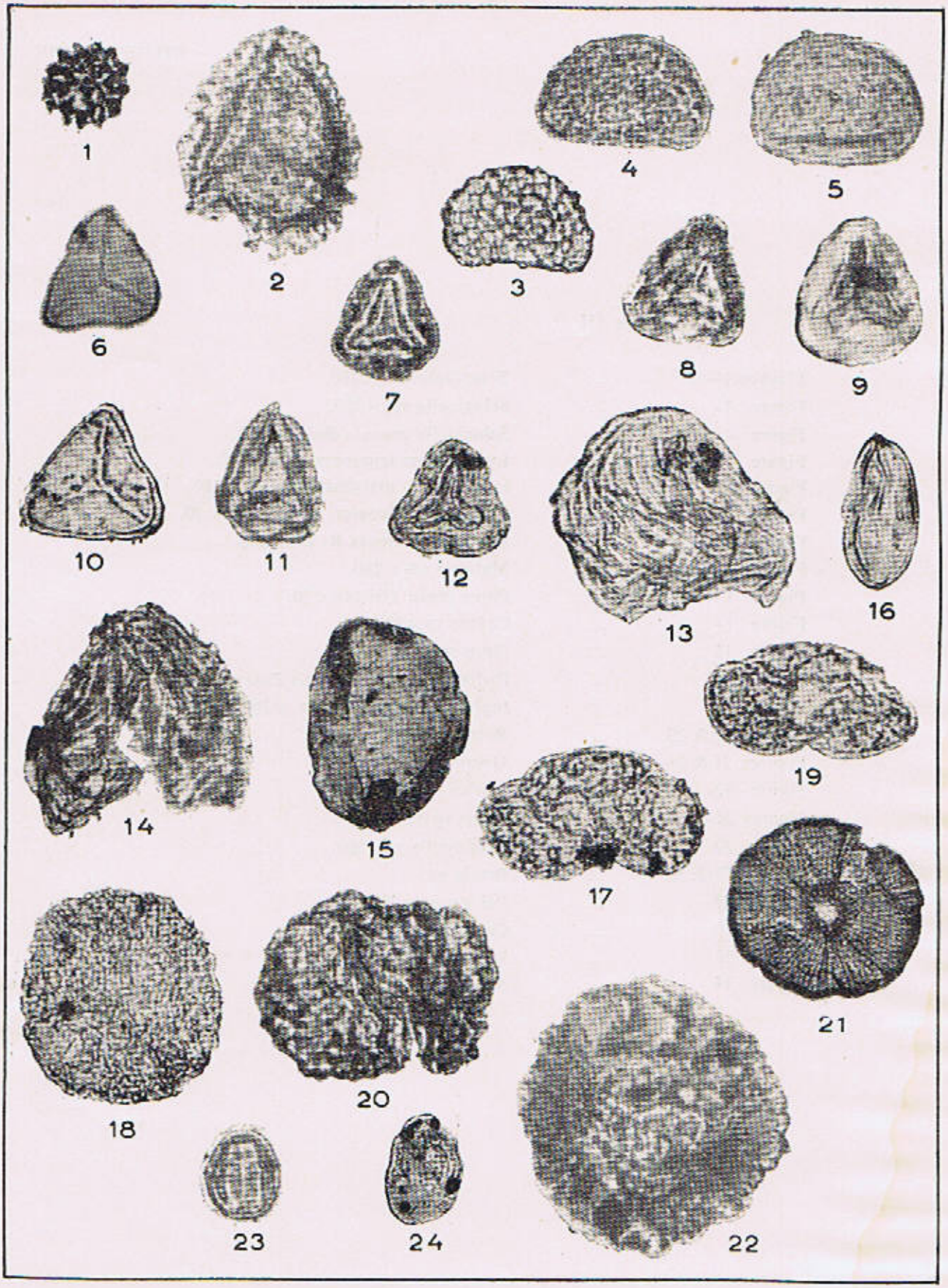

Geol. Bull. Panj. Univ. no. 6 Plate 2

Plate III

Figures 1—2	...	Selaginella $sp_1 \times 280$.
Figure 3	...	Selaginella $sp_2 \times 280$.
Figure 4	...	Selaginella granata Bolch $\times 280$.
Figure 5	...	Lycopodium trigonum K-M $\times 280$.
Figure 6	...	Lycopodium marginatum K-M $\times 280$.
Figures 7—8	...	Polypodium Scouleri Hook $\times 280 \times 70$.
Figures 9—10	...	Matonia pectinata R. Br. $\times 280$.
Figures 11—12	...	Matonia $sp_3 \times 280$.
Figure 13	...	Pinus peuce Grisech $\times 70$.
Figure 14	...	Cedrus sp $\times 280$.
Figure 15	...	Pinus sp $\times 70$.
Figure 16	...	Podocarpus nageiaformis Zakl $\times 280$.
Figure 17	...	Juglans polyporata Vojc. $\times 280$.
Figures 18 & 20	...	Betula americana $\times 560$.
Figures 21 & 24—25	...	Quercus sp $\times 560$.
Figure 22	...	Myrica sp.
Figures 26—27 & 31	...	Alnus sp $\times 560$.
Figure 23	...	Trudopolis sp $\times 560$.
Figures 28 & 33	...	Betula sp.
Figure 29	...	Palmae sp $\times 70$.
Figure 30	...	Corylus sp. $\times 560$.
Figure 32	...	Magnolia sp $\times 70$.
Figure 34	...	Acer $\times 560$.

Plate IV

Figure 1	...	Selaginella $sp_3 \times 280$.
Figure 2	...	Acrostichum axillare Cav. × 560
Figure 3	...	Nephrolepis acuminata Houff. Kuchm × 560.
Figures 4—6	...	Dryopteris immersa (BL) Kuntze × 560.
Figure 7	...	Adiantum sp × 560.
Figure 8	...	Polypodiaceae (Acrostichum axillare Cav) × 560.
Figure 9	...	Dicksonia $sp_5 \times 280$.
Figures 10—11	...	Schizaea $sp_2 \times 280$.
Figures 12—15	...	Pinus subgen Diploxylon × 280.
Figure 16	...	Palmae sp × 280.
Figure 17	...	Betula sp × 560.
Figures 18—22	...	Corylus americana Walt × 560.
Figure 19	...	Castanea sp × 560.
Figures 20—21	...	Carpinus japonica Benme × 560.

AN ESTIMATION OF TEMPERATURES OF FORMATION OF SOME GRANITIC ROCKS OF THE MANSEHRA-AMB STATE AREA, NORTHERN WEST PAKISTAN, AND ITS BEARING ON THEIR PETROGENESIS.

BY

F.A. SHAMS AND FAZAL-UR-REHMAN*

Abstract : *Temperatures of formation of some granitic rock of the Mansehra-Amb State area, have been estimated on the basis of mineralogical reactions and transformations, and by Barth's method of two-feldspar geothermometry. The estimated temperatures range from 580° to 670°C and therefore are in the range of granitic magmas both as products of differentiation as well as that of anataxis.*

INTRODUCTION

The Mansehra-Amb State area, about 600 square miles in extent, makes the crystalline core of a major syntaxial loop of the northwest Himalayas. The area (Fig. 1) consists of pelitic to psammitic schists and quartzites, which have suffered Barrovian-type regional metamorphism upto the kyanite grade. These rocks occur as continuous belts that bound a large granitic complex—The Hazara Granitic Complex. Basic minor bodies cut the entire area sporadically. A preliminary account of the geology of the area was published by Shams (1961) while the petrochemistry of the granitic complex has been discussed by Shams and Fazal-ur-Rehman (1966).

On the basis of field relations, the granitic complex can be subdivided as below :

(*i*) Older Gneiss-Granite Members :

This group consists of gneissic (Susalgali gneiss) to granitoid rocks (Mansehra granite and the andalusite-bearing granite) and the associated acid minor intrusives, such as pegmatites, aplites and rare porphyry bodies.

(*ii*) Younger Tourmaline-bearing Granite Members :

This group consists of granitoid rocks (Hakale granite, Karkala granite, Sukal granite etc.) and the associated acid minor intrusives such as pegmatites and aplites.

The field and laboratory investigations, to be published elsewhere, have shown that the granitic complex does not represent material of entirely foreign origin ; rather it represents portions of pre-existing metamorphic rocks that suffered regional granitization. Comparison of chemistry of the granitic and the metamorphic rocks of the area has shown that granitization involved addition essentially of lime and soda, alongwith regional recrystallization. The nature of the chemical changes are well brought out in a Brammell projection based on normative recasting of the analyses, which also shows that the trend of progressive granitization, exhibited by the Mansehra-Amb State area, is comparable to complexes of similar nature that have been described from some other parts of the world.

There could be atleast two ways in which the addition of necessary material had taken place ; through the agency of magmatic fluids or low temperature hydrothermal fluids. The possibility of solid diffusion is not considered favourable. In order to decide between magmatic and metasomatic granitization, an estimation of temperatures prevalent during formation of the granitic rocks is thought to be atleast one of the important criteria.

* Department of Geology, Panjab University, Lahore.

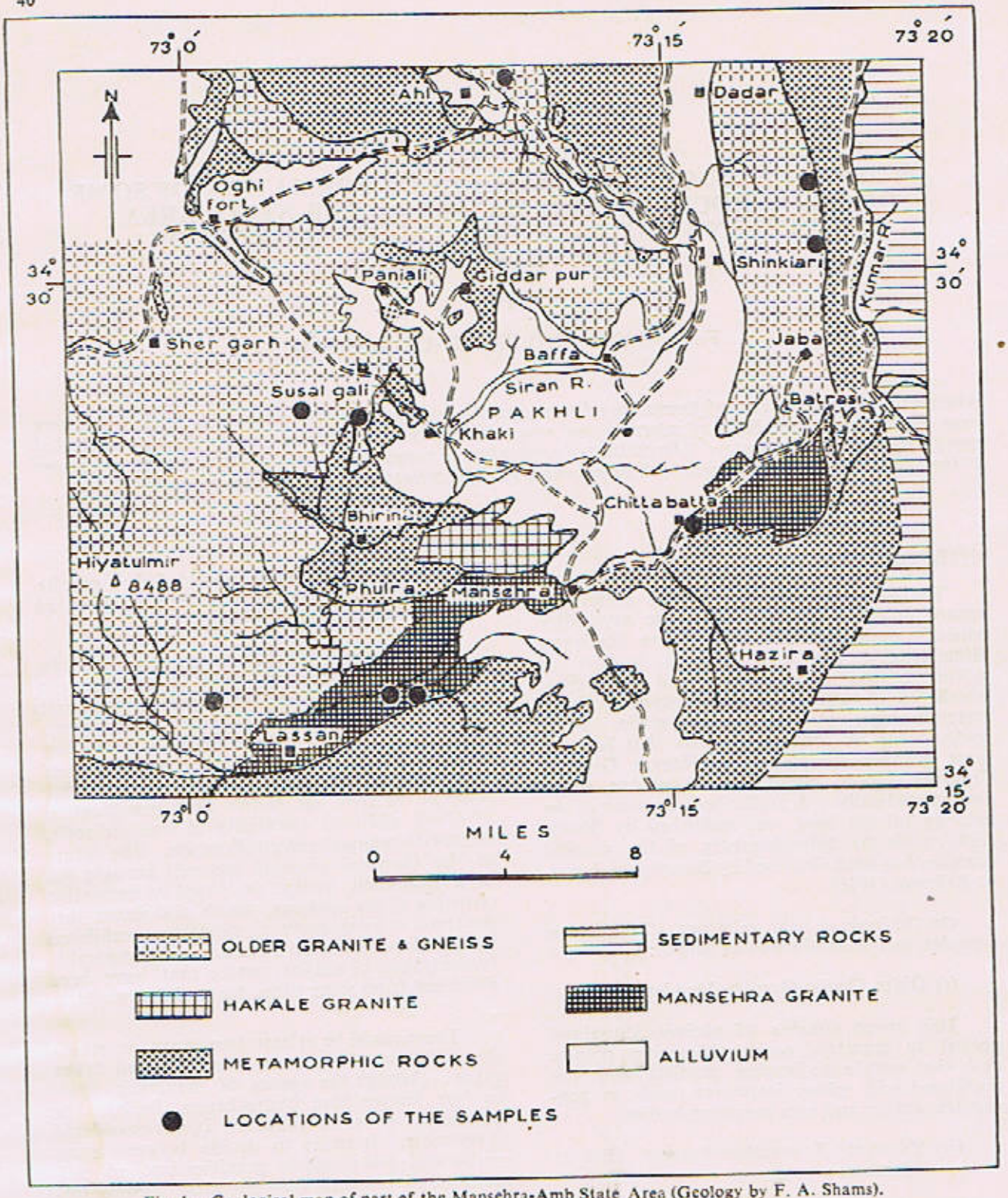

Fig. 1. Geological map of part of the Mansehra-Amb State Area (Geology by F. A. Shams).

ESTIMATION OF TEMPERATURES

There are many methods in vogue :

(*a*) The decrepitation method : It is applied to the fluid inclusions in minerals and quartz is considered to be the most suitable material for this study. However, in the present case, this method is not considered to be very suitable, firstly, as the method is applicable up to temperature levels

around 500°C only and secondly, the petrographic evidence shows that most of the quartz of the granitic rocks was derived from the pre-existing metamorphic formations.

(*b*) Mineralogical reactions and transformations :

There is evidence of the following phenomena of interest :

(*i*) Reaction : Muscovite+quartz= Al.Silicate+Orthoclase+Water

Evidence, that this reaction took place, is seen in the hornfelsed schists, the andalusite granite and in certain xenoliths. According to Segnit and Kennedy (1961), in geological environments, this reaction should take place between 650° and 750°C.

(*ii*) Transformation : andalusite=sillimanite :

The evidence of this transformation is seen in the hornfelsed schists, the andalusite granite and in certain xenoliths.

Although the entire field of the system Al_2Si0_5 has not been explored experimentally, yet on the basis of data available (Bell, 1963 ; Clark, 1961) and the geological and thermodynamical considerations (Miyashire, 1960 ; Thompson, 1955), an appreciable understanding has been achieved.

The lower limit of the p, t conditions for this transformation, is shown by the triple point which lies in the range (Pitcher and Flinn, 1965) :

t=300° to 450°C.
p=4 to 8 kilobars

If the pressure is assumed to be of a purely hydrostatic nature, then a depth of 15 to 30 km. is indicated. Although, the presence of a sedimentary (or a meta-sedimentary) cover of some intermediate thickness was not improbable, it is thought that tectonic forces could also have contributed significantly in building up the regional pressures.

(*iii*) Cordierite genesis and breakdown :

Two varieties of cordierite are known to occur in nature-hydrous and anhydrous ; the latter being formed at high temperatures. The variety that formed in the Mansehra-Amb State area, was most probably an hydrous one. However, as no unaltered cordierite could be found, it was not possible to estimate the water content, although, the mineral is known to contain only 2.7 to 2.9% of water (Deer, et al., 1962).

The hydrous cordierite has been synthesized by Schreyer and Yoder (1960) at 600°C. and 1200 bars water vapour pressure. Above 750°C., only the anhydrous cordierite is formed, whatever is the pressure of water vapour so that the temperatures prevalent during formation of this mineral, in the Mansehra-Amb State area, must have been lower than 750°C, say around 700°C.

(*c*) Two-feldspar Thermometry : The basis of this method (Barth, 1956) is that the distribution of albite molecule between co-existing plagioclase and alkali feldspar is a function of the temperature at which the fildspar phases are formed within a common medium.

TABLE NO. 1

Chemical Data and Estimated Temperatures of Crystallization of Feldspar Pairs.

Rock No.*	6451	6447	6553-A	7556	7214	7457-B	6738	7776	7557
wt.% of :									
Na_20	2.97	2.79	3.72	3.59	3.50	3.41	2.57	2.32	2.79
K_20	9.54	11.98	10.05	9.54	10.95	10.95	11.32	7.75	9.40
mol% of :									
albite	34.86	25.34	34.78	35.11	31.26	30.88	24.85	29.84	29.78
k-feldspar	65.14	74.66	65.22	64.89	68.74	69.12	75.15	70.16	70.22
albite% of the associated plag.	90	84	90	91	83	82	84	89	89
distribution ratio (K_t)	0.387	0.301	0.386	0.386	0.377	0.376	0.296	0.355	0.354
estimated temperature (Centigrade)	670°	585°	670°	670°	660°	660°	580°	620°	620°

*These numbers refer to the catalogued collection of the Deptt. of Geology, Panjab University, Lahore.

Alkali feldspars from 9 granitic rocks of random distribution (Map 1) were hand-picked, cleaned and analysed by flame photometer for soda and potash ; the oxide values were converted into the respective feldspar molecules. The percentage contents of albite molecule in the associated plagioclase feldspars were estimated by the universal stage method. From this data K_t, the distribution ratios of the albite molecule, were calculated and the temperature of formation of each pair of feldspar phases was determined from the determinative curve of Barth (loc. cit., p. 15). The entire data is given in Table No. 1 and projected on feldspar diagram in Fig. 2.

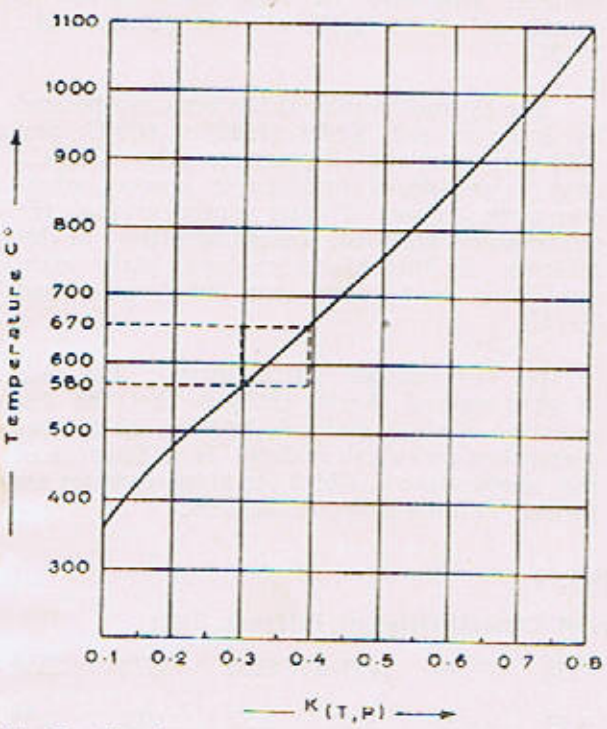

Fig. 2. Showing range of plotted positions on the Barth's curve ; based on data given in Table I.

The range of the estimated temperatures lies between 580° and 670°C.

DISCUSSION

The range of temperatures, estimated on the basis of above considerations, lies between 450°C. ($Al_2 Si0_5$ transformation) and 700°C. (muscovite+quartz reaction).

In nature, these reactions can be influenced by a number of factors. For instance, Waston (1948) has shown that, in addition to inversion from another aluminium silicate polymorph, sillimanite can grow through the agency of metasomatizing fluids as well. Furthermore, the aluminium silicate formed, as a result of reaction between muscovite and quartz, could be andalusite as well as sillimanite ; this being the case in the Mansehra-Amb State area. According to Harker (1939), muscovite breakdown should always yield andalusite, while Ramberg (1952) has suggested that this is possible only at lower pressures and that sillimanite will develop instead at higher pressures. In the inner aureole hornfelses of the area under study, sillimanite is formed in preference to andalusite. It appears that, in this case, an increase in temperature was the dominant factor rather than an increase in pressure.

The phase equilibrium between feldspar pairs of the plutonic rocks could also be affected during the post-crystallization period. This may happen in response to falling temperature, or due to tectonic deformation. These factors may have operated in the Mansehra-Amb State area and might be responsible for the somewhat lower range of geothermal temperatures, estimated on the basis of feldspar equilibrium, as compared with those estimated from mineralogical considerations. From the above considerations, it is concluded that temperatures in the range of 600° to 700°C. were prevalent during formation of the granitic complex. These temperatures are known to be in the range of granitic magmas both as products of differentiation (Tuttle and Bowen, 1958, p. 121) as well as that of anataxis (Winkler and von Platen, 1961).

REFERENCES

Barth, Tom. F.W. 1956 Studies in gneiss and granite. *Skr. Norsk. Videns. Akad. I. Mat. Nat. Kl.* No. **1**, 1-34.

Bell, P.M. 1963 Aluminium silicate system : Experimental determination of the triple point. *Science* **139**, 1055-1056.

Clarke, S.P. Jr. 1961 A redetermination of equilibrium relations between kyanite and sillimanite. *Amer. Journ. Sci.* **259**, 641-650.

Deer, W.A. et al. 1962 Rock Forming Minerals. vol. I, Longmans, London.

Harker, A. 1939 Metamorphism. 2nd Ed. Methuen, London.

Miyashiro, A. 1960 Thermodynamics of reactions of rock-forming minerals with silica, Part IV, Decomposition reactions of muscovite. *Japan Journ. Geol. Geog.* **41**, 113-120.

Pitcher, W.S. 1965 The aluminium silicate polymorphs, *In* Controls of Metamorphism. Ed. Pitcher and Flinn, Oliver and Boyd, Edinburgh and London, 325-341.

Ramberg, H. 1952 The Origin of Metamorphic and Metasomatic Rocks. Univ. Chicago Press.

Segnite, R.E. and Kennedy, G.C. 1961 Reactions and melting relations in the system muscovite-quartz at high pressures. *Amer. Journ. Sci.* **259**, 280-287.

Shams, F.A. 1961 A preliminary account of the geology of the Mansehra area, District Hazara, West Pakistan. *Geol Bull. Panjab Univ.* No. **1**, 57-62.

..... and Rehman, F. 1966 Petrochemistry of the granitic complex of the Mansehra-Amb State Area, Northern West Pakistan. *Journ. Sci. Res. Panjab Univ.*, **1**, 47-55.

Thompson, J.B. Jr. 1955 The thermodynamic basis for the mineral facies concept. "*Amer. Journ. Sci.*" **253**, 650-103.

Tuttle, O.F. and Bowen, N.L. 1958 Origin of granite in the light of experimental studies in the system $NaAlSi_3O_8$-$KAlSi_3O_8$-SiO_2-H_2O. *Mem. Geol. Soc. Amer. No.* **74**.

Watson, J. 1948 Late sillimanite in the migmatites of Kildonen. *Geol. Mag.* **85**, 149-162.

Winkler, H.G.F. and Platen, H. von 1961 Experimentelle gesteinmetamorphose—V. Experimentelle anatektischeschmelzen und ihre petrogenetische bedentung. *Geochem. Cosmochem. Acta.* **24**, 250-259.

THE OCCURRENCE OF COCCOLITHS AND RELATED FORMS IN THE LAKI AND RANIKOT FORMATIONS FROM SARI, WEST PAKISTAN

BY

SHAIKH M. AMIN*

Abstract: *Six genera and eighteen species of Coccoliths and related forms are described from the Palaeogene deposits encountered in Sari Test well-1, from the depth interval* 1160 *to* 1440 *metres.*

Four of the species recorded appear to be new. The commonly occurring forms are Discolithus and Coccolithus. A marine tropical environment is thought to have prevailed during formation of these deposits.

INTRODUCTION

In the course of palynological studies on the core-amples, obtained from Sari Test Well-1, which is located about 50 miles north-east of Karachi, fairly rich assemblages of nannofossils (coccoliths and related forms) were isolated from rocks of the Laki and Ranikot formations that are of Lower Eocene and Palaeocene ages respectively; the rocks were obtained from the depth interval 1160 to 1440 metres. This is the first time that nannofossils from Pakistan are being described.**

Nannofossils are planktonic unicellular algae with calcareous shells. They were first recorded in 1836 by Ehrenberg, from the Tertiary rocks of Germany but they received serious attention only after 1930 when it was realized that they can be useful in solving stratigraphical problems. However, the main development came after 1954, with the discovery of large number of such fossils in the Cainozoic sediments of Europe, North Africa, and the U.S.A. Since then, they have received great attention as, due to their limited vertical ranges, they are of great stratigraphic value.

CLASSIFICATION

Nannofossils have been classified by Deflandre (1950) on the basis of their morphological characters into the following main groups.

Group A Heliolithae (2 Families)

Family A) Syracosphaeridae Lohmann 1902 (3 Genera)

Family B) Coccolithidae Lohmann 1902 (2 Genera)

Group B Ortholithae (2. Families)

Family A) Brasrudosphaeridae Deflandre 1947 (2 Genera)

Family B) Discoasteridae Tan Sin Hok 1927 (2 Genera)

MACERATION OF SAMPLES

The maceration of samples was carried out by the hydrofluoric acid, as follows:—

(*a*) 3 grams of powdered sample was taken in polythene beaker and 200

* Oil and Gas Development Corporation, Karachi.

** See Haq, this No., p. 55.

c.c. of 20% HF-acid was added and the material was thoroughly stirred. The sample was left for about 2 hours in acid.

(*b*) HF-acid was removed, as much as possible, with the help of a siphon and then distilled water was added to the sample to dilute the remaining HF-acid. The process of dilution was continued till a p_H value between 6 and 7 was obtained.

(*c*) The sample was stirred and left for 10 to 15 minutes. With the help of a pipette 1 to 2 drops from middle of the suspension were taken over the cover slip, dried over an electric heater and mounted on slide with the help of 1 to 2 drops of Canada Balsam.

METHOD OF STUDY

Two slides* from each sample were examined under compound microscope N. AY-26 with magnification x 20. All photos were taken using normal light and with magnification x 40.

SYSTEMATIC DESCRIPTION

Group: Ortholithae Deflandre 1950

Family: Braarudosphaeridae

Genus: *Braarudosphaera* Deflandre 1947. Gran and Braarud.

Braarudosphaera bigelowi Gran and Braarud 1935, pl.1, Figs. 1-6.

Pentagonal in shape, having 5 crual units. Every unit is more or less trapezoidal and strongly united with each other but separate and independently orientated. A small rounded cavity is present in the centre. When the microfossils are examined under normal light all the five units have same appearance, while using the polarised light two units become dark in colour.

Size: 13-14 Microns.

Family: Discoasteridae

Genus: *Discoaster* Tan Sin Hok 1927.

Discoaster barbadiensis, pl. 1, Fig 7.

Circular in shape, with 8 arms which are more or less fused with each other. The distal faces are free and round. A small cavity is present in the centre.

Size: 12 Microns.

Discoaster lenticularis Bramlette and Sullivan 1961, pl. 1, Figs. 8-9.

Circular in outline with two zones; small central circular zone and outer serrated zone. The ridges are radial and longitudinal, 16 to 20 in number.

Size: 10 Microns.

Discoaster elegans Bramlette and Sullivan 1961, pl. 1, Figs. 10-12.

This species is very similar to *D. barbadiensis*. Each arm is narrow and elongated when observed from the concave face. If the same spacies is observed from the opposite side, each arm is divided into 4 to 5 equal segments by transversal furrows. The arms are also angular.

Size: 8 Microns.

Discoaster binodosus Martini 1959, pl. 1, Figs. 13-14.

Circular in outline, with 8 arms which are separated at the apex while united at the base. Each arm has bulbous-like swelling at the distal face.

Size : 12 Microns.

Discoaster brouweri Tan Sin Hok 1927, pl. 1, Figs. 15-18.

Asterolith with six as well as five rays are common in Lower Miocene. Central part has small knob-like structure with thin and elongated 5 to 6 arms (rays), tapering towards the end.

Size : 14 Microns.

Discoaster exilis Martini 1959, pl. 1, fig. 19.

Asterolith with 6 rays central area with small knob, which is stellate. The long and slender rays have slightly notched ends.

Size : 15 Microns.

* All slides are preserved in Palynological branch of G. & A. Lab. of OGDC, Karachi.

Discoaster Sp. 1, pl. 1, fig. 20.

Asterolith with large central portion, circular in outline, having eight long and slender rays tapering towards the distal end. A small cavity is present in the central disc. This species differs from other described species of this genus in having eight arms.

Size : 11 Microns.

Discoaster sp. 2, pl. 2, Fig. 21.

Asterolith with large central disc and eight knob-like rays. A small rounded cavity in the centre. This species can be distinguished by the club-shaped arms.

Size : 11 Microns.

Discoaster sp. 3, pl. 2, Figs. 22-23.

Asterolith with large central disc having a small cavity in the centre. The disc has 14 to 16 medium size rays which are slightly tapering towards the outer end.

Size : 16 Microns.

Group : Heliolithae Deflandre 1950

Family : Coccolithidae Lohmann 1902

Genus : *Coccolithus* (Schwarz 1893) Kamptner 1956.

Cyclococcolithus leptoporus (Murray and Blademan 1928 Kamptner 1954) pl. 2, figs. 30-32.

A large central opening with 2 to 3 circular bands. The outer band is larger than inner.

Size : 9 Microns.

Coccolithus danicus (Brotzen), pl. 2, figs. 36-37.

The species has two closely appressed elliptical plates with sigmoid curving cross bars spanning the nearly central opening. Striae at the rims show sinistral curvature from the distal side.

Size : 9 Microns.

Coccolithus aff. pelagicus (Wallich) Schiller 1930, pl. 2, figs. 42-43.

The species is oval in outline and has two elliptical discs which are united by large and thick intermediate cylinder. There is a big cavity in the centre.

Size : 7 and 8 Microns.

Coccolithus sp. 1, pl. 2,figs. 44-45

Circular in outline having a large central cavity, which is surrounded by elliptical plates and is divided into 4 segments by two septa, one radial and one transversal.

Size : 8 Microns.

Coccolithus sp. 2, pl. 2, figs. 35, 47-48.

Circular to oval in outline, single central cavity is surrounded by 2 to 3 circular bands.

Size : 7-8 Microns.

Family : Syracosphaeridae Lohmann 1902

Genus : *Discolithus* Kamptner 1946

Discolithus Pulcher Deflandre, pl. 2, figs. 38 and 41.

Elliptical or oval in outline. The rim, which is more or less thick, is perforated by radial fissures, the central portion has two pores which are separated by a thick transversal septum.

Size : 7 Microns.

Genus : *Zygolithus* Kamptner 1949.

Zygolithus erectus : Deflandre 1954, pl. 2, fig. 46.

Oval in outline, the species is divided into two equal halves by transversal septa.

Size : 6 Microns.

Discolithus cf. numerousa (Gorka), pl. 2, fig. 50.

This species has wavy outline and perforated central part. The striae are not visible at the rim.

Size : 10 Microns.

During the studies of nannofossils, microforaminifera and the spicules (Triradiatus) of sponges were frequently found. These are illustrated in pl.2, figs. 24 and 29.

PALAEOECOLOGY

The Core sample No. 1 (play No. NF 101) from the Laki formation from 1160.20 to 1164. 24 m. interval was very rich in microfossils as compared to other samples and yielded most of the described types. The core samples No. 2 to 5 (Play. No. NF 102 to 105 respectively) from 1185 to 1238.5 m. interval were also fairly rich in fossils. From the habitat and occurrence in abundance of nannofossils it may be concluded that at the time of deposition a

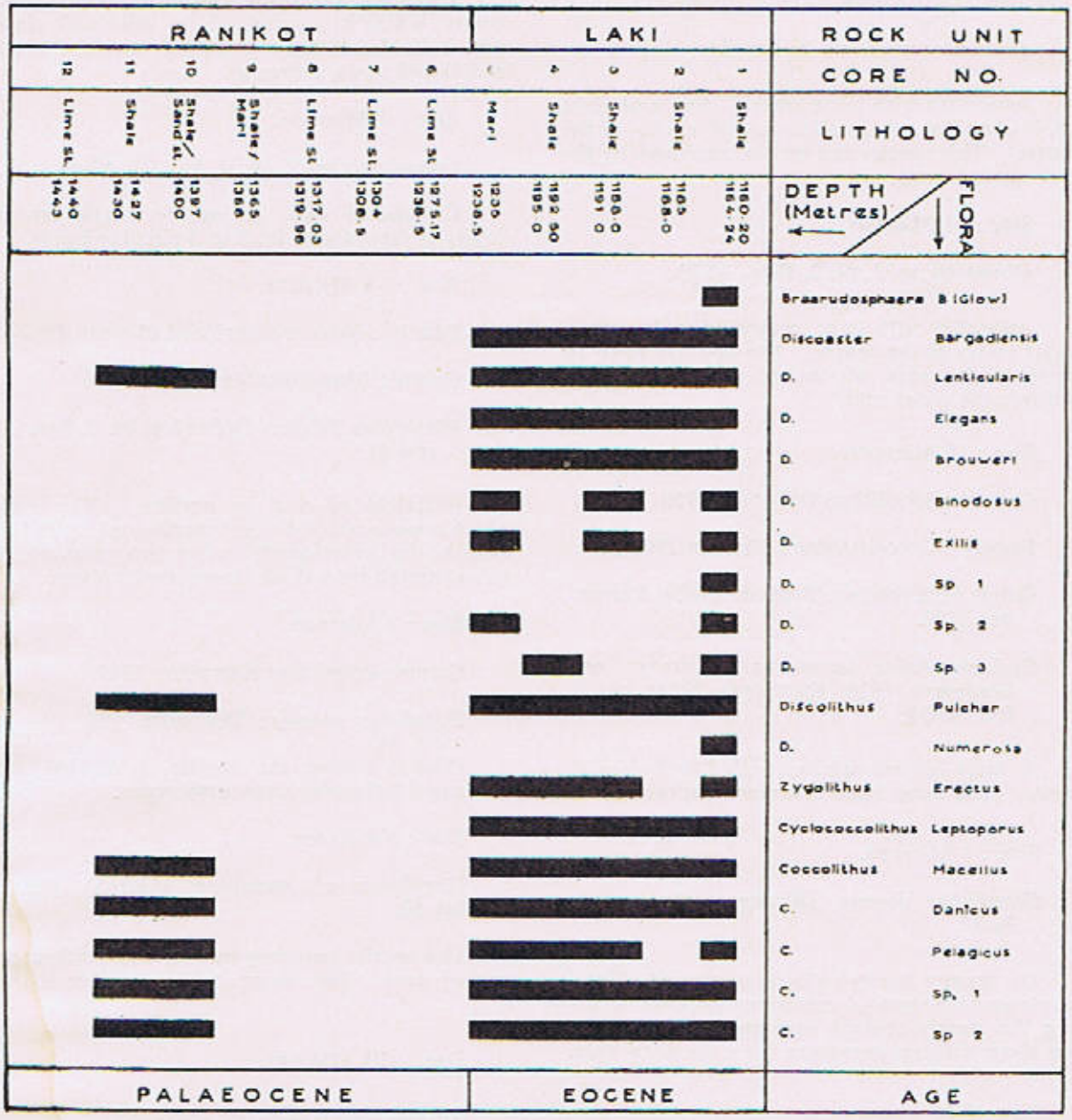

Fig. 1 Range chart of Nannofossils occurring in Sari well No. 1

marine tropical enviornment was prevailing.

CONCLUSIONS

The present study has shown that the nannofossil assemblages of the Laki and Ranikot formations are distinct (Fig. 1). Further the coccolithus, although they occur in both the formations, yet they are much smaller in size in the Ranikot formation as compared to the Laki formation.

The following species of nannofossils and coccolithus are confined to the Laki formation :

Braarudosphaera biglowi, Discoaster barbadiensis, D. elegans, D. binodosus, D. exilis, D. sp. 1, *D.* sp. 3, *Discolithus numerosa, Zygolithus erectus,* and *Cyclococcolithus leptoporus.*

From the habitat and occurrence in abundance of these fossils, it may be concluded that at the time of deposition a marine tropical environment was prevailing.

Further studies which are now in progress in the Palynology branch of the G and A Labs. will furnish data for defining the characteristic palynological assemblages of various geological formations. These studies will be valuable, particularly for the correlation of the geological formations in East Pakistan.

ACKNOWLEDGEMENT

The author is grateful to Dr. M. H. Khan, Chief of Laboratories, Oil and Gas Development Corporation, for his invaluable suggestions during the course of this investigation.

BIBLIOGRAPHY

Bouché, P.M. 1962 Nannofossiles tertiaires du Bassin de Paris. *Somm. Soc. Fr.*, **4**, 106,

.....1962 Nannofossiles calcaires du Lutétien du Bassin de Paris. *Rev. Micropal.*, **5**, 75-103.

Bramlette, M.N. and Riedel, W.R. 1954 Stratigraphic value of Discoasters and some other microfossils related to Recent Coccolithophores. *Journ. Pal.*, **28**, 385-403.

.....and Sullivan, F.R. 1961 Coccolithophorids and related Nannoplankton of the Early Tertiary in California. *Micropal.*, **7**, 129-188.

Cookson, I.C. and Singleton, O.P. 1954 The preparation of transluscent fossils by treatment with Hydroflouric acid. *Geol. Soc. Australia, News Bull.*, **2**.

Deflandre, G. 1947 Braarudosphaera nov. gen. type d'une famille nouvelle de coccolithophoridés actuels á éléments composites. *Acad. Sci., C.R.*, **225**, 439-441.

.....1950 Observations sur les Coccolithophoridés, á propos d'un nouveau type de Braarudosphaeridae Micrantholithus á éléments clastiques. *Acad. Sci. C.R.*, **231**, 1156-1158.

Gorka, H. 1963 Coccolithophororidés, Dinoflagellés, Hystrichosphaeridés et Microfossles incertae sedis du Crétacé supérieurde Pologne.. *Acta Pal. Polonica*, **8**, 1-24.

Kamptner, E. 1949 Fossile Coccolithineen-Skelettreste aus dem Molukken-Archipel. *Osterr. Akad. Wiss., Math.—Naturwiss. Kl,, Awz,*, **86**, 77-80.

Lohman, H. 1902 Die Coccolithophoridae, eine Monographie der Coccolithen-bildenden Flagellaten. *Archiv. Protistenk*, **1**, 89-165.

Martini, E. 1959 Pemma angulatum und Micrantholithus basquensis, zwei neue Coccolithophoriden-Arten aus dem Eozän. *Senckenbergiana Leth* **40**, 415-421.

Schiller, J. 1930 Coccolithinae. In: Rabenhorst, L., *Kryptogamen Flora, Leipzig*, **10**, 89-267.

Tan Sin Hok 1927 Over de Samenstelling en het ontstaan van Krijt en mergelgesteenten van de Molukken. *Mijnw. Ned. Oost-Indie, Jarb.* (1926), 1-165.

Plate I

(All sketches are diagrammatic)

Figure 1	...	*Braarudosphaera bigelowi* (without separating suture and central cavity).
Figure 2	...	*Braarudosphaera bigelowi* (Well developed central cavity but without separating suture).
Figure 3	...	*Braarudosphaera bigelowi* (ill developed separating suture).
Figure 4	...	*Braarudosphaera bigelowi* (Separating sutures not upto equator).
Figure 5	...	*Braarudosphaera bigelowi* (Separating sutures upto equator).
Figure 6	...	*Braarudosphaera bigelowi* (with rounded angles).
Figure 7	...	*Diccoaster barbadiensis.*
Figures 8—9	...	*Discoaster lenticularis.*
Figures 10—12	...	*Discoaster elegans.*
Figure 13	...	*Discoaster binodosus* (Proximal view).
Figure 14	...	*Discoaster binodosus* (Distal view).
Figures 15 & 17	...	*Discoaster brouweri* (Six rays).
Figures 16 & 18	...	*Discoaster brouweri* (Five rays).
Figure 19	...	*Discoaster exilis.*
Figure 20	...	*Discoaster* sp_1.

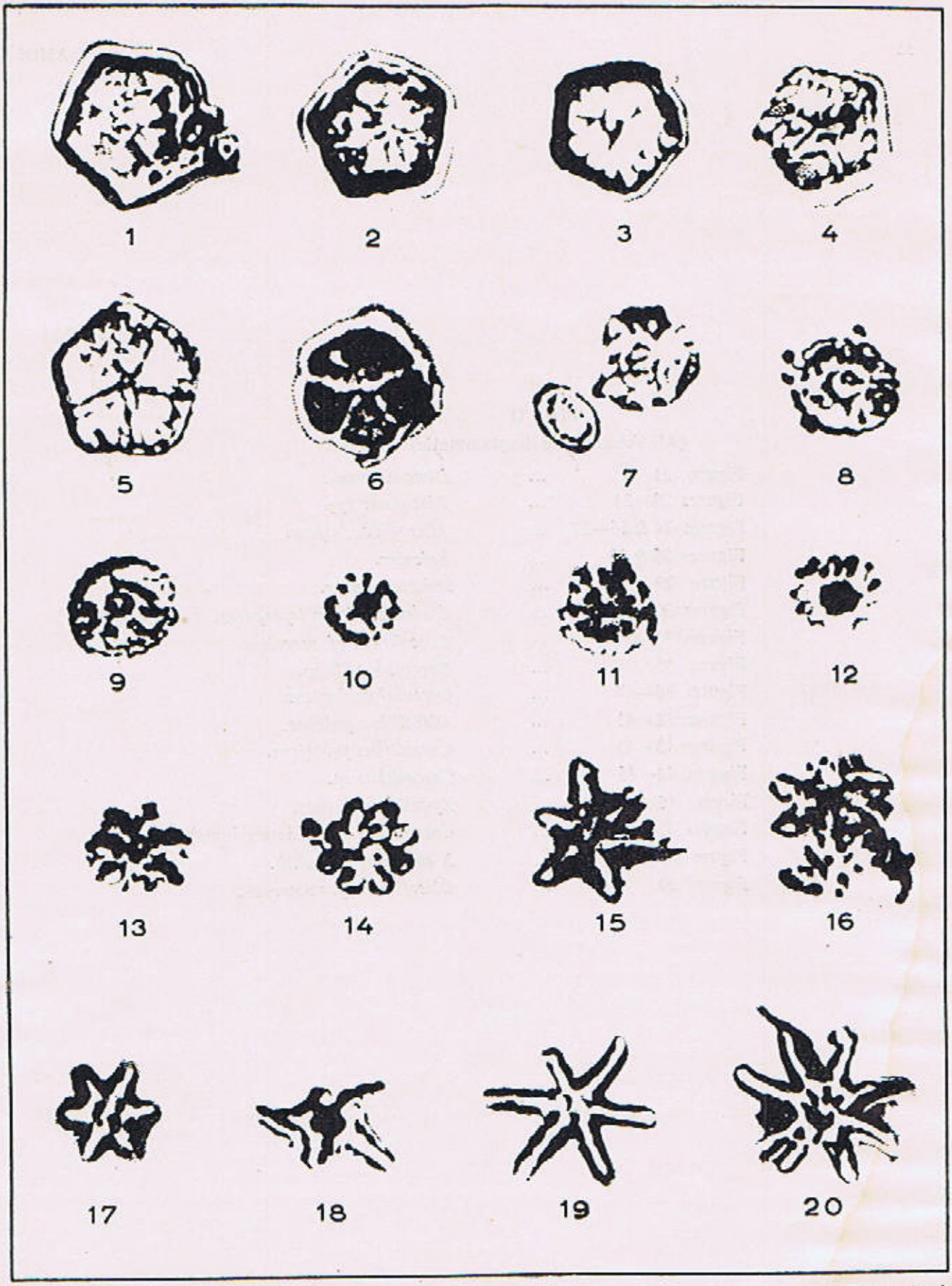

Geol. Bull. Panj. Univ. no. 6 Plate 1

Plate II

(All sketches are diagrammatic)

Figure 21	...	*Discoaster* sp_2.
Figures 22—23	...	*Discoaster* sp_3.
Figures 24 & 26—27	...	*Microforaminifera.*
Figures 25 & 28	...	*Spicules.*
Figure 29	...	*Inderterminate.*
Figures 30—32	...	*Cyclococcolithus leptoporus.*
Figures 33—34	...	*Coccolithus cf. macellus.*
Figure 35	...	*Coccolithus (?) sp.*
Figures 36—37	...	*Coccolithus danicus.*
Figures 38—41	...	*Discolithus pulcher.*
Figures 42—43	...	*Coccolithus pelagicus.*
Figures 44—45	...	*Coccolithus sp.*
Figure 46	...	*Zygolithus erectus.*
Figures 47—48	...	*Coccolithus sp.* (indeterminate).
Figure 49	...	A group of *Coccolith.*
Figure 50	...	*Discolithus cf. numerosa.*

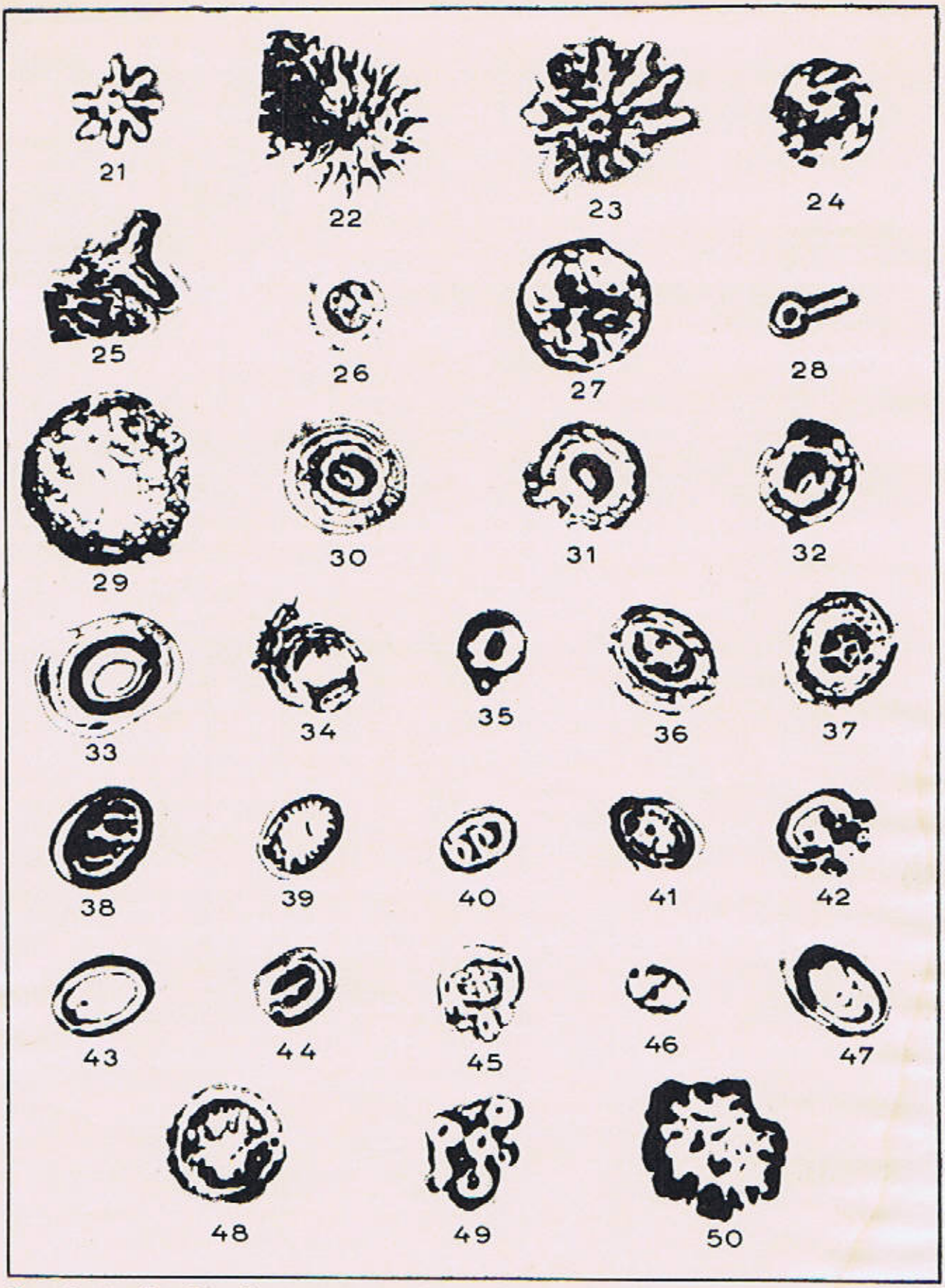

Geol. Bull. Panj. Univ. no. 6 Plate 2

CALCAREOUS NANNOPLANKTON FROM THE LOWER EOCENE OF THE ZINDA PIR, DISTRICT DERA GHAZI KHAN, WEST PAKISTAN.

BY

U. Z. BILAL UL HAQ*

Abstract : *Twenty-eight species of calcareous nannoplankton are recorded from the Ghazij Shales of the Zinda Pir area, District Dera Ghazi Khan, West Pakistan. The abundant presence of Marthasterites tribrachiatus (Bramlette & Riedel) Deflandre confirms their Lower Eocene age.*

INTRODUCTION

Calcareous nannoplankton include the living and fossil representatives of the extremely small (4-25μ) unicellular 'flagellate algae' (Coccolithophorales) and some morphologically different but related forms with calcareous skeleton. They constitute an important part of the phytoplanktonic content of the present day seas, prefering the $CaCO_3$-rich water of the lesser latitudes, although some species occur in great abundance in the higher latitude seas as well.

Fossil representatives of this group have been described from sediments of Lower Jurassic to Recent. Since Bramlette & Riedel (1954) first pointed out their value as stratigraphic indicators, this group of microfossils has been very effectively used for stratigraphic zonations of sequences in many parts of Europe and North America. They become extremely valuable as guide fossils when other microfossils are absent, or when zonations based upon other fossil assemblages are of doubtful nature. The short vertical and wide horizontal distributions of many species of nannoplankton makes them very desirable material for biostratigraphy and intercontinental correlation.

A single sample from Ghazij Shales of the Zinda Pir area, District Dera Ghazi Khan, West Pakistan, which formed a part of samples studied by Bramlette and Sullivan (1961), was put at the author's disposal by Professor M. N. Bramlette who received the same from late Dr. Y. Nagappa, then of the Burmah Oil Company, India. The present study of this sample records 16 genera and 28 species of coccoliths and discoasters.

DESCRIPTION OF THE MATERIAL

The Zinda Pir area is located in the northern part of the Sulaiman Range where rocks of Cretaceous, Paleocene, Eocene and Lower Miocene are exposed (Fig. 1). A more or less complete Eocene section is present. Except in the lowermost Eocene, the sequences of the Zinda Pir section are very similar to those of the Rakhi Nala section which is exposed towards south of the Zinda Pir area (Eames, 1951a).

The Ghazij Shales of the Zinda Pir area contain some important faunal assemblages of larger forminifera, bryozoa and mollusca (Eames, 1951b). The present study confirms the age of these Shales as Lower Eocene from the abundant presence of *Marthasterites tribrachiatus* (Bramlette & Riedel) Deflandre, a species reported to be restricted to the Lower Eocene sediments of many parts of the world.

METHODS OF INVESTIGATION**

The investigation was mainly carried out with the help of a light microscope and a transmission electron microscope. For the light microscopy a Leitz research microscope with an oil immersion lens was used and the slides were

*Geological Institution, University of Stockholm, Sweden. Student of Geology Department, Punjab University from 1959 to 1963.

**All type negatives and slides are deposited in the type collection of the Geological Institution, University of Stockholm, Sweden.

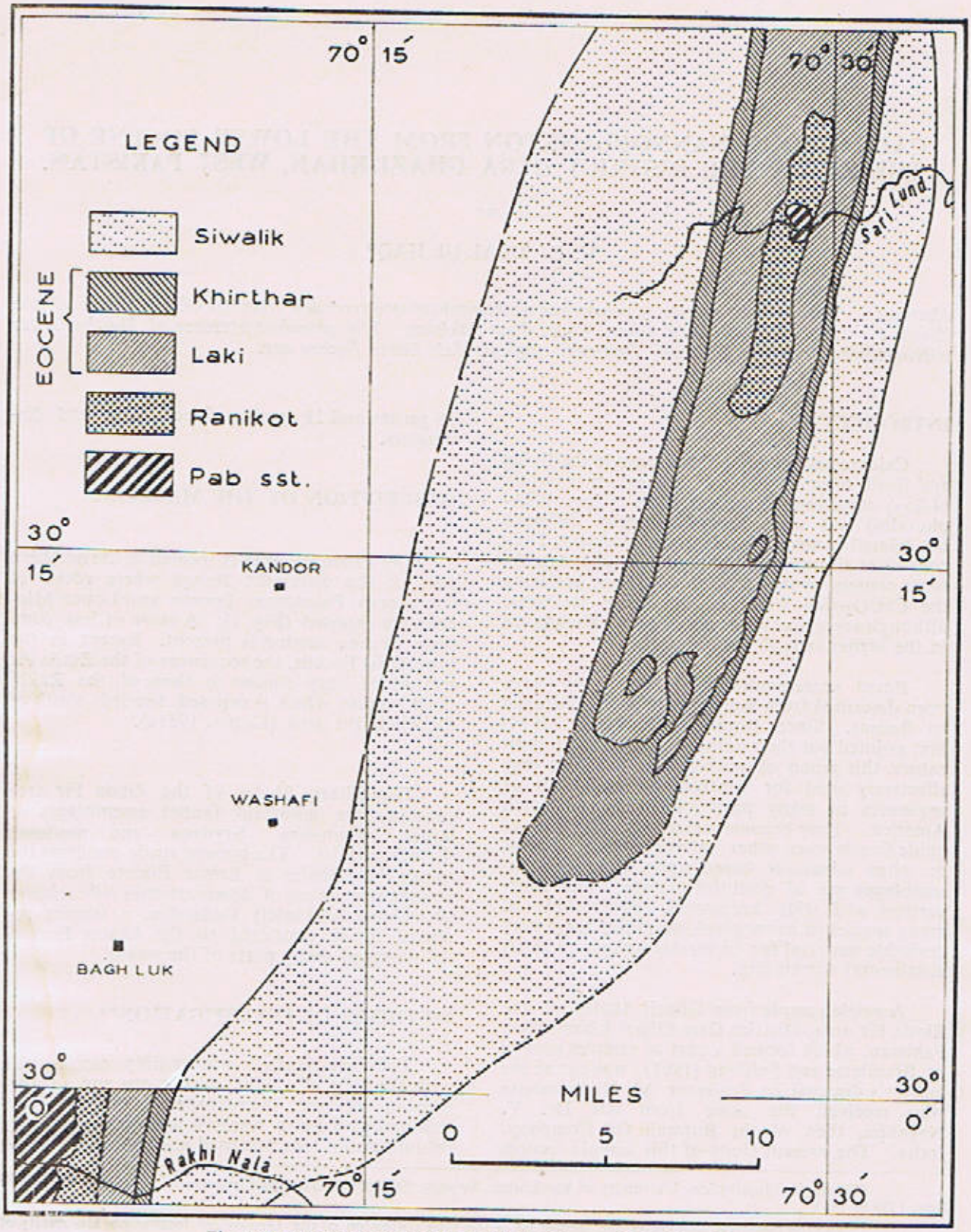

Fig. 1 Geological sketch map of the Zinda Pir area, D.G. Khan Distt.

prepared using Caedax. The photomicrographs were taken under normal light at a magnification of 414 X.

For transmission electron microscopy, carbon replication methods were used, which have already been discussed in some detail by the author (1968). Due to comparative poor preservation of the material and due to the large size of discoasters which fall-off the carbon film when it is removed from the glass slide during preparation, only a few electronmicrographs were available. A Zeiss EM9 electron microscope was used at the Geological Institution of Stockholm University. Most of the electronmicrographs were photographed at a magnification of 6300 X.

A single scanning electronmicrograph of *Marthasterites tribrachiatus* is also recorded. Scanning electron microscope has recently achieved great importance as an instrument which is able to reproduce a three-dimensional image of objects at a wide range of magnifications (15-20,000 X) and at appreciably high resolutions (upto 200 A).

ACKNOWLEDGEMENT

The author expresses his thanks to Professor M. N. Bramlette (La Jolla, California) for providing sample for the present study.

SYSTEMATIC DESCRIPTIONS

The following systematics is adapted for the description of genera and species described in this paper :

Family *Coccolithaceae* Kamptner 1928

Tribe *Coccolitheae* Kamptner 1958 :
- Genus *Coccolithus* Schwarz 1894
- Genus *Cycloplacolithella* Haq 1968
- Genus *Ericsonia* Black 1964
- Genus *Rhabdosphaera* Haeckel 1894

Tribe *Pontosphaereae* Hay 1966 :
- Genus *Discolithina* Loeblich & Tappan 1963
- Genus *Helicosphaera* Kamptner 1954
- Genus *Zygodiscus* Bramlette & Sullivan 1961
- Genus *Zygolithus* Kamptner 1956

Tribe *Lophodolitheae Haq, n.t.*:
- Genus *Lophodolithus* Deflandre 1954

Tribe *Zygosphaereae* Kamptner 1958 :
- Genus *Zygrhablithus* Deflandre 1959

Family *Lithostromationaceae Haq n.f.*

Genus *Lithostromation* Deflandre 1942

Family *Discoasteraceae* Vekshina 1959

Genus *Discoaster* Tan Sin Hok 1927
Genus *Discoasteroides* Bramlette & Sullivan 1961
Genus *Marthasterites* Deflandre 1959

Family *Ceratolithaceae* Norris 1965

Genus *Ceratolithus* Kamptner 1950

Incertae sedis

Genus *Polycaldolithus* Deflandre 1954

Genus **COCCOLITHUS** Schwarz 1894

Type species : *Coccolithus oceanicus* Schwarz

Coccolithus pelagicus (Wallich) Schiller 1930, pl. I, figs. 1, 2.

1877 *Coccosphaera pelagica* Wallich, p. 348, pl. 17, figs. 1, 2, 5, 11, 12.
1930 *Coccolithus pelagicus* (Wallich) Schiller, p. 246.
1954 *Coccolithus pelagicus* (Wallich) Schiller, Kamptner, p. 20, figs. 14-15.
1963 *Coccolithus pelagicus* (Wallich) Schiller, Black, pp. 41—45, pl. 1, fig. 7.
1963 *Coccolithus pelagicus* (Wallich) Schiller, Stradner in Bachmann, Papp & Stradner, p. 156.
1963 *Coccolithus pelagicus* (Wallich) Schiller, Martini and Bramlette, p. 849.
1965 *Coccolithus pelagicus* (Wallich) Schiller, Cohen, p. 12, pl. 1, figs. a-d.
1966 *Coccolithus pelagicus* (Wallich) Schiller, Haq, p. 31, pl. 1, fig. 5.
1967 *Coccolithus pelagicus* (Wallich), Levin & Joerger, p. 165, pl. 1, figs. 4-5.

Remarks : Pl.1, fig. 1 shows a distal view similar to the specimen illustrated by Black (1963), however, due to rupture of the carbon film the specimen illustrated here seems more circular than elliptical. Pl. 1, fig. 2 is most probably a proximal view of a corroded specimen of this species.

Distribution : Middle Jurassic to Recent. Wide occurrence in the present day seas.

Coccolithus delus (Bramlette and Sullivan) 1961, pl.VI, fig. 7.

1961 *Coccolithites delus* Bramlette & Sullivan, pp. 151-152, pl.7, figs. 1a-c, 2a-b.
1964 *Coccolithites delus* Bramlette & Sullivan, Sullivan, p. 180, pl. 1, figs. 8-9.
1965 *Coccolithites delus* Bramlette & Sullivan, Sullivan, p. 31.

Remarks : The specimens of this species are usually poor preserved and often with the central bars partly or completely broken away.

Distribution : Reported by Bramlette and Sullivan (1961) from the Paleocene to Middle Eocene of California, Middle Eocene of Weches Formation, Texas, Middle Eocene of Donzacq, France and from the present material from Lower Eocene of the Zinda Pir, West Pakistan.

Coccolithus aff. ***C. staurion*** Bramlette & Sullivan 1961, pl. VI, fig. 9.

Remarks : The specimen illustrated here shows affinity to *Coccolithus staurion*, but the small central cross is only partly preserved due to poor preservation of material.

Distribution : Described by Bramlette & Sullivan (1961) from Middle Eocene of California, Middle Eocene of Weches Formation, Texas, and Middle Eocene of Gibret, France.

Genus **CYCLOPAYCOLITHELLA** Haq 1968

Type species : *Cycloplacolithella foliosa* (Kamptner).

Cycloplacolithella sp., pl.I, fig. 3.

Remarks : A single transmission electronmicrograph shows distal view of the specimen with a circular outline and a well marked central opening. Crystal-rays are broad and flat and few (ca 12) in number and show smoothened extremities.

Genus **DISCOLITHINA** Loeblich & Tappan 1963

Type species : *Discolithina multipora* (Kamptner) Martini.

Discolithina plana (Bramlette & Sullivan) Levin 1965, pl. VI, figs. 1-3.

1961 *Discolithus planus* Bramlette and Sullivan, p. 143, pl.3, figs. 7a-c.
1964 *Discolithus crassus* Deflandre, Cohen, p. 236, fig. c.
1965 *Discolithus planus* Bramlette and Sullivan, Cohen, p. 13, pl.2, figs. p.s.
1965 *Discolithina plana* (Bramlette and Sullivan) Levin, p. 266, pl. 41, figs 9a-c.
1967 *Discolithina plana* (Bramlette and Sullivan) Levin and Joerger, p. 167, pl.2, figs. 3a-b.

Distribution : Reported from Lower to Middle Eocene of California, Weches Formation, Texas and Middle Eocene of Donzacq, France (Bramlette and Sullivan, 1961). Upper Eocene to Middle Oligocene of Alabama and Mississippi (Levin & Joerger, 1967) and also recorded from Pleistocene and (sub) Recent sediments of the Adriatic (Cohen, 1965).

Genus **ERICSONIA** Black 1964

Type species : *Ericsonia occidentalis* Black

Ericsonia ovalis Black 1964, pl. V, fig. 6.

1964 *Ericsonia ovalis* Black, p. 312, pl. 52, figs. 5-6.
1964 *Coccolithus muiri* Black, p. 309, pl.50, figs, 3-4.
1966 *Coccolithus muiri* Black, Haq, p. 29, pl.1, fig. 3.
1967 *Ericsonia ovalis* Black, Stradner in Stradner & Edwards (in press).
1968 *Ericsonia ovalis* Black, Haq, p.21, p.l. 1, figs. 4-9; pl. 2, figs. 1-4; pl. 4, figs. 1-2.

Remarks : A single transmisson electronmicrograph is illustrated here. Comprehensive illustrations and descriptions have already been rendered by Stradner in Stradner & Edwards (1967) and by Haq (1968).

Distribution : Described from the Middle Eocene of Atlantic seamounts (Black, 1964), Upper Eocene of Syria and NW Germany (Haq, 1966, 1968). Upper Eocene of Oamaru, New Zealand (Stradner in Stradner and Edwards, 1967). Rare occurrence in the present material and probably reworked.

Genus **HELICOSPHAERA** Kamptner, 1954

Type species : *Helicosphaera carteri* (Wallich) Kamptner.

Helicosphaera carteri (Wallich) Kamptner, 1954, pl.1, fig. 4, pl. VI, 8.

1877 *Coccosphaera carteri* Wallich, p.348, pl.17 figs. 3,4,6,7,17.
1899 *Coccosphaera pelagica* var. *carteri* Wallich, Ostenfeld, p. 436.
1944 *Coccolithus carteri* (Wallich), Kamptner, pp. 93, 111, pl.13, fig. 136.
1954 *Helicosphaera carteri* (Wallich) Kamptner, p.21, text-figs. 17,19.
1954 *Helicosphaera carteri* (Wallich), Deflandre & Fert, p. 38, text-figs. 10.11, 75.
1961 *Helicosphaera carteri* (Wallich) Kamptner, Black & Barnes; p. 139, pls. 22-23.
1963 *Helicosphaera carteri* (Wallich) Kamptner, Stradner in Bachmann, Papp and Stradner, p. 157, pl.24, fig. 9, text-figs. 3, figs, 2, 2a.
1964 *Helicosphaera carteri* (Wallich) Kampter, Cohen, p.238, pl.3., figs. 2a-f, pl.4, figs. 1a-c.
1967 *Helicosphaera carteri* (Wallich) Kamptner, McIntyre, Bé, and Preikstas, p.12, pl.6, figs, A.B.
1967 *Helicosphaera carteri* (Wallich) Kamptner, Levin and Joerger, p. 168, pl.2, figs. 12a-c.

Remarks : One transmission electronmicrograph (Pl.1, fig. 4) of a distal view of a partly broken specimen and one photomicrograph of a distal view of a complete specimen (Pl. VI, fig. 8) are recorded here. Black and Barnes (1961) have illustrated excellent transmission electronmicrographs of this species.

Distribution : Widespread occurrence reported from Cretaceous to Recent sediments.

Genus **RHABDOSPHAERA** Haeckel, 1894

Type species : *Rhabdosphaera clavigera* Murray and Blackmann.

Rhabdosphaera perlonga (Deflandre) Bramlette and Sullivan 1961, pl.III, figs, 4,5.

1954 *Rhabdolithus perlongus* Deflandre in Deflandre and Fert, p.44, pl.12, figs. 34, 35, text-fig. 86.
1961 *Rhabdosphaera perlonga* (Deflandre), Bramlette and Sullivan, p, 146, pl.5, figs. 7a-c
1964 *Rhabdosphaera perlonga* (Deflandre), Sullivan, p. 185, pl.7, fig. 8.
1965 *Rhabdosphaera perlonga* (Deflandre), Sullivan, p.36, pl.7, figs. 7a,b.
1967 *Rhabdosphaera perlonga* (Deflandre), Levin and Joerger, p. 168, pl.2, figs. 13a-c.
1968 *Rhabdosphaera perlonga* (Deflandre) Bramlette and Sullivan, Haq, p. 34, pl. 11, fig.19.

Distribution : Reported from Lower to Middle Eocene of California, Middle Eocene of Weches Formation, Texas, Lower Lutetian of Donzacq, France (Bramlette and Sullivan, 1961), from Upper Eocene to Middle Oligocene of Alabama and Mississippi (Levin and Joerger, 1967), and from Upper Eocene of NW Germany (Haq, 1968).

Rhabdosphaera spinula Levin 1965, pl.III, figs. 1,2,3.

1965 *Rhabdosphaera spinula* Levin, p.267, pl.42, fig. 3.
1967 *Rhabdosphaera spinula* Levin, Levin and Joerger, p.169, pl.2, figs. 15a-c,
1967 *Rhabdosphaera spinula* Levin, Gartner and Smith; p.5, pl.1, figs. 1,2.
Distribution : Upper Eocene of Yazoo Formation, Mississippi (Levin, 1965), and Upper Eocene to Middle Oligocene of Alabama (Levin and Joerger, 1967). Common in the present material from Lower Eocene of Zinda Pir, West Pakistan.

Rhabdosphaera sp., pl.II, fig. 1.

Remarks : The form so designated is only provisionally included under this taxon. It shows a circular basal shield composed of a number of broad and flat crystal-rays radiating from a thick stem. The robust stem seems to have been formed of thin needle-like crystals arranged in slightly helicoid manner. The stem has been broken away almost completely.

Genus **LOPHODOLITHUS** Deflandre, 1954

Type species: Lophodolithus machlophorus Deflandre.

Lophodolithus nascens Bramlette and Sullivan, 1961, pl. VI, fig. 4.

1961 *Lophodolithus nascens* Bramlette and Sullivan, p. 145, pl. 4, figs. 7a-c, 8a-c.
1964 *Lophodolithus nascens* Bramlette and Sullivan, Sullivan p. 185, pl. 6, figs. 7a, b.
1965 *Lophodolithus nascens* Bramlette and Sullivan, Sullivan p. 36,

Distribution : Reported from Paleocene to Middle Eocene of California, Lower Eocene and Lower Leutetian of France and from the present material of Lower Eocene of the Zinda Pir, West Pakistan (Bramlette and Sullivan, 1961).

Genus **ZYGODISCUS** Bramlette and Sullivan, 1961

Type species : *Zygodiscus adamas* Bramlette and Sullivan.

Zygodiscus aff. ***Z. plectopons*** Bramlette and Sullivan, 1961, pl.VI, fig. 5.

1961 *Zygodiscus* aff. *Z. plectopons* Bramlette and Sullivan, p. 148, pl. 4, figs. 13a-c.
1966 *Zygodiscus* sp. aff. *Z.plectopons* Bramlette and Sullivan, Edwards, p. 489, fig. 27.
Distribution : Reported from Paleocene and Lower Eocene of California (Bramlette and Sullivan, 1961) and from the Teurian Stage of Waipara, New Zealand (Edwards, 1966).

Genus **ZYGOLITHUS** Kamptner 1956

Type species: Zygolithus dubius Deflandre.

Zygolithus chiastus Bramlette and Sullivan 1961, pl. V, figs. 1,2,5.

1961 *Zygolithus chiastus* Bramlette and Sullivan, p. 149, pl, 6, figs. 1a-d, 2a, b, 3a, b.
1963 *Zygolithus chiastus* Bramlette and Sullivan; Stradner in Gohrbandt, p. 77, pl. 10, figs. 1-3
1964 *Zygolithus chiastus* Bramlette and Sullivan; Sullivan, 187, pl. 7, fig. 12.

Distribution: Paleocene to Lower Eocene of California, Paleocene of Alabama, type Thanetian, type Danian and Paleocene of France (Bramlette and Sullivan, 1961), Helvetian of Salzburg, Austria (Stradner in Gohrbandt, 1963)

Zygolithus sp., Pl. V, figs. 3,7.

Remarks: The light micrograph shows an elliptical form with a broad rim and a single bar crossing the central opening at right angles to the long axis of the ellipse. The transmission electron—micrograph, on the hand shows the central opening to be filled in with secondary material. It shows some similarity to *Zygolithus disentus* Bramlette and Sullivan (1961, pl.6, fig.6a).

Genus **ZYGRHABLITHUS** Deflandre 1959.

Type species : Zygrhablithus bijugatus (Deflandre) Deflandre.

Zygrhablithus bijugatus (Deflandre) Deflandre 1959, pl. III, fig. 8.

1954 *Zygolithus bijugatus* Deflandre in Deflandre and Fert, p. 148, pl. 11, figs. 20,21.
1954 *Rhabdolithus costatus* Deflandre in Deflandre and Fert, p. 157, pl. 11, figs. 8-11, text-figs. 41, 42 77-79.
1959 *Zygrhablithus bijugatus* (Deflandre) Deflandre, p. 135.
1961 *Zygrhablithus bijugatus* Deflandre, Bramlette and Sullivan, p.151, pl.6, figs. 16-18.
1962 *Zygrhablithus bijugatus* Deflandre, Bouché, p.84,pl.1, figs.4,9,11.
1964 *Zygrhablithus bijugatus* Deflandre, Sullivan, p.187,pl.7,figs.9-10.
1965 *Zygrhablithus bijugatus* Deflandre, Sullivan, p.38.
1965 *Zygrhablithus bijugatus* Deflandre, Levin, p.267, pl.42,figs.1a,b.
1967 *Zygrhablithus bijugatus* (Deflandre), Levin and Joerger, p.170, pl.2, figs. 24a, b, pl.3, figs. 1-4
1967 *Zygrhablithus bijugatus* (Deflandre), Gartner and Smith, p.5, pl.8, figs. 1-6.
1967 *Zygrhablithus bijugatus* Deflandre, Stradner in Stradner and Edwards.
1968 *Zygrhablithus bijugatus* (Deflandre) Deflandre, Haq, p. 40, pl. 7, fig. 10; pl. 9, figs. 10-11.

Distribution : Described from the Eocene of many parts of the world.

Zygrhablithus sp., pl.III, fig. 6.

Description : A Zygrhablith with a comparatively small basal shield mounted by thick and long knife-like stem which tapers upwards and ends sharply. A deep notch is produced between the basal plate and the stem which seems to be formed of four separate elements at right angles to each other.

Occurrence : Rare in the present material from Lower Eocene of the Zinda Pir, West Pakistan.

Genus **LITHOSTROMATION** Deflandre 1942

Type species : Lithostromation perdurum Deflandre.

Lithostromatian sp., pl.VI, fig. 6.

Remarks : A single specimen is recorded here. It shows a triangular form with about five depressions on its surface that are separated by ridges. The specimen shows some similarity to *Lithostromation robustum* Martini, 1961.

Genus **MARTHASTERITES** Deflandre 1959

Type species : *Marthasterites furcatus* Deflandre.

Marthasterites tribrachiatus (Bramlette and Riedel) Deflandre 1959, pl. II, figs. 2-5, pl. III, fig. 7.

1954 *Discoaster tribrachiatus* Bramlette and Riedel, p. 397, pl. 38, fig. 11.
1958 *Discoaster tribrachiatus* Bramlette and Riedel, Stradner, p. 181, fig. 5.
1958 *Discoaster tribrachiatus* Bramlette and Riedel, Martini, p. 357, pl. 2, fig. 8a, b.
1959 *Discoaster tribrachiatus* Bramlette and Riedel, Stradner, p. 477, figs. 5,6,10.
1959 *Marthasterites tribrachiatus* (Bramlette and Riedel) Deflandre, p. 138, pl.2, fig. 1.
1960 *Discoaster tribrachiatus* Bramlette and Riedel, Martini, p.81, pl, 10, fig. 30.
1961 *Discoaster tribrachiatus* Bramlette and Riedel, Bramlette and Sullivan, p.162, pl. 13, figs, 6-9, 11-13.
1961 *Marthasterites tribrachiatus* (Bramlette and Riedel) Deflandre, Stradner in Stradner and Papp, p. 110. pl. 35, figs. 1-4, 7, text-figs. 11/5, 6;2/3; 20/2.
1963 *Marthasterites tribrachiatus* (Bramlette and Riedel) Deflandre, Stradner in Gohrbandt, p.83, pl, 11, fig. 10.

Remarks: Pl.II, figs. 2 and 4 illustrated here are most probably juvenile forms of this species. Figs.3 and 5,on the other hand, show fully developed forms in transmission electron microscope and light microscope, respectively. The scanning electronmicrograph (pl.III,fig.7) shows this species in three dimensions, indicating the arch-shaped form of the arms.

Distribution : Reported to be restricted to the Lower Eocene deposits of many parts of the world. It is one of the most common species in the present material.

Genus **DISCOASTEROIDES** Bramlette and Sullivan 1961.

Type species : *Discoasteroides kuepperi* (Stradner) Bramlette and Sullivan.

Discoasteroides kuepperi (Stradner) Bramlette and Sullivan 1961, pl. IV, figs. 1-6.

1959 *Discoaster kuepperi* Stradner, p. 478, text-figs. 17-21.
1961 *Discoaster kuepperi* Stradner, Martini; p. 14, pl. 3, fig. 29.
1961 *Discoasteroides kuepperi* (Stradner) Bramlette and Sullivan, p. 163, pl. 13, figs. 16-19.
1961 *Discoaster kuepperi* Stradner, Stradner in Stradner and Papp, p. 93, pl. 27, figs. 1-6, text-figs. 9/6, 16.
1962 *Discoasteroides kuepperi* (Stradner), Hay and Towe, p. 515, pl. 10, fig. 1.
1964 *Discoasteroides kuepperi* (Stradner), Sullivan, p. 192, pl. 12, figs. 1a, b, 2a, b.
1965 *Discoasteroides kuepperi* (Stradner), Sullivan, p. 44.
1968 *Discoasteroides kuepperi* (Stradner) Bramlette and Sullivan, Haq, p. 47, pl. 10, fig. 6.

Remarks : Two transmission electronmicrographs (Pl. IV, fig. 1 and 2) showing the proximal and distal views, and four photomicrographs (figs. 3-6) showing proximal and side views are illustrated here. A description of this species based on electronmicroscopic observations has already been rendered by Hay and Towe (1962) and by Haq (1968).

Distribution : Reported from Lower and Middle Eocene of California and Paleocene of Austria (Bramlette and Sullivan, 1961) Lutetian of Donzacq, France (Hay and Towe, 1962) and Upper Eocene of NW Germany (Haq 1968).

Genus **DISCOASTER** Tan Sin Hok 1927

Type species : *Discoaster pentaradiatus* Tan Sin Hok

Discoaster sublodoensis Bramlette and Sullivan 1961, pl. VIII, figs. 1-3.

1961 *Discoaster sublodoensis* Bramlette and Sullivan, p. 162, pl. 12, figs. 6a, b
1962 *Discoaster sublodoensis* Bramlette and Sullivan, Bouché, p. 90, pl. 3, figs. 18, 19, text-figs. 25,26
1965 *Discoaster sublodoensis* Bramlette and Sullivan, Sullivan, p. 43, pl. 10, fig. 11

Distribution : Reported from Middle Eocene California, and Weches Formation, Texas (Bramlette & Sullivan, 1961), Middle Eocene of France (Bouché, 1962) and Lutetian of Paris Basin. Rare in the present material and probably reworked.

Discoaster lodoensis Bramlette and Riedel 1954, pl. VII, figs. 3, 6, 7

1954 *Discoaster lodoensis* Bramlette and Riedel, p. 398, pl. 39, figs. 3a, b
1958 *Discoaster lodoensis* Bramlette and Riedel ; Stradner, p. 182, fig. 8
1958 *Discoaster lodoensis* Bramlette and Riedel ; Martini, p. 366, pl. 6, figs. 28a-d
1959 *Discoaster lodoensis* Bramlette and Riedel ; Stradner, p. 1083, fig. 5
1959 *Discoaster lodoensis* Bramlette and Riedel ; Manivit, p, 31, pl. 6, fig. 4-5
1960 *Discoaster lodoensis* Bramlette and Riedel ; Martini, p. 76, pl, 8, fig. 11
1961 *Discoaster lodoensis* Bramlette and Riedel ; Martini, p. 11
1961 *Discoaster lodoensis* Bramlette and Riedel ; Bramlette and Sullivan, p. 161, pl. 12, figs. 4-5
1961 *Discoaster lodoensis* Bramlette and Riedel, Stradner in Stradner & Papp, p. 92, pls. 25, 26, text-figs. 9/3, 24/9
1962 *Discoaster lodoensis* Bramlette and Riedel, Hay and Towe, p. 514, pl. 10, figs. 2, 4,6
1964 *Discoaster lodoensis* Bramlette and Riedel, Sullivan, p. 191, pl. 11, fig. 14.
1965 *Discoaster lodoensis* Bramlette and Riedel, Sullivan, p. 12, pl. 10, fig. 14
1965 *Discoaster lodoensis* Black, fig. 20
1965 *Discoaster lodoensis* Bramlette and Riedel, Cohen, p. 33, pl. 25, fig. e

Distribution : Widespread in the Eocene deposits of many parts of the world. Abundant in the present material.

Discoaster barbadiensis Tan Sin Hok 1927, pl. VII, figs, 1-2

1927 *Discoaster barbadiensis* Tan Sin Hok (proparte), p. 119
1954 *Discoaster barbadiensis* Tan, Bramlette and Riedel, p. 398, pl. 39, figs .5a, b
1955 *Discoaster barbadiensis* Tan Sin Hok, Gardet, p. 526, pl. 7, figs. 68a, b
1958 *Discoaster barbadiensis* Tan Sin Hok, Stradner, p. 183, fig. 11
1958 *Discoaster barbadiensis* Tan Sin Hok, Martini, p. 366, pl. 5, figs. 24a-c
1959 *Discoaster barbadiensis* Tan Sin Hok, Manivit, p. 39, pl. 10, fig. 3
1959 *Discoaster barbadiensis* Tan Sin Hok, Stradner, p. 1082, fig. 2
1961 *Discoaster barbadiensis* Tan Sin Hok, Bramlette and Sullivan, p. 158, pl. 11, fig. 2.
1961 *Discoaster barbadiensis* Tan Sin Hok, Stradner in Stradner and Papp, p. 95, pl. 28, figs. 1-2, text-fig. 9/7, 18/6, 24/3
1962 *Discoaster barbadiensis* Tan Sin Hok, Hay and Towe, p. 515, pl. 10, figs. 3, 5
1964 *Discoaster barbadiensis* Tan Sin Hok, Sullivan, p. 189, pl. 10, figs. 1, 2
1965 *Discoaster barbadiensis* Black, fig. 20
1965 *Discoaster barbadiensis* Tan Sin Hok, Cohen, p. 32, pl. 7, figs. a-d
1965 *Discoaster barbadiensis* Tan Sin Hok, Sullivan, p. 41
1967 *Discoaster barbadiensis* Tan Sin Hok, Levin, and Joerger, p. 172, pl. 3, figs. 17 a, b
1967 *Discoaster barbadiensis* Tan Sin Hok, Gartner and Smith, p. 6, pl. 12, figs. 1-3

Distribution : Widespread occurrence in the Eocene deposits of many parts of the world. Abundant in the present material.

Discoaster aff. ***D. septemradiatus*** (Klumpp) Martini 1958, pl. VII, figs. 4-5

Remarks : Forms thus designated show a distinct affinity to *Discoaster septemradiatus* in the bifurcation of the rays but the surface ornamentation and the central knob are not clearly discernable. This could be due to the poor state of preservation of the material.

Occurrence : Common in the present material from Lower Eocene of the Zinda Pir, West Pakistan.

Discoaster aff. ***D.mediosus*** Bramlette and Sullivan 1961, pl. VIII, fig. 5

Remarks : This form shows similarity to *Discoaster mediosus* in size, number of rays, and the structure of the rays, however there seems to be two-rayed stem or an upwards broadening funnel-like structure rising from the central disc, which in the specimen illustrated here, has broken and fallen down.

Occurrence : Rare in the present material.

Discoaster saipanensis Bramlette and Riedel 1954, pl. VIII, figs. 4, 6, 7

1954 *Discoaster saipanensis* Bramlette and Riedel, p. 398, pl. 39, fig. 4.
1958 *Discoaster saipanensis* Bramlette and Riedel, Martini, p. 367, pl. 6, fig. 29
1959 *Discoaster saipanensis* Bramlette and Riedel, Stradner, p. 1083, fig. 3
1960 *Discoaster saipanensis* Bramlette and Riedel, Martini, p. 76, pl. 8, fig. 12
1961 *Discoaster saipanensis* Bramlette and Riedel, Stradner in Stradner and Papp, p.90, pl.22, figs. 5-7,9, text-figs. 9/5.
1965 *Discoaster saipanensis* Bramlette & Riedel, Levin, p. 270, pl.43, figs 2a, b.
1966 *Discoaster saipanensis* Bramlette & Riedel; Hay, Mohler & Wade, p.396, pl.11, figs. 8-9,pl.13, fig. 1.
1967 *Discoaster saipanensis* Bramlette & Riedel; Levin and Joerger, p.172, pl.3, fig. 16.
1967 *Discoaster saipanensis* Bramlette and Riedel; Gartner and Smith, p.6, pl.12, figs. 4.5

Distribution : Described from the Upper Eocene of Saipan, Upper Eocene of California, Mississippi and Alabama, Louisiana, Germany and from the Middle Eocene of Austria.

Discoaster sp., pl.VIII, fig. 8

Remarks : The specimen illustrated here shows similarity to *Discoaster* sp. of Bramlette and Sullivan (1961, pl.13, fig. 5), however, it does not show the elaborate ornamentation of the latter. A broad central disc from which radiate out eight rays dividing into three parts at the tips, each part ending pointedly.

Occurrence : Rare in the present material.

Genus **CERATOLITHUS** Kamptner, 1950

Type species: *Ceratolithus cristatus* Kamptner

Ceratolithus sp., pl.V, fig. 4

Remarks : A single specimen illustrated here shows two broad, downwards tapering equi-dimensional arms so as to form a crescent-shaped structure.

Occurrence : Rare.

Genus **POLYCLADOLITHUS** Deflandre, 1954

Type species: *Polycladolithus operosus* Deflandre

Polycladolithus operosus Deflandre, 1954, pl. VII, fig. 8

1954 *Polycladolithus operosus* Deflandre in Deflandre and Fert, p.170, pl.12, figs, 3-6, text-fig. 125
1961 *Polycladolithus operosus* Deflandre, Bramlette and Sullivan, p.165, pl.14, figs. 13a-c
1962 *Trochoaster operosus* (Deflandre), Bouché, p.92, pl.4, figs. 7,8, text-fig. 32
1964 *Polycladolithus operosus* Deflandre, Sullivan, p.194, pl.9, figs. 8a-c
1965 *Polycladolithus operosus* Deflandre, Sullivan, p.45

Remarks : The fragmentary specimen illustrated here (pl.VII, fig.8) clearly shows the structure of this species.

Distribution : Reported from the Lower and Middle Eocene of California, Middle Eocene of Weches Formation, Texas, Upper Eocene of Oamaru, New Zealand and Lutetian of Donzacq, France (Bramlette and Sullivan, 1961). Rare in the present material.

REFERENCES

Black, M. 1963 The fine structure of the mineral parts of Coccolithophoridae. *Proc. Linn. Soc. Lond.* **174**, 41-46.

..... 1964 Cretaceous and Tertiary coccoliths from Atlantic seamounts. *Palaeont.* **7**, 306—316.

..... 1965 Coccoliths. *Endeavour*, **24**, 131—137.

Black, M. and Barnes, B. 1961 Coccoliths and discoasters from the floor of the South Altantic Ocean. *Journ. Roy. Micr. Soc.* (*Lond.*) **80**, 137—147.

Bouché, P. M. 1962 Nannofossiles calcaires du Lutétien du Bassin de Paris. *Rev. Micropal.* **5**, 75—103.

Bramlette, M. N. and Riedel, W. R. 1954 Stratigraphic value of discoasters and some other microfossils related to Recent coccolithophores. *Journ. Pal.* **28**, 385—403.

Bramlette, M. N. and Sullivan, F. R. 1961 Coccolithophorids and related nannoplankton of the early Tertiary in California. *Micropal.* **7**, 129—188.

Cohen, C.L.D. 1964 Coccolithophorids from two Caribbean deep-sea cores. *Micropal.* **10**, 231—250.
..... 1965 Coccoliths and discoasters from Adriatic bottom sediments. *Proefschrift Univ. Leiden*, 44 pp.

Deflandre, G. 1942 Possibilités morphogénétiques comprées du calcaire et de la silice, à propos d'un nouveau type de microfossile calcaire de structure complexe, *Lithostromation perdurum* n. g. n. sp. *C.R. Acad. Sci.* (*Paris*). **214**, 917—919.

..... 1959 Sur les nannofossiles calcaire et leur systématique. *Rev. Micropal.* **2**, 127—152.

Deflandre, G. and Fert, C. 1954 Observations sur les Coccolithophoridés actuels et fossiles en microscopie ordinaire et électronique. *Ann. Pal.* **40**, 115—176.

Eames, F. E. 1951a A contribution to the study of Eocene in western Pakistan and western India : A. The geology of standard sections in the western Punjab and in Kohat district. *Quart. Journ. Geol. Soc. Lond.* **107**, 159—171.

Eames, F. E. 1951 b A contribution to the study of Eocene in western Pakistan and western India : D. Discussion of the faunas of certain standard sections, and their bearing on the classification and correlation of the Eocene in western Pakistan and western India. *Ibid.* 173—200.

Edwards, A. R. 1966 Calcareous nannoplankton from the uppermost Cretaceous and lowermost Tertiary of the Mid-Waipara section, South Island, New Zealand. *New Zealand Journ. Geol. Geophy.* **9**, 481—490.

Gardet, M. 1955 Contribution á l'étude des coccolithes des terrains Néogéne de l'Algérie. *Publ. Serv. Carte, Geol. Algerie*, ser. 2, Bull. **5**, 477—55.

Gartner, S. and Smith, L.A. 1967 Coccoliths and related calcareous nannofossils from the Yazoo Formation (Jackson, Late Eocene) of Louisiana. *Univ. Kansas Paleont. Contr.* Paper **20**, 7 pp.

Haeckel, E. 1894 Systmatische Phylogenie der Protisten und Pflanzen. Berlin, Reimer., 1—400.

Haq, U.Z.B. 1966 Electron microscope studies on some Upper Eocene calcareous nannoplankton from Syria. *Stockholm Contr. Geol.* **15**, 23-37.

..... 1968 Studies on Upper Eocene calcareous nannoplankton from NW Germany. *Ibid.* **18**, 13-74.

Hay, W. W., Mohler, H. and Wade, M.E. 1966 Calcareous nannofossils from Nal'chik (NW Caucasus). *Eclog. Geol. Helv.* **59**, 379-399.

Hay, W. W. and Towe, K. M. 1962 Electronmicroscopic examination of some coccoliths from Donzacq (France). *Ibid.* **55**, 497-517.

Kamptner, E. 1941 Die Coccolithneen der Suedwestkueste von Istrien. *Ann. Naturh. Mus. Wien*, **51**, 54-149.

..... 1950 Ueber den submikroskopischen Aufbau der Coccolithen. *Anz. Oesterr. Akad. Wiss., Math. Naturw. Kl.* **87**, 152-158.

..... 1954 Untersuchungen ueber den Feinbau der Coccolithen. *Arch. Protistk.*, **100**, 1-90.

Levin, H.L. 1965 Coccolithophoridae and related microfossils from the Yazoo Formation (Eocene) of Mississippi. *Journ. Paleont.* **39**, 265-272.

Levin, H. L. and Joerger, A. P. 1967 Calcareous nannoplankton from the Tertiary of Alabama. *Micropaleont.* **13**, 163-182.

Loeblich, A.R. and Tappan, H. 1963 Type fixation and validation of certain calcareous nannoplankton genera. *Proc. Biol. Soc. Wash.* **76**, 191-196.

Manivit, H. 1959 Contribution á l'étude des coccolithes de l' Eocéne. *Publ. Serv. Carte. Geol. Algerie*, ser. 2, Bull, **25**, 331-382.

Martini, E. 1958 Discoasteriden und verwandte Formen in NW-deutschen Eozaen (Coccolithophorida). 1. Taxonomische Untersuchung. *Senckenb. Leth.* **39**, 353-388.

..... 1960 Braarudosphaeriden, Discoasteriden, und verwandte Formen aus den Rupelton des Mainzer Beckens. *Notizbl. Hess. Landesant. Bodenforsch. Wiesbaden*, **88**, 65-87.

Martini, E. 1961 Der stratigraphische Wert der Lithostromationidae. *Erdoel Z.*, **77**, 100-103.

..... and Bramlette, M.N. 1963 Calcareous nannoplankton from the experimental Mohole drilling. *Journ. Paleont.* **37**, 845-856.

McIntyre, A., Bé, A.W.H. and Preikstas, R. 1967 Coccoliths and the Pliocene-Pleistocene boundary. Progress in Oceanography, 4 : The Quaternary history of the Ocean basins. Pergamon Press (Oxford & New York), 3-25.

Ostenfeld, C.H. 1899 Ueber *Coccosphaera* und einige neue Tintinniden in Plankton des nordlichen Atlantischen Oceans. *Zool. Anz.* **22**, 433-439.

Schiller, J. 1930 Coccolithineae. *In* Dr. L. Rabenhorst's Kryptogamen-Flora von Deutschland, Osterreich und der Schweiz. 10. *Abt. Leipzig : Akademische Verlagsgesselschaft*, 89-267.

Stradner, H. 1958 Die fossilen Discoasteriden Oesterreichs. I. Teil. Die in den Bohrkernen der Tiefbohrung Korneuburg 1 enthaltenen Discosteriden. *Erdoel. Z.* **74**, 178-188.

..... 1959 Die fossilen Discoasteriden Oesterreichs. II. Teil. *Ibid.* **75**, 472-488.

..... 1963 *In* Bachmann, A., Papp, A., and Stradner, H., Mikropalaeontologische Studien im "Badener Tegel" von Fraettingsdorf N. O. *Mitt. Goel. Ges. Wien* **56**, 117-210.

..... 1963 *In* Gohrbandt, K., Zur Gliederung des Palaeogen im Helvetikum nordlich Salzburg nach planktonischen Foraminiferen. *Ibid.*, 1-116.

Stradner, H. and Edwards, A. R. 1967 Electron microscopic studies on Upper Eocene coccoliths from the Oamaru Diatomite, New Zealand. *Jahrb. Geol. Bundesanst. wien* (in press).

Stradner, H. and Papp, A. 1961 Tertiaere Discoasteriden aus Oesterreich und deren stratigraphischen Bedeutung mit Hineisen auf Mexiko, Rumanien und Italien. *Ibid.* **7**, 159 pp.

Sullivan, F. R. 1964 Lower Tertiary nannoplankton from the California coast ranges. I Paleocene. *Univ. Calif. Publ. Geol. Sc.* **44**, 163-277.

..... 1965 Lower Tertiary nannoplankton from the California coast ranges. II Eocene. *Ibid.*, **53**, 1-75.

Tan Sin Hok 1927 Over de samenstelling en het onstaan van krijt en mergelgesteenten van de Molukken. *Jaarb. Mijnw. Nederl., Indie* **55**, 111-122.

Wallich, 1877 Observations on the coccosphere. *Ann. and Mag. Nat. Hist.* ser. 4, **19**, 242.

PLATE III

Figure 1	...	Photomicrograph of *Rhabdosphaera spinula* LEVIN, specimen with basal plate broken away. 3300X.
Figures 2—3	...	Photomicrographs of *Rhabdosphaera spinula*. 4100X.
Figures 4—5	...	Photomicrograph of *Rhabdosphaera perlonga* (DEFLANDRE) BRAMLETTE & SULLIVAN. 4500X.
Figure 6	...	Photomicrograph of *Zygrhablithus* sp. 4500X.
Figure 7	...	Scanning electronmicrograph of *Marthasterites tribrachiatus* (BRAMLETTE & RIEDEL) DEFLANDRE, showing the arch formed by two arms. Negative SM 3/31. 7850X.
Figure 8	...	Photomicrograph of *Zygrhablithus* (DEFLANDRE) DEFLANDRE, 4500X.

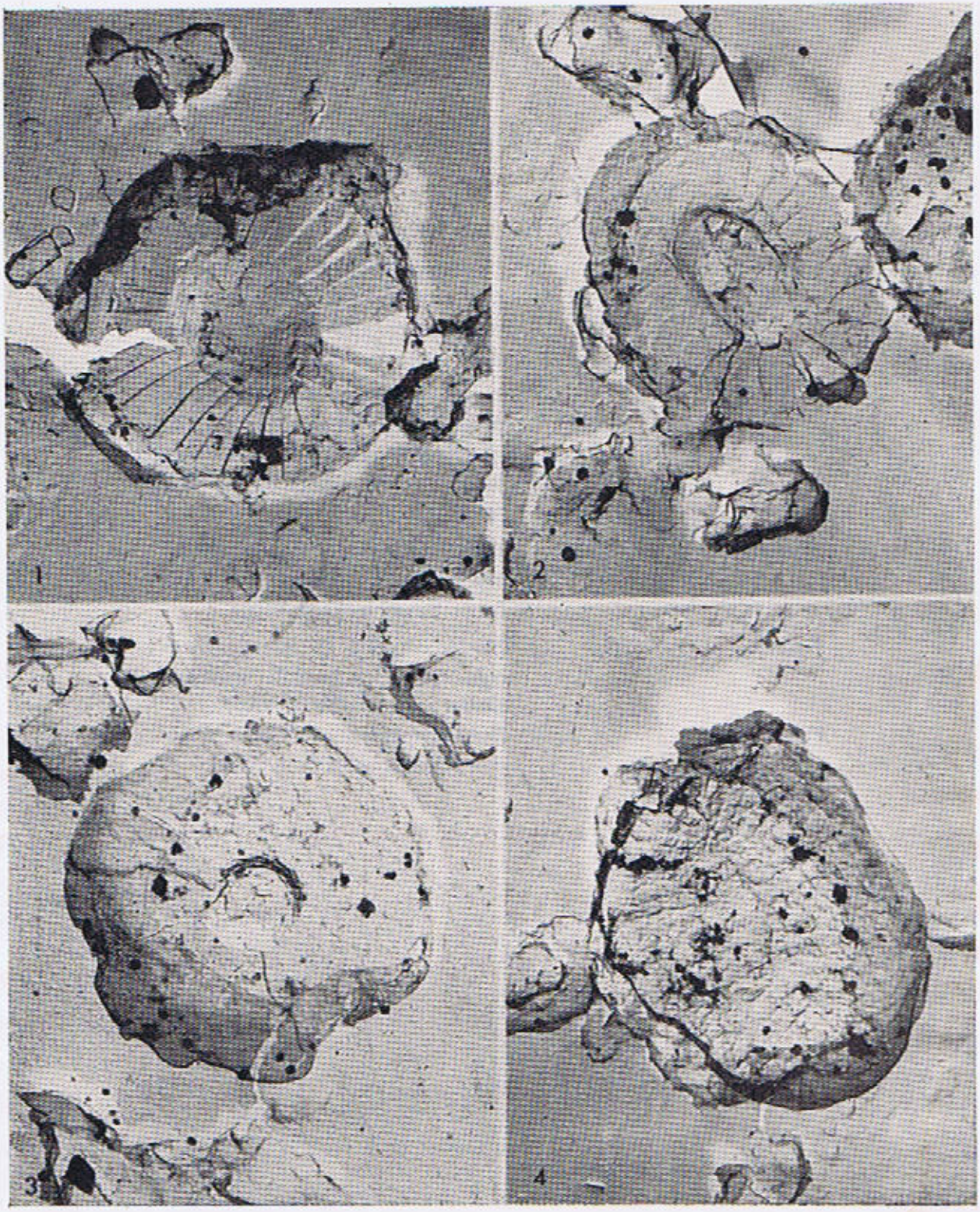
1
2
3
4

PLATE II

Figure 1 ... Transmission electronmicrograph of *Rhabdosphaera* sp., distal view with stem broken away from the basal shield. Negative FO 21. 12700X.

Figure 2 ... Transmission electronmicrograph of *Marthasterites tribrachiatus* (BRAMLETTE & RIEDEL) DEFLANDRE, juvenile form. Negative FO 20. 3600X.

Figure 3 ... Transmission electronmicrograph of *Marthasterites tribrachiatus*, adult form. Negative FO 32. 9000X.

Figure 4 ... Photomicrograph of *Marthasterites tribrachiatus*, a juvenile specimen similar so that in fig. 2. 3300X.

Figure 5 ... Photomicrograph of *Marthasterites tribrachiatus*, adult form. 3300X.

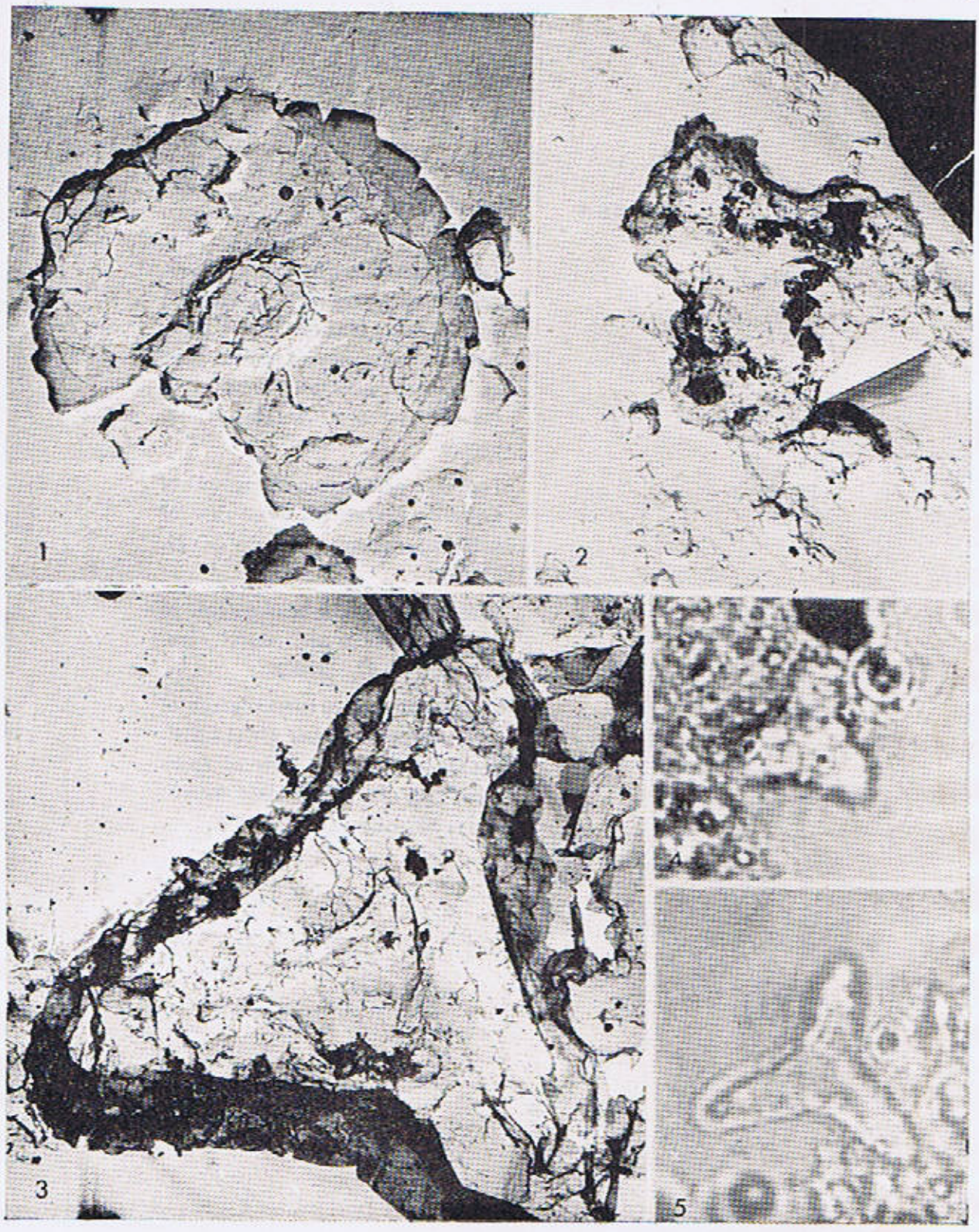
1
2
3
4
5

PLATE I

Figure 1 ... Transmission electronmicrograph of *Coccolithus pelagicus* (WALLICH) SCHILLER, proximal view. The carbon film is ruptured so as to give an apparent subspherical shape to this elliptical form. Negative FO 22. 9000X.

Figure 2 ... Transmission electronmicrograph of *Coccolithus pelagicus*, distal view of corroded specimen. Negative FO 23. 12700X.

Figure 3 ... Transmission electronmicrograph of *Cycloplacolithella* sp., distal view. Negative FO 27. 12700X.

Figure 4 ... Transmission electronmicrograph of *Helicosphaera carteri* (WALLICH) KAMPTNER, distal view of specimen with proximal shield broken away. Negative FO 15.12700X.

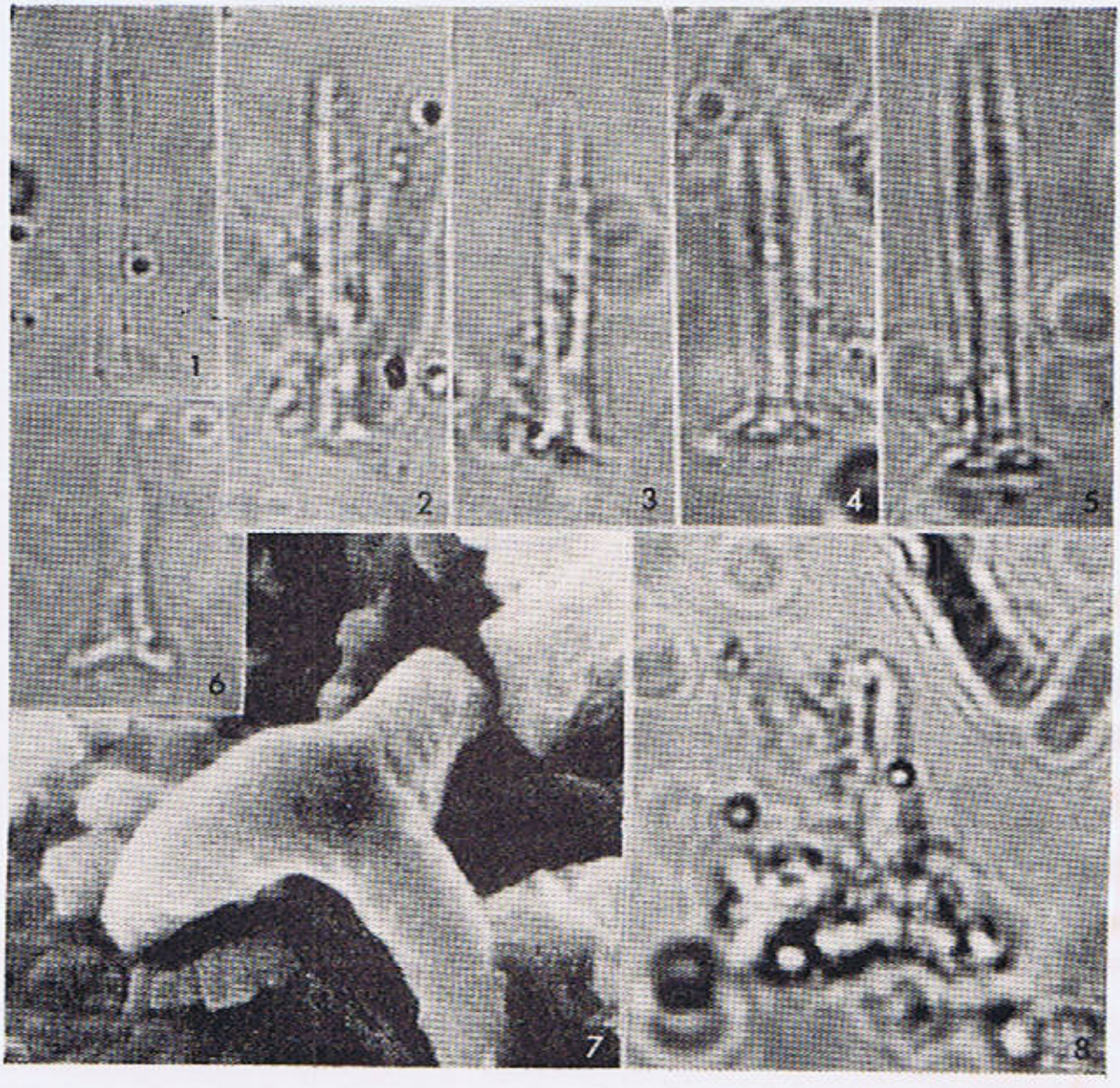
1
2
3
4
5
6
7
8

PLATE IV

Figures 1—2	...	Transmission electronmicrographs of *Discoasteroides kuepperi* (STRADNER) BRAMLETTE & SULLIVAN; fig. 1 : proximal view, fig. 2 : distal view. Negatives FO 14 and FO 25. 5400X.
Figures 3—4	...	Photomicrographs of *Discoasteroides kuepperi*, proximal view. Fg. 3 : 2070X ; fig : 4.4500X.
Figures 5—6	...	Photomicrographs of side view of *Discoasteroides huepperi*. 4500X.

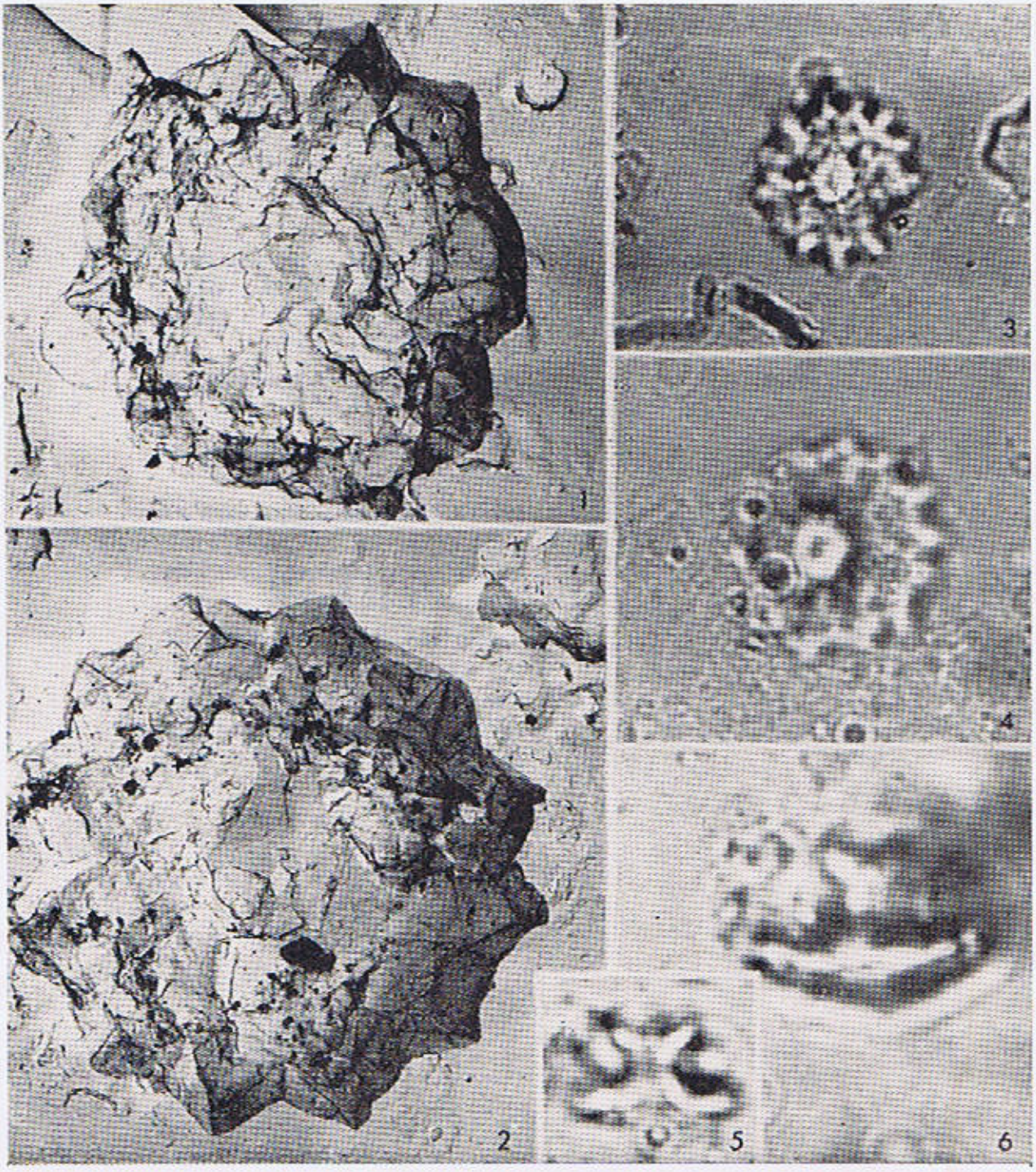
1
2
3
4
5
6

PLATE V

Figures 1, 2 & 5	...	Photomicrographs of *Zygolithus chiastus* BRAMLETTE & SULLIVAN, distal views. Fig. 1 : 4100X; fig. 2 : 4500X; fig. 5 : 3300X.
Figure 3	...	Photomicrograph of *Zygolithus* sp. 3300X.
Figure 4	...	Photomicrograph of *Ceratolithus* sp. 3300X.
Figure 6	...	Transmission electronmicrograph of distal view of *Ericsonia ovalis* BLACK, poor preserved specimen. Negative FO 24. 9000X.
Figure 7	...	Transmission electronmicrograph of *Zygolithus* sp. distal view of a specimen similar to fig. 3, central area filled-in with secondary material. Negative FO 29. 12700X.

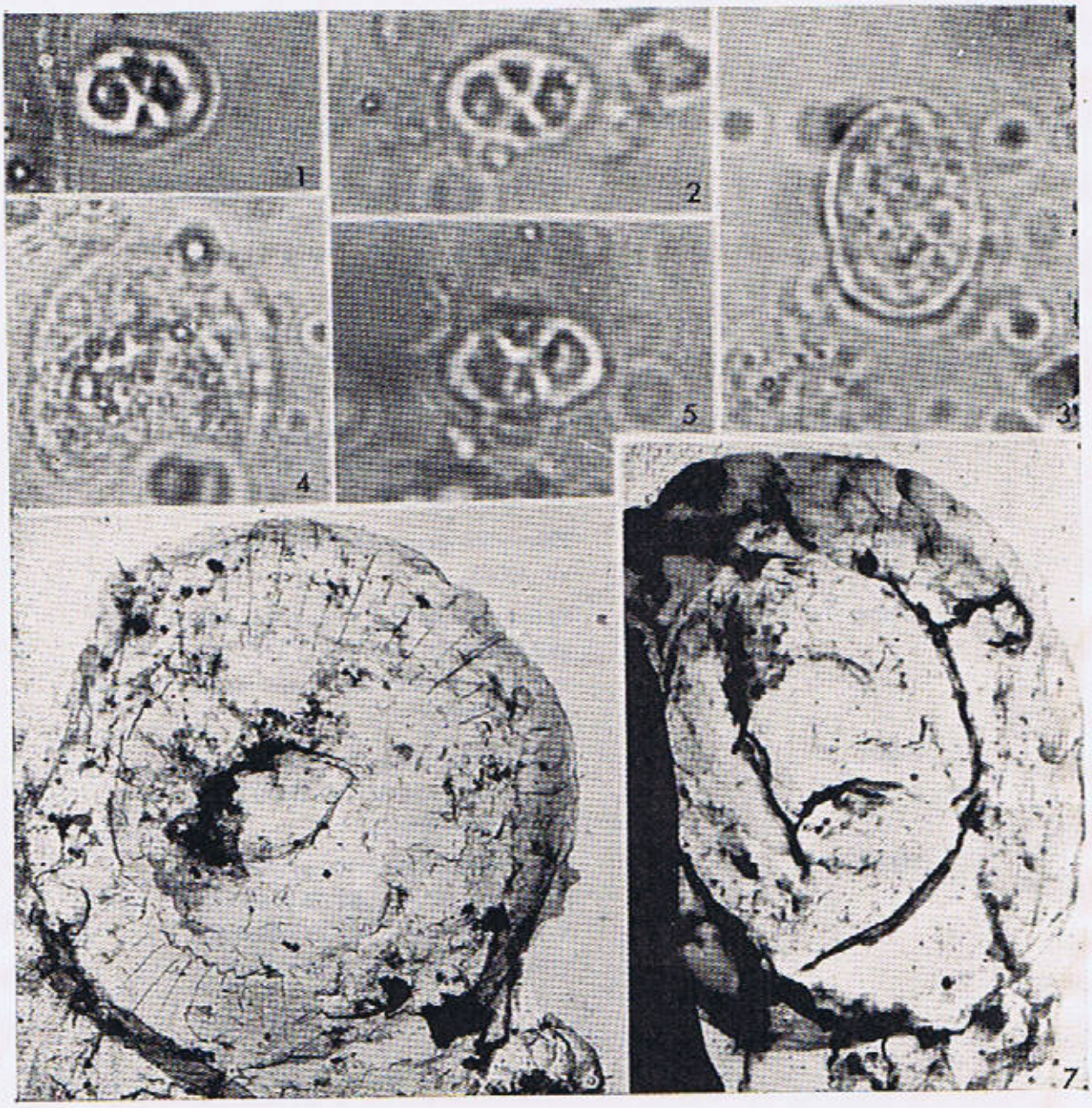
1
2
3
4
5
7

PLATE VI

Figures 1—3	...	Photomicrographs of *Discolithina-plana* (BRAMLETTE & SULLIVAN) LEVIN, distal views. Fig. 1 : 3300X; figs. 2 & 3 : 4100X.
Figure 4	...	Photomicrograph of *Lophodolithus nascens* BRAMLETTE & SULLIVAN, distal view. 4500X.
Figure 5	...	Photomicrograph of *Zygodiscus* aff. *Z. plectopons* BRAMLETTE & SULLIVAN, 3300X.
Figure 6	...	Photomicrograph of *Lithostromation* sp. 4100X.
Figure 7	...	Photomicrograph of *Coccolithus delus* (BRAMLETTE & SULLIVAN) of a specimen with central cross partly broken. 3300X
Figure 8	...	Photomicrograph of *Helicosphaera carteri* (WALLICH) KAMPTNER, distal view. 4100X.
Figure 9	...	Photomicrograph of *Coccolithus* aff. *C. staurion* BRAMLETTE & SULLIVAN, proximal view of specimen with central cross broken. 3300X.

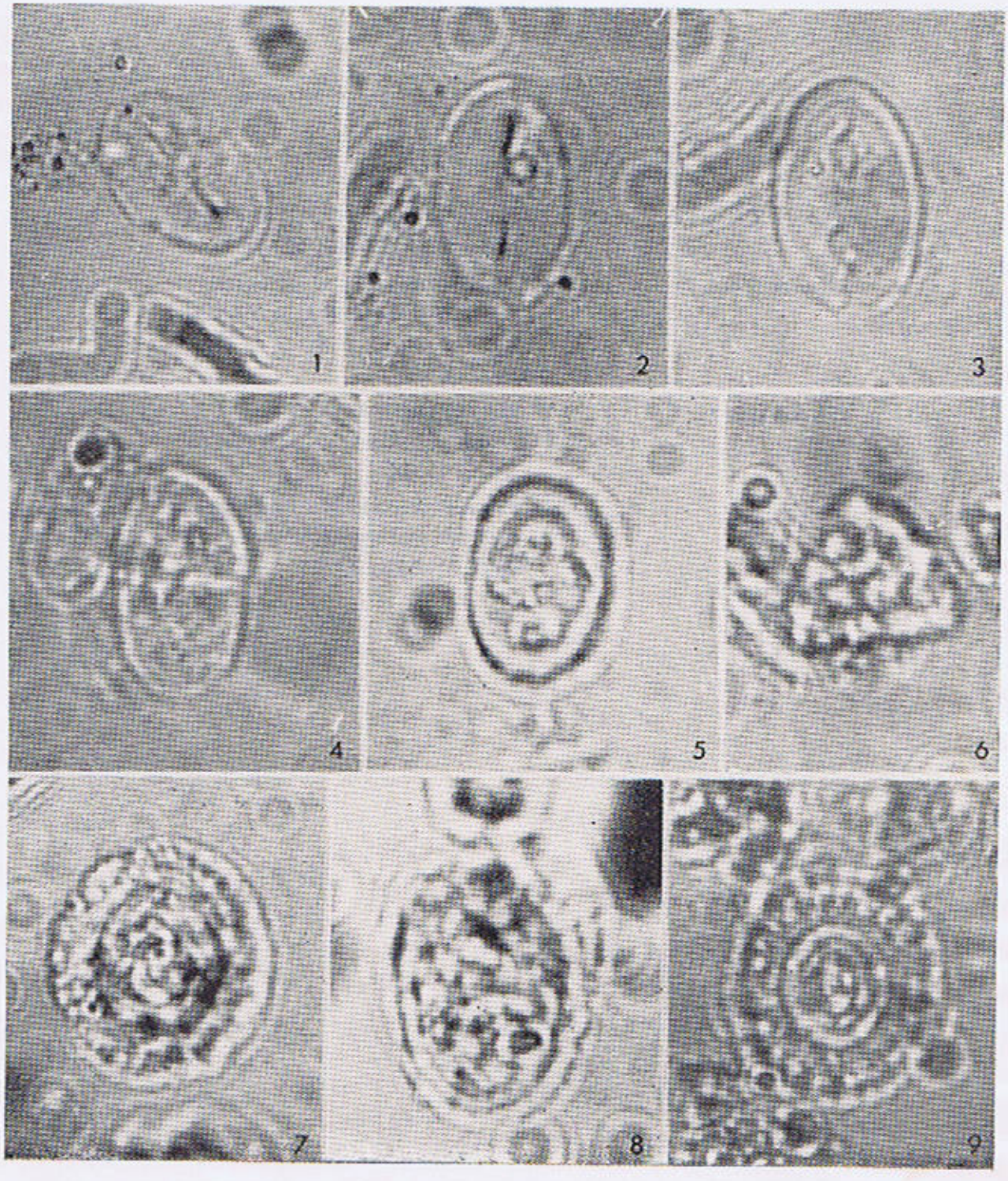
1
2
3
4
5
6
7
8
9

PLATE VII

Figures 1 & 2	...	Photomicrograph of *Discoaster barbadiensis* TAN SIN HOK, 4100X.
Figures 3, 6 & 7	...	Photomicrographs of *Discoaster lodoensis* BRAMLETTE & RIEDEL, Fig. 3 : 2070X ; fig. 6 : 3300X; fig. 7 : 4100X.
Figures 4 & 5	...	Photomicrographs of *Discoaster* aff. *D. septemradiatus* (KLUMPP) MARTINI. 3300X.
Figure 8	...	Photomicrographs of a partly broken specimen of *Polycladolithus operosus* DEFLANDRE. 3300X.

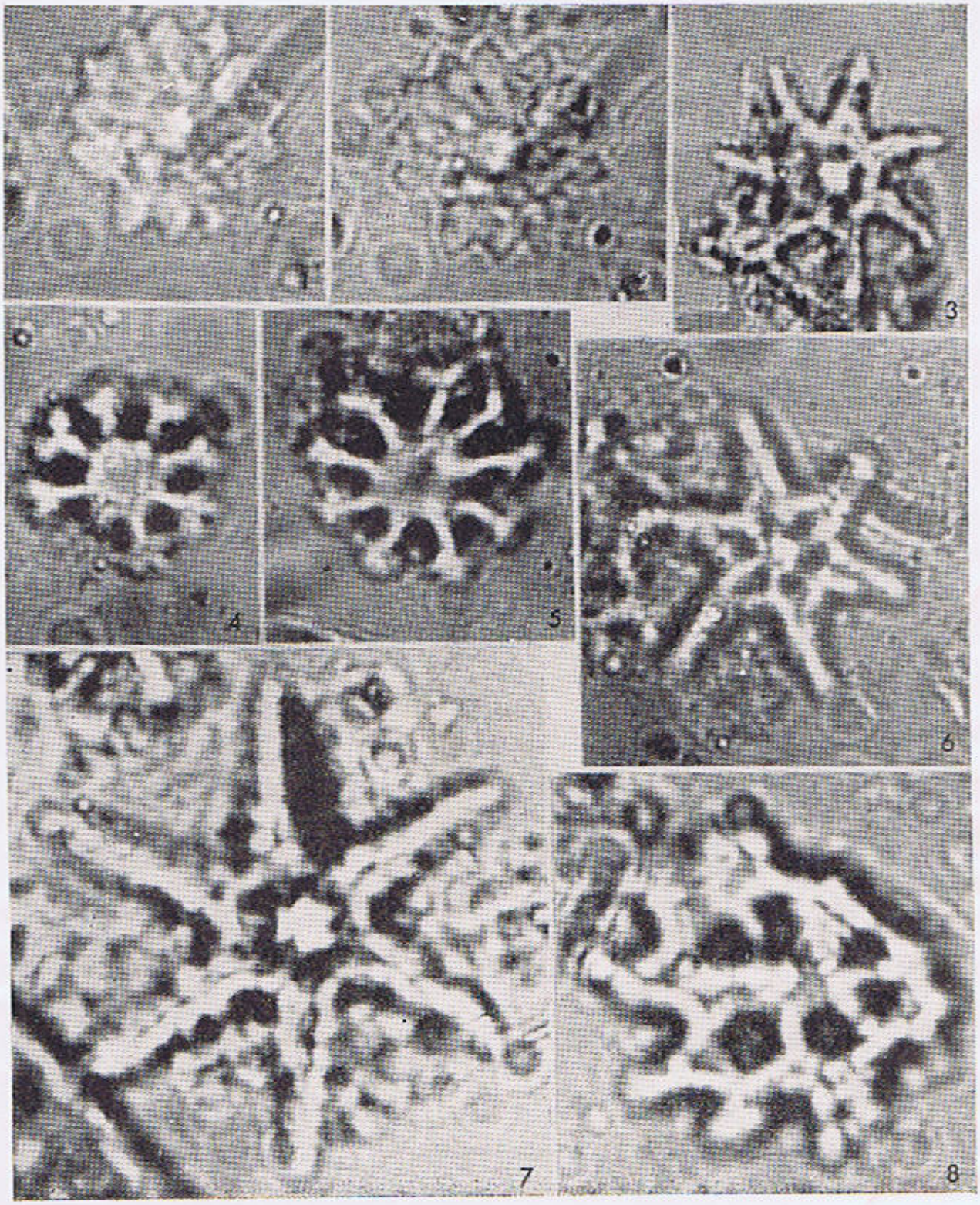
1
2
3
4
5
6
7
8

PLATE VIII

Figures 1—3	...	Photomicrographs of *Discoaster sublodoensis* BRAMLETTE AND SULLIVAN. Figs. 1 & 3 : 3300 X ; fig. 2 : 4100 X.
Figures 4, 6 & 7	...	Photomicrographs of *Discoaster saipanensis* BRAMLETTE AND RIEDEL. Figs. 4 & 7 : 4100 X ; fig. 6 : 3300 X.
Figure 5	...	Photomicrograph of *Discoaster* aff. *D. mediosus* BRAMLETTE AND SULLIVAN. 4500 X.
Figure 8	...	Photomicrograph of *Discoaster* sp. 4100 X.

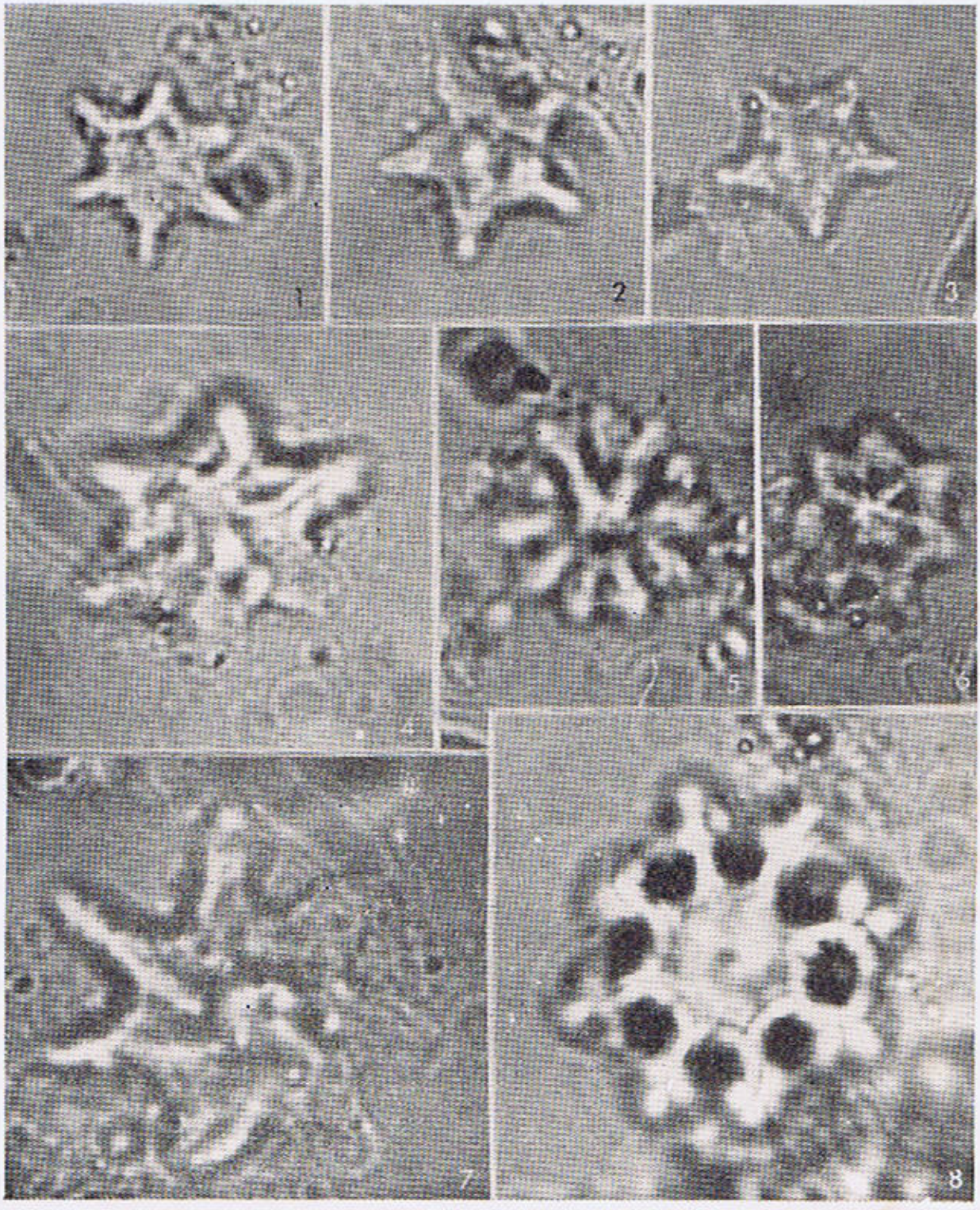
1
2
3
4
5
6
7
8

NOTICES, ABSTRACTS AND REVIEWS

NOTE ON THE DISCOVERY OF CARBONATITE ROCKS IN THE CHAMLA AREA, SWAT STATE WEST PAKISTAN

HISTORY OF DISCOVERY

Following the discovery of an alkaline rock complex in Swat (Siddiqui, 1965), detailed mapping of the area was undertaken and presence of some "calcite" veins in the syenite was noticed by A. Shakoor and two M.Sc. students of the Geology Department, Panjab University. This information was passed on to the author who visited the area during August 1966, and found that the veins, mentioned above, contained pyroxene and feldspar in addition to carbonate minerals. Subsequent petrographic work showed that the pyroxene was aegiritic in nature and that apatite was also present in abundance.

The field relations and mineralogy of the rock was thus found to have features similar to some known carbonatite rocks. For further confirmation, two samples were submitted to Dr. T. Deans of the Institute of Geological Sciences, Great Britain, who arranged their X-ray fluorescence analysis at his laboratory (Special Report No. 252, 1967). The results showed heavy traces of Ba, Sr and the rare earths Ce and Y, with minor traces of La (See Table No. 1).

On the basis of these investigations it was concluded that these rocks are in fact carbonatite and an announcement to the effect was made in the Commonwealth Liaison Office Newsletter for October and November 1967.

The present note is intended to report further progress on the work being conducted by the author. The rocks have been named as the "Naranji Kandao Carbonatite" in reference to the place where the occurrence was first noticed.

FIELD RELATION

The alkaline complex (named the Koga Alkaline Complex of which the carbonatite makes a part) is an oval shaped body with the long axis approximately 5 miles and the short axis about 2½ miles in length (Fig. 1). It is intrusive into the granitic portion of the Ambela Granitic Complex (Martin et. al. 1962).

Modally, the alkaline rocks range from undersaturated aegirine and feldspathoid-bearing syenites to slightly oversaturated biotite-bearing nordmarkites. Further field work is in progress to map the various units within the complex and to establish their genetic and age relations.

The carbonatite rocks are confined to the western part of the syenite body and occur in the form of lenses, pockets and veins, that may vary from a few inches to a few feet in thickness, with lengths of upto a few yards. The host rock at Naranji Kandao is a medium grained nepheline syenite with flow structure marked by the parallel alignment of feldspar laths. Biotite is present in small amounts and is probably the sole mafic mineral present apart from minor amounts of magnetite.

In contrast, the carbonatite is coarse grained and generally lacks prominent mineral orientation. Its veins cut across the flow structure in the syenite.

STRUCTURES WITHIN THE CARBONATITE VEINS.

Majority of veins are filled with massive carbonate-silicate material. Flow structure, in which the constituent crystals lie with their largest surfaces parallel to the walls of the veins, such as observed at Mountain Pass (Olson, 1954) and Chilwa Island (Garson, 1955) has not been observed in the Naranji Kandao carbonatite so far.

Instead, in a few veins, where layering is present, tabular or acicular crystals tend to lie with their longest dimensions perpendicular to the walls of the vein. This feature is strikingly displayed in a detached slab (6′ × 3′ size) of carbonatite, lying on the slope just west of Naranji Kandao. The slab shows a cross-section of a composite vein consisting of at least five parallel layers or strands. Four of these strands are about 3″ thick each, while the fifth one is

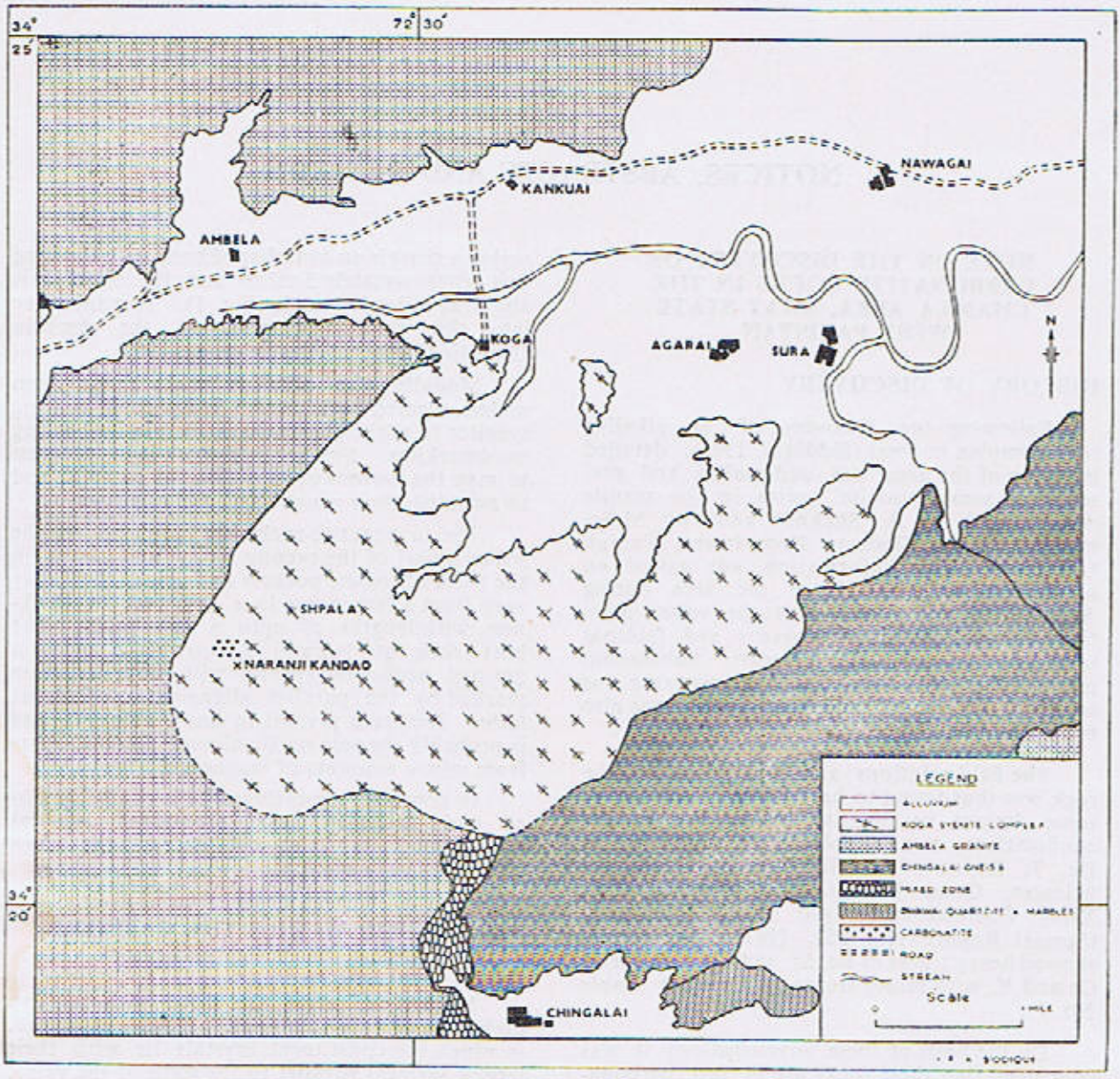

Fig. 1. Geological Map of Koga area showing carbonatite occurrence in Koga syenite complex.

more than a foot thick. Each of the four strands shows slightly divergent growth of acicular pyroxene crystals, almost at right angles to the walls of the strands (Fig. 2). The fifth strand shows the same arrangement but the grain size is much coarser and crystals of pyroxene upto six inches long are present (Fig. 3).

The middle portion of each strand is occupied by carbonate minerals, mainly calcite with minor dolomite, while the margins have abundant apatite. It is interesting to note that pyroxene crystals show a progressive thickening towards the middle of the srands (Figs. 2 & 3).

MINERALOGY AND PETROGRAPHY

Minerals present in the Naranji Kandao Carbonatite include: calcite, dolomite, aegirine augite, arfvedsonite, albite, microcline microperthite, biotite, sphene, apatite, monazite, barite and pyrite (now mainly pseudomorphed by goethite) and rare quartz.

Fig. 2. Pyroxene cyrstals (dark) in divergent growth almost perpendicular to the wall of veinlets of carbonatite. The photograph is a specimen broken from the junction of two adjacent strands in a composite vein. Carbonate (white).

Calcite is the most common carbonate mineral present. Its grain size ranges from a fraction of an inch to two or three inches. One peculiarity of this calcite is that it shows parting parallel to (0001). Often present along such partings are crystals of apatite, albite and aegirine augite, giving a streaky appearance on cleavage faces. Dolomite occurs as minute discrete crystals, normally visible only under the microscope.

Next to carbonate minerals in abundance is pyroxene and the carbonate-pyroxene assemblage is the most common (Fig. 4). Pyroxene is mostly aegirine-augite which occurs as coarse crystals, often partially or completely replaced by arfvedsonite (negative elongation, $c \wedge X = 28°$, pleochroism dark green to pale yellowish green).

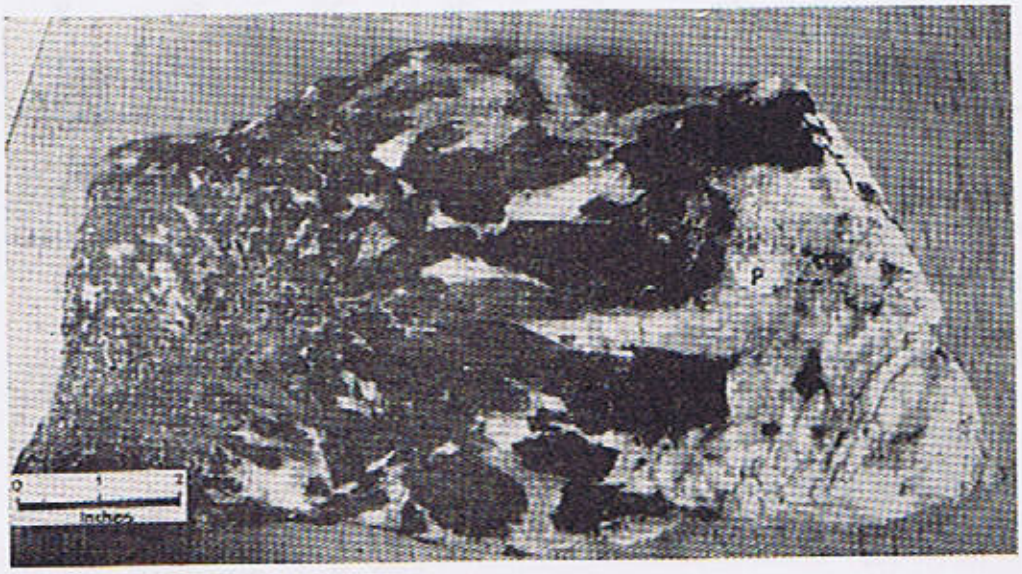

Fig. 3. Divergent growth of coarse pyroxene cyrstals (black) almost perpendicular to the walls of a carbonatite vein. White areas near the scale contain abundant apatites rest of white area mainly carbonates. P, plagioclase. Note thickening of pyroxene crystals towards the middle of the veins.

A common feature of pyroxene crystals is the presence, in them, of abundant microscopic, drop like inclusions of carbonate and of prismatic apatite.

K-feldspar is microcline with microperthitic intergrowth of albite. Microcline often shows strong undulose extinction or patchy chessboard like extinction which in some crystals resolves into sharp cross-hatched twinning. Apart from its presence in microperthite, albite (3-4%An) is also present as separate subhedral grains. Biotite (pleochroic from yellow to dark brown) occurs as minute grains showing curved

Fig 4. Pyroxene (black) in coarse carbonate matrix.

lamellae. Apatite is a rather abundant mineral in many specimens ; in some cases it may make up as much as 50% of the bulk of the rock. It occurs as euhedral to subhedral, short prismatic crystals. Sphene, monazite, barite and pyrite occur only in accessory amounts. A few microscopic grains of quartz have been noticed in one specimen.

At the contact of carbonatite veins etc., the commonly hard syenite becomes weak and yields easily to hammer. This appears to have happened due to calcite deposition along the grain boundaries and in the cracks within the constituent grains of the syenite. Furthermore, at the calcite-feldspar contact, the latter crystals are embayed, which indicates replacement by the former.

GEOCHEMISTRY

The trace element content of these rocks compares well with the characteristic range in known carbonatites elsewhere in the world. The results of X-ray fluorescence analysis at the Institute of Geological Sciences, Great Britain are reproduced in Table No. 1.

TABLE No. 1

Trace element contents of Naranji Kandao Carbonatite (Reproduced from Institute of Geological Sciences London, Special Rep. 252, 1967)

		Approximate Percentage of Metal					
		Ce	La	Ba	Nb	Sr	Y
Sample	8855	0.07	Trace	0.09	n.d.	2.46	0.005
Sample	8945	0.07	n.d.	0.08	n.d.	0.90	0.005

n.d.=not detected.

CONCLUSIONS

This preliminary study has suggested that Naranji Kandao Carbonatite may be classed together with 'Apatite-Magnetite variety of Pecora (1956) (as against the rare-earth mineral variety) : examples of which include such classic occurrences as Fen, Alnö, Kaiserstuhl and Magnet Cove etc.

The present carbonatite differs from those mentioned above, in its geologic occurrence. It is one of the few carbonatites which occur in a fold mountain belt and its discovery encourages further search for carbonatites in the Himalayas.

Further work is in progress on detailed field mapping, petrology and geochemistry of the entire alkaline rock complex in Chamla area, Swat State.

ACKNOWLEDGEMENTS

I am grateful to Mr. F. A. Shams for critically reading the manuscript. Thanks are due to Prof. R. G. Davies for arranging analysis of rocks through Dr. T. Deans whose help is hereby grateful acknowledged.

FUZAIL A. SIDDIQUI
Department of Geology,
Panjab University, Lahore
November, 1967.

REFERENCES

Bradshaw, N.A., and Livingstone A. 1967 Special Report No. 252, Institute of Geological Sciences, Great Britain.

Garson, M.S. 1955 Flow phenomena in Carbonatites in Southern Nyasaland : *Colonial Geol. and Min. Res.* 5, No. 3, 311-318.

Martin, N.R., Siddiqui, S.F.A. and King B. H. 1962 A geological reconnaissance of the region between the Lower Swat and Indus Rivers of Pakistan, *Geol. Bull. Panjab Univ.* No. 2, 1-14.

Olson, J.C., Shaw, D. R. Pray, L. C. and Sharp, W. N. 1954 Rare-earth mineral deposits of the Mountain Pass district, San Bernardino county, California, *U. S. Geol. Survey Prof. Paper* **261**, 47.

Pecora, W. T., 1956 Carbonatites : A Review. *Bull. Geol. Soc. Amer.* 67, 1537-1556.

Siddiqui, S. F. A. 1965 Alkaline Rocks of Swat, Chamla, *Geol. Bull, Punjab Univ.* No. 5, 52.

A NOTE ON RADIOMETRIC AGES OF MICAS FROM SOME GRANITES OF THE MANSEHRA-AMB STATE AREA, NORTHERN WEST PAKISTAN

One of the controversial aspects of Himalayan geology is age of the granitic intrusions that form voluminous outcrops along almost all the Himalayan belt. Right from the beginning of geological work in the Himalayas, it was generally felt that these intrusives bodies could be grouped into two types (Pascoe, 1963) :—

(*i*) dominently foliated calc-alkaline granites, with essential biotite and/or hornblende and subordinate muscovite, and accessory ore, garnet, apatite, tourmaline and zircon. This was called the Central Gneiss or the Himalayan Gneiss. It occurs as sheet-like bodies which form continuous outcrops over long areas and show remarkable parallelism between their strike and dip and that of the foliation of the enclosing strata.

(*ii*) dominently unfoliated sodaclase granites with essential muscovite, tourmaline and sometime hornblende, and subordinate biotite and accessory garnet, epidote and ore minerals. In the field, they occur as small plutons or sheet-like bodies that are rather sporadically distributed and frequently intrude the Central Gneiss.

Perusal of the literature shows that there has never been any major difference of opinion about the age of second group of granites ; assuming their essentially unfoliated nature, they are believed to have been emplaced during the period of waning Himalayan orogeny, and are loosely called Tertiary granites, although as Pascoe (loc. cit.) writes "the actual evidence of such sofar found is not as widespread as it was at first supposed" (p. 1420).

The controversy turned upon the question of the age of the Central Gneiss. The proposed ages range from Palaeozoic (Carboniferous, Auden (1932); Infra-Triassic, Middlemiss (1896) to Tertiary (Tertiary, Hayden (1907); early Miocene, MacMahon (1833). These ideas were based on the general concepts of the writers rather than direct evidence. On record, however, is an important discovery, made by Auden (loc.cit.) of a granitic pebble in the breccia at the base of the "Purple Series" of Garhwal. Lithologically, this pebble was found to be identical to the Arwa granite, a member of the Central Gneiss, and therefore Auden claimed that the Central Gneiss cannot be younger than Carboniferous.

According to Wadia (1939) there are three types of granites in Kashmir Himalayas :—

(*i*) A biotite granite, most widespread from Kashmir to Assam.

(*ii*) A hornblende granite, less common than (*i*) but similar in structure and composition. It is thought to be post-Cretaceous, as it was found to be intrusive into an orbitolina limestone at the head of the Burzil valley.

No age is suggested for the biotite granite, but it is considered to be earlier than the hornblende granite ; it will be pre-Cretaceous anyway.

(*iii*) Tourmaline granite, more recent than (*i*) and (*ii*) as it intrudes them.

Misch (1949) has been concerned with the Nanga Parbat granites. He claims that the various types, as described by him and earlier recognized by Wadia (1939), have so close affinites that no real age sequence can be found. According to him the granite of Nanga Parbat is a product of syntectonic granitization while the tourmaline granites are the product of the continuation of this process in the post-tectonic period. It follows from this that the main granite is post-Cretaceous and the tourmaline granites are much younger.

Among various problems posed by Mansehra-Amb State by this area is that of the age of the granites. In view of the contradictions outlined above, no conclusions from the other areas could be applied to the area under investigation. It was thought useful to find out whether the granites were older or not than the Himalayan orogeny that is Tertiary in the main. Mica concentrates from three specimens, representative of the major intrusive bodies, were sent to the Department of Geophysics, Australian National University for examination, and their ages, based on the K/Ar ratio, are given below :—

Rock	*Locality*	*Mineral*	*Age (m. years).*
1. Susalgali gneiss.	Near Susalgali.	Biotite	79
2. Mansehra granite.	Near Mansehra Rest House.	Biotite	83
3. Hakale granite.	Near Thakra	Muscovite	165

Although the number of age determinations is very small, they all indicate an age definitely older than the Himalayan orogeny. It is note-

worthy that while the Hakale granite is intrusive into the Mansehra granite, its age has turned out to be older. According to Dr. MacDougall (personal communication) this may be due to the fact that muscovite retains radiogenic argon better than biotite. Another reason may be that while the Hakale granite is essentially unfoliated, the main granitic complex is foliated so that its geological time-clock might have been readjusted during Himalayan orogeny. Considering the conclusion (to be published elsewhere) that the granitic complex originated by magmatic granitization of pre-existing rocks, the mica minerals do not seem to be very useful ingradients for age determination. As these are believed to have been mostly derived from pre-granitic metamorphic rocks, any age data based on them may not be applied to the granitic rocks ; rather their ages may give ideas about certain phases of metamorphism that may or may not be related to the period of genesis of the granitic complex. Feldspar minerals are considered more reliable and are being subjected to age determination.

F. A. SHAMS
Department of Geology,
Panjab University, Lahore.
September, 1967.

REFERENCES

Auden, J.B. 1932 On the age of certain Himalayan granites. *Rec. Geol. Surv. India* 66, 461-471.

Hayden, H.H. 1913 Notes on the relationship of the Himalayas and the Indo-gangetic plain and the Indian peninsula. *Rec. Geol. Surv. India* 43, 138-167.

MacMahon, C.A. 1833 On the microscopic structure of some sub-Himalayan rocks of Tertiary age. *Rec. Geol. Surv. India* 16, 186-192.

Middlemiss, C.S. 1896 The geology of Hazara and the Black mountain. *Rec. Geol. Surv. India* 26, 1-302.

Misch, P. 1949 Metasomatic granitization of batholithic dimensions. *Amer. Jour. Sci.* 247, 209-245, 673-705.

Pascoe, E. 1963 Manual of Geology of India, Govt. of India Press, Vol. III.

Wadia, D.N. 1939 The Geology of India, MacMillan, London, revised Ed. 1961, 90-92.

"CRYSTDEM"—A SIMPLE MODEL OF THREE CO-CENTRAL AXES FOR USE IN TEACHING CRYSTALLOGRAPHY.

INTRODUCTION

In geological training as well as in research we generally deal with problems that require three dimensional perspective. This is particularly true of the science of Crystallography in which every crystalline material is classified and oriented in terms of crystallographic axes.

The crystalline matter is classified into six crystal systems, namely, the cubic, the tetragonal, the hexagonal, the orthorhombic, the monoclinic and the triclinic systems. Crystals belonging to the hexagonal system have three equal horizontal axes, making angles of 120° with each other and a vertical axis at right angle to the horizontal axes. The other five systems have only three axes, out of which, the cubic, the tetragonal and the orthorhombic systems have three axes at right angles to one another, while in the monoclinic system there are three axes, one vertical, one at right angles to the vertical and the third making an oblique angle with the plane containing the other two. The triclinic system has three axes, none of which is at right angles to any other.

From the above it is clear that a model for teaching crystallography and illustrating the position of the axes in different systems should be manoeuvrable so as to allow the manipulation of the axes. There are some such models available in the market, but they are either too expensive or not versatile enough to enable the students to grasp these concepts. During course of routine teaching of crystallography in this Department, a need was felt for a simple and yet inexpensive model. Consequently the author designed and prepared a prototype of a model to meet this demand. The model is described below in some detail.

DESCRIPTION AND CONSTRUCTION OF THE MODEL

The construction of this model is done in three stages. First stage consists of the preparation of parts, A, B, C, C_1 and a_3, a_4, b_3, b_4,

(Figure 1). These components govern the movements of the north-south axis.

Component "A" is a ball of mild steel with arms a_1 and a_2. The diameter of this ball is 15 mm. and the threaded arms have a diameter of 5mm. and a length on each side of 20mm.

Component "B" is a block of mild steel with initial dimension of 100mm. ×22mm × 18mm. Cylindrical hole "H" is drilled through the block in the centre and at right angle to the 22mm. × 100mm. face. The diameter of this hole should be controlled with piston precision to accommodate ball "A". The two ends of the hole "H" are then widened to 20mm. diameter, to a depth of 7mm. on both sides leaving a 4mm. long hole in the midddle to retain the original diameter. The two wider ends of the hole "H" are then subjected to thread cutting.

Components C, C_1 are a pair of rings 7mm. in width to be screwed on either sides of hole "H". The inner diameter of the two rings is a shade less than that of ball "A" so that the ball may remain fixed in between the rings while the arms are allowed to move freely. To increase the angle of movement of arms a_1 and a_2, the inner diameter of rings is tapered.

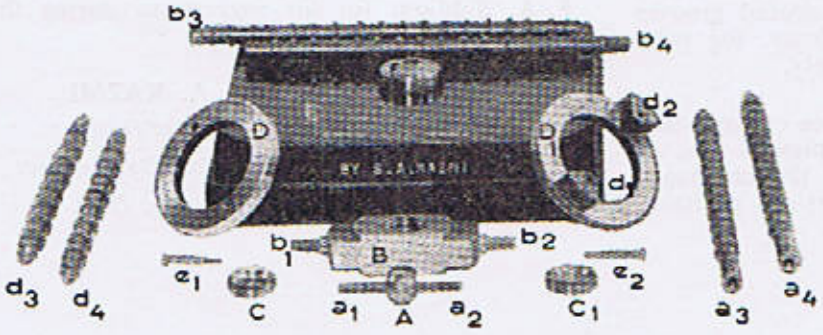

fig. 1

fig. 2

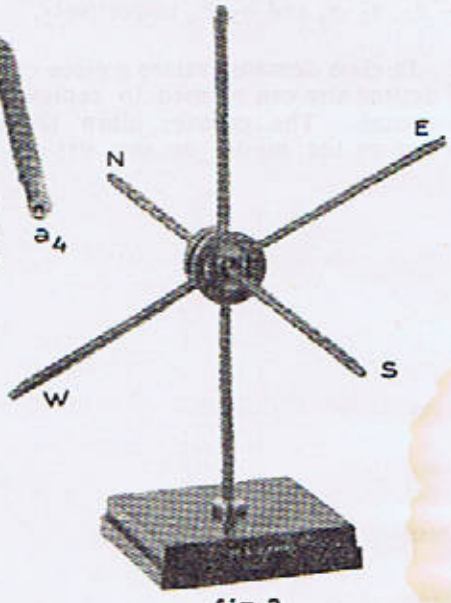

fig. 3

For any further machining the author recommends the use of a tool of mild steel 5cm. long, threaded at one end to fit into hole "H". Proper orientation of component "B" is facilitated by use of such a tool. The rest of the machining on component "B" is carried out according to the dimensions shown in the Fig. 2.

Brass rods a_3 and a_4 will be fixed in position a_1, a_2 and brass rods b_3, b_4 in positions b_1 and b_2. The dimensions for the brass bars are given towards the end of this paper.

In the second stage relatively simple parts, such as D, D_1, d_1, d_2, d_3, d_4 and e_1, e_2 are to be prepared. This stage will govern movements of the east-west axis.

Component D, D_1 consists of two identical brass rings, each with inner diameter 45.5mm., outer diameter 68mm. and thickness 7mm. Component d_1, d_2 consists of a pair of supports roughly triangular in shape which are placed in diametrically opposite positions, in between the two rings D, D_1, after placing the latter on either side of component "B". D, D_1 are held together with the help of screws e_1, e_2 which also pass through d_1, d_2. Care should be taken to see that the thickness of d_1, d_2 is a little over 12mm. so that it does not jam movement of rings D, D_1. Finally, bars d_3, d_4 are screwed into the curved face of the parts d_1, d_2.

Third and the last stage is to prepare a base which can take b_3, b_4 vertically to establish the vertical axis of this model.

Component "E" is a wooden board with dimensions roughly 18cm. ×18cm.× 4cm. The function of the vertical axis is served by bars b_3, b_4 screwed to either ends of component B, in position b_1, b_2. The free end of bar b_4 is fixed to the centre of the wooden board E by a bolt and screw mechanism "f".

The three pairs of brass bars, namely a_3 -a_4, b_3 -b_4, and d_3 -d_4 are identical and have a diameter of 1cm. The length of the brass bars is so arranged that the distance of the free end of all the bars is 22cm. from the centre of the device. The free ends of the bars are extendable by a telescopic arrangement. Each pair of bars is also marked by evenly spaced grooves with intervals of 20, 15 and 10mm. for pairs d_3- d_4, a_3 -a_4 and b_3 -b_4 respectively.

In class demonstrations a piece of cardboard of desired size can be used to represent face of a crystal. The grooves allow the cardboard to rest on the model in any desired position. For further stability of the cardboard piece, rings from a polythene tube may be superimposed on the grooves.

It may be mentioned that since this is an experimental model, modifications and improvements are possible and suggestions for the same will be welcomed by the author.

ACKNOWLEDGEMENTS

I am much grateful to Mr. F. A. Shams for having acquainted me of the need for the construction of such an apparatus and for his help and guidance. Thanks are due to Dr. S. F. A. Siddiqui for his suggestions during the preparation of this paper.

S. A. KAZMI

Department of Geology,

Panjab University, Lahore.

October, 1967.

STAFF LIST OF THE DEPARTMENT OF GEOLOGY, UNIVERSITY OF THE PANJAB (AT THE 31st DECEMBER, 1967)

1. Teaching Staff

Name and Qualifications	*Subject*	*Appointed*
Professor of Geology.	Vacant	
Readers :		
Mr. F. A. Shams, M.Sc. (Pb.), M.A. (Cantab). Head of the Department.	Mineralogy, Petrology, X-Ray Crystallography.	November, 1956.
Mr. M. A. Latif, M.Sc. (Pb.), M.Sc. D.I.C. (London)*	Micropalaeontology, Stratigraphy.	July, 1957.
Dr. Aziz-ur-Rehman, M.Sc. (Pb.), D. Rehr. Nat. (Munich).	Applied Geophysics	February, 1960.
Mr. A. H. Gardezi, M.Sc. (Pb.), M.Sc., D.I.C. (London)**	Petroleum Geology, Structure.	March, 1962.
Lecturers :		
Dr. M. A. Chaudhry, M.Sc. (Pb.), Ph.D. (Reading)	Sedimentology, Geomorphology.	June, 1959.
Dr. A. A. Butt, M.Sc. (Pb.), Ph.D. (Utrecht)	Micropalaeontology Stratigraphy.	June, 1959.
Dr. S. F. A. Siddiqui, M.Sc. (Pb.), Ph.D. (London)	Mineralogy, Petrology, Mapwork.	July, 1960.
Mr. Z. A. Saleem, M.Sc. (Pb.)***	Geohydrology, Geophysics.	June, 1961.
Mr. F. Z. Khan, M.Sc. (Pb.).****	Palaeontology	January, 1965.
Mr. M. Ghazanfar, M.Sc. (Pb.)*****	Structural Geology	January, 1965.
Mr. M. H. Malik, M.Sc. (Pb.), M.Sc., D.I.C. (London)	Engineering Geology	March, 1965.
Mr. A. Shakoor, M.Sc. (Pb.)******	Petrology	May, 1965.
Mr. Krishan Ahmad, M.Sc. (Pb.)	Structural Geology	August, 1967.
Mr. Zulfiqar Ahmad, M.Sc. (Pb.)	Mineralogy, General Geology.	August, 1967.

* On duty leave at Vienna, Austria.
** On duty leave at E.N.I. School of advanced studies on Hydrocarbons, Milano, Italy.
*** On duty leave at the Department of Hydrology, University of New Mexico, Socorro, U.S.A.
**** On duty leave at the Department of Geology, University of Leeds, Leeds, U.K.
***** On duty leave at the Department of Geography, Sheffield University, Sheffield, U.K.
****** On duty leave at the Department of Geology, University of Leeds, Leeds, U.K.

Name and Qualifications	*Subject*	*Appointed*
Mr. Farooq A. Khan, M.Sc. (Pb.), M. Phil. D.I.C. (London).	Subsurface Geology, Stratigraphy.	October, 1967.
Mr. A. Baset, M.Sc. (Pb.)	Palaeontology	October, 1967.
Dr. Ali Rahmat, M.Sc. (Pb.), D.E.A., Ph.D. (Montpellier).	Hydrology	November, 1967.
Research Assistants :		
Mr. S. Taseer Hussain, M.Sc. (Pb.)*	Palaeontology	April, 1966.
Mr. Fazal-ur-Rehman, M.Sc. (Pb.)	Geochemistry	December, 1966.
Mr. Shafeeq Ahmad, M.Sc. (Pb.)	Geochemistry	January, 1967.
Mr. Tasneem Noorani, M.Sc. (Pb.)	Petroleum and Structural Geology.	May, 1967.
Part-time Lecturers :		
Mr. M. S. Zafar, M.Sc. (Pb.), M.Sc. (London) Physics Department.	Mathematical Physics	November, 1967.
Dr. A. Q. Rathur, M.Sc. (Pb.), Ph.D. (Birmingham)	Structural Geology and Mapwork.	October, 1967.
Mr. Riaz M. Khan, M.A. (Pb.), Mathematics Department.	Applied Mathematics	November, 1967.
Mr. Anis A. Abbasi, M.A. (Pb.), M.Sc. (Syracuse, U.S.A.).	Geomorphology	October, 1966.
Demonstrators :		
Mr. Liaqat A. Shaikh	Palaeontology	November, 1967.
Mr. Zahid A. Roomana	Mineralogy	November, 1967.
Mr. Iqbal A. Malik	Mineralogy	November, 1967.
Mr. Ghazanfar Riaz	Geophysics	November, 1967.
Mr. Kaleem A. Qureshi	Structural Geology	November, 1967.
2. Technical and Service Staff :		
Mr. S. A. Kazmi, M.I.S.T. (London)	Chief Technician	March, 1963.
Mr. M. Aslam	Junior Technician	June, 1964.
Mr. H. Siddiqui	Junior Technician	June, 1965.
Mr. Arshad Hussain	Geological Illustrator	March, 1966.
Mr. Mahmood Ahmad	Draftsman	January, 1967.
Mr. G. R. Bhatti, B.A. (Pb.)	Secretary/Assistant	September, 1963.
Mr. K. Ahmad, B.A. (Pb.)	Library Assistant	August, 1965.
Office and Library Staff	6	
Laboratory Assistants	9	
Drivers	1+1 (summer only)	
Service Staff	3	

* On duty leave at the Geological Institute, Utrecht, Holland.